# Holocene Evolution of the Upper Western Channel within Tauranga Harbour

A thesis

Submitted in partial fulfilment

of the requirements for the degree

of

**Masters of Science (Research) in Earth Science**

at

**The University of Waikato**

by

**ALYOSHA PODRUMAC**

THE UNIVERSITY OF WAIKATO

*Te Whare Wānanga o Waikato*

2016

# ABSTRACT

The Tauranga Harbour is a mesotidal lagoon that is actively infilling with sediment. The southern basin of the harbour is important from both ecological and socio-economic standpoints. An understanding of sediment dynamics is necessary for the management of the harbour. Previously, the Tauranga Harbour Sediment Study (THSS) analysed the terrigenous flux of sediments into the harbour. It identified predominantly silt-sized sediment yields, from catchments, which remains confined to entry points into the harbour, or get exported out to the open coast. However, mapping of the tidal inlet and parts of the Western Channel through to Rangiwaea Island, has identified that accretion involves sand-sized sediment. The presence of eroding cliffs has provided speculation that sediment is primarily derived by local source erosion, as opposed to terrestrial or marine inputs. However, little is known about the sediment dynamics through the central harbour region.

This thesis involved seismic reflection surveying through the Western Channel, from Rangiwaea Island to Matakana Point, utilising a Knudsen Sub-Bottom Profiler that operates on a chirp sonar system. Through the seismic analysis, patterns of sandwave occurrence were analysed to discover how sediment dynamics varied along the Western Channel. Additionally, three fault sites were identified in the seismic profiles. Two of these faults occur parallel to a previously mapped fault at Omokoroa, where doming has been suggested. The third fault occurs in the southeast where subsidence has been identified.

Vibracoring was utilised to collect intact, contiguous, and undisturbed cores through the field area. Sand is identified as the primary contribution to ongoing sedimentation in the harbour. A general coarsening trend of sedimentary texture is observed from the central intertidal flats through the upper Western Channel towards the tidal inlet. This pattern is disrupted where current amplification or close proximity to a sediment source is associated with the accretion of coarser sediment to form sandwaves. Rates of sedimentation through the Western Channel over the last 7,200 years, ranged from 0.0482 mm/yr approaching the tidal flats, to 0.436 mm/yr where extensive sandwave were identified. A sedimentation rate of 0.0977 mm/yr was calculated within the channel where no sandwaves were present. The primary source of sediment appears to be local erosion of coastal cliffs, with sedimentation rates strongly correlating to erosional sites.

# Acknowledgements

Firstly, I would like to thank my chief supervisor Dr Willem de Lange. Your guidance and vast knowledge through this experience has been amazing and much appreciated. Also thanks to my secondary supervisor Vicki Moon, whose assistance was always appreciated.

Thanks to the Western Bay of Plenty District Council for funding part of the research

I am also thankful to staff of the Earth Science programme who have taught me much in my long six year journey from the start of undergrad in 2010, to the completion of my Masters Degree.

Special thanks also to the Earth Science technicians, in particular Dean Sandwell and Chris Morcom for helping with my Vibracoring field work, and Annette Rodgers for assistance with the Laser Sizing.

Thank you to all my fellow MSc students. From late nights spent in D.2.13 during the first year and half of Masters (Alex and Berengere), to the crew down in F.1.02 over the final months of my research (Tyler and Francesca), and all the others who have helped me along the way.

Finally, thanks to all my friends and family. Constantly motivating me through the journey, especially in the last couple months where longer days and nights were spent at University. Also, thanks mum for proof reading almost every report and chapter I wrote since beginning my Masters.

# Contents

**List of Figures** ..... **vii**

**List of Tables** ..... **xii**

**CHAPTER 1: INTRODUCTION** ..... **1**

1.1 Background ..... 1

1.2 Thesis Aim and Objectives ..... 3

1.3 Thesis Structure ..... 4

**CHAPTER 2: LITERATURE REVIEW** ..... **5**

2.1. Introduction ..... 5

2.2. Estuaries ..... 6

2.3. Regional Geology ..... 9

2.3.1. Volcanism ..... 10

2.3.2. Faulting in the Tauranga Harbour ..... 14

2.4. Holocene Evolution of the Tauranga Harbour ..... 14

2.4.1. Sedimentary Evolution ..... 15

2.5. Hydrodynamics ..... 16

2.5.1. Tidal Currents ..... 16

2.5.2. Wind Waves ..... 17

2.5.3. Storm Surge ..... 17

2.5.4. Residence Times, Salinity and Temperature ..... 18

2.6. Sedimentation Studies ..... 20

2.6.1. Tauranga Harbour Inlet ..... 20

2.6.2. Catchment Sediment Studies ..... 23

2.6.3. Sand Sedimentation ..... 29

2.7. Summary ..... 33

**CHAPTER 3: SEISMIC SURVEY INTERPRETATION** ..... **35**

3.1. Introduction ..... 35

3.2. Seismic Reflection ..... 35

3.3. Methods ..... 36

3.3.1. Field Methods ..... 36

3.3.2. Laboratory Interpretation ..... 38

3.4. Sedimentation Patterns ..... 40

3.4.1. Sandwaves ..... 40

3.4.2. Sandwaves Identified ..... 42

3.4.3. Discussion ..... 55

3.5. Structural Interpretation ..... 58
3.5.1. Faulting Discussion ..... 67
3.6. Summary ..... 69
**CHAPTER 4: SEDIMENT CORING INTERPRETATION ..... 71**
4.1. Introduction ..... 71
4.2. Vibracoring ..... 71
4.3. Core Sites ..... 73
4.3.1. Core Group 1 ..... 73
4.3.2. Core Group 2 ..... 74
4.3.3. Core Group 3 ..... 74
4.4. Field Methods ..... 75
4.4.1. Equipment ..... 75
4.4.2. Coring Procedure ..... 76
4.4.3. Post Coring ..... 78
4.5. Analytical Methods ..... 79
4.5.1. Visual Logging ..... 79
4.5.2. Laser Sizing ..... 80
4.5.3. Stratigraphic Logs ..... 80
4.6. Stratigraphic Analysis ..... 81
4.6.1. Core Site 1 ..... 81
4.6.2. CS2 ..... 85
4.6.3. CS3 ..... 89
4.6.4. CS4 ..... 92
4.6.5. CS5 ..... 95
4.7. Facies Interpretation ..... 98
4.7.1. CG1 ..... 98
4.7.2. CG2 ..... 98
4.7.3. CG3 ..... 99
4.7.4. Silt Composition ..... 99
4.8. Summary ..... 99
**CHAPTER 5: DISCUSSION ..... 101**
5.1 Introduction ..... 101
5.2 Evolution of Upper Western Channel Sedimentary Deposits ..... 101
5.2.1 Fluvial Deposits ..... 102
5.2.2 Pre Holocene ..... 110

5.3 Structural Interpretation ..... 111
5.3.1 Doming Evidence ..... 112
5.3.2 Subsidence Evidence ..... 114
5.4 Summary ..... 114
**CHAPTER 6: CONCLUSIONS ..... 117**
6.1 Summary of Research Findings ..... 117
6.2 Future Work ..... 119
**REFERENCES ..... 121**

# List of Figures

Figure 1.1: Satellite image of the Tauranga Harbour with an image of New Zealand in the top right corner for reference (orange dot marks the location of Tauranga Harbour). ..... 2

Figure 1.2: Hydrographic chart of the southern Tauranga Basin. Western Channel marked with a solid red line. From LINZ (2016) ..... 3

Figure 2.1: Stratigraphy of the Tauranga Region (From Jorat et al., 2016) ..... 11

Figure 2.2: Geological map of the Tauranga area and Southern Kaimai Range showing the major units and their ages where known (from Briggs et al., 2005) ..... 12

Figure. 2.3: Bathymetry of the ebb tidal delta and the tidal inlet. The data show the progressive narrowing and deepening of the tidal inlet associated with the progradation of Panapane Pt, and the changing morphology of the ebb tidal delta between 1852 and 1954. From de Lange et al., 2015 ..... 21

Figure 2.4: Representative frequency grain size frequency curves around the Tauranga Basin Inlet. Three curves given for each site with (i) the dashed line showing percent by weight frequency curve for the total sample, (ii) the solid line showing frequency for the acid insoluble fraction, and (iii) the cumulative line showing cumulative percent by weight frequency curve for the acid-insoluble fraction. Taken from Davies-Colley et al. (1978) ..... 22

Figure 2.5: Contour map of (a) mean grain size and (b) sorting of non-carbonate materials. From Davies-Colley et al. (1978) ..... 23

Figure 2.6: Subdivision of the southern Tauranga Harbour into subestuaries and the association of subcatchments with subestuaries. The black numbers mark subestuaries. The white numbers in the black boxes mark subcatchments. From Hume et al. (2009). ..... 24

Figure 2.7: Fine sedimentation rates and composition at each subetuary. From Hume et al. (2009). ..... 28

Figure. 2.8: Sedimentation rates calculated based on radiometric dates and inferred Holocene – Pleistocene Boundary. From Christophers (2015). ..... 31

Figure 2.9: Map of Matakana Barrier Island showing former landforms and shorelines. EHS = Early Holocene Shoreline, S1 and S2 = former eroded shorelines, S3 – Kaharoa Shoreline. From Shepherd et al., 1997 ..... 32

Figure 3.1: Example of Seismic Reflection utilizing a chirp sonar system. Solid lines are emitted waves, and dashed are reflected ..... 36

Figure 3.2: Map of the field area. Matakana, Rangiwaea and Motuhoa Islands, and Omokoroa Peninsula are all labelled. The Western Channel is marked by a solid black line from the inlet and approaching the tidal flats ..... 37

Figure 3.3: Transect I of the seismic data consisting of the initial route from Rangiwaea Island to Matakana Point ..... 38

Figure 3.4: Transect II of the seismic data, consisting of the first section of the reverse route from Matakana Point to just north of the Omokoroa Peninsula ..... 39

Figure 3.5: Transect III of the seismic data, consisting of the second section of the reverse route from the Omokoroa Peninsula to the southernmost tip of Matakana Island ..... 39

Figure 3.6: Sandwave profile with principal morphological features and measurements labelled. From Allen (1980) ..... 42

Figure 3.7: Locations through the harbour where sandwaves have been identified in the seismic interpretation with the bold numbers marking the sites. The lines mark the respective profile length of each sandwave length with the colours corresponding to the transects that the profiles are derived from, Orange = Transect I, Purple – Transects II & III. ..... 43

Figure 3.8: Modelled residual current speed and direction calculated over a 28 day period. Black arrows with circles are the observed residual currents. From Tay et al. (2013). ..... 44

Figure 3.9:Modelled residual velocity over two representative tidal cycles. The greyscale indicates velocity magnitude (m/s). Sample locations are indicated by black dots. From Kwoll and Winter (2011). ..... 44

Figure 3.10: Two seismic profiles taken at SS1. Both profiles are split into two halves, with the lower half continuing on the right of the upper half. For both profiles the left marks the southeastern side and the right the northwestern. (a) is sourced from Transect I with a total length of 264 m, (b) is sourced from Transect III with a total length of 255 m ..... 46

Figure 3.11: Two seismic profiles taken at SS2. Both profiles are split into two halves, with the lower half continuing on the right of the upper half. For both profiles the left marks the eastern side and the right the western. (a) is sourced from Transect I with a total length of 265 m, (b) is sourced from Transect III with a total length of 245m ..... 48

Figure 3.12: Two seismic profiles taken at SS3. Both profiles are split into two halves, with the lower half continuing on the right of the upper half. For both profiles the left marks the southeastern side and the right the northwestern. (a) is sourced from Transect I with

a total length of 330 m, (b) is sourced from Transect III with a total length of 380 m ..... 50

Figure 3.13: Two seismic profiles taken at SS4. Both profiles are split into two halves, with the lower half continuing on the right of the upper half. For both profiles the left marks the southeastern side and the right the northwestern. (a) is sourced from Transect I with a total length of 260 m, (b) is sourced from Transect II with a total length of 185 m ..... 52

Figure 3.14: Two seismic profiles taken at SS5. Both profiles are split into two halves, with the lower half continuing the right of the upper half. For both profiles the left marks the southeastern side and the right the northwestern. (a) is sourced from Transect I with a total length of 195 m, (b) is sourced from Transect II with a total length of 128 m ..... 54

Figure 3.15: Locations where faults have been identified in the seismic interpretations with the bold numbers marking the site. The lines mark the respective seismic profile lengths for each fault site. The colours correspond to the transects the profiles are derived from, Orange = Transect I, Purple – Transect II & III ..... 59

Figure 3.16: Seismic profile of FS1 from Transect III. The solid orange line marks the bottom of a layer identified under the surface. The arrows display a constant thickness with the subsurface layer. ..... 61

Figure 3.17: Seismic profile of FS2 from Transect I. The total length of the profile is 600 m with the lower image continuing from the right of the upper image. The left side marks the southeast (inlet side of the harbour) and the right the northwest (tidal flat side of the harbour). Solid yellow lines mark the boundaries of subsurface layers. ..... 63

Figure 3.18: Seismic profile of FS2 from Transect III. The total length of the profile is 990 m with the lower image continuing from the right of the upper image. The left side marks the southeast (inlet side of the harbour) and the right the northwest (tidal flat side of the harbour). Solid yellow lines mark the boundaries of subsurface layers. The solid red line marks the presumed fault location ..... 64

Figure 3.19: Seismic profile of FS3 from Transect II. The total length of the profile is 200 m. The left side marks the south and the right the north, which coincides with a fork in the Western Channel with both directions leading towards tidal flats. Solid yellow lines mark the boundaries of subsurface layers. ..... 66

Figure 3.20: Models of fault propogation folds. (A) Geometric kick-band model. (B), (C), (D) Analog experimental models of folds above (B) thrust, (C) reverse, (D) normal faults. From Erslev (1991) ..... 67

Figure 3.21: Example of the reverse fault fracture presumed at FS2 ..... 68

Figure 4.1: Example of a vibracore setup. A generator powers a vibrating head, sending a vibrations through the core barrel and allowing penetrations of the surface under the weight of the unit. ..... 72

Figure 4.2: Locations of core sites through the harbour. CS = Core Site. Tidal inlet is found southeast of Rangiwaea Island. Tidal flats occur northwest of CS5 ..... 73

Figure 4.3: Example of the vibracorer deployment. Features of the vibracorer are labelled (frame, head and core barrel). The vessel crane lifts the unit and deploys it off the vessel into the water. ..... 77

Figure 4.4: An idealised example of a retrieved core indicating penetration depth..... 77

Figure 4.5: Example of the labelling system utilised across both two and three piece core series..... 78

Figure 4.6: Saw table for splitting cores. Cores are laid flat in the central groove of the table, the PVC an the exposed side is split, the core is rotated 180° and once again the exposed PVC is split ..... 79

Figure 4.7: Image of two open cut core sections from CS1. Colour wheel present as a reference for cross-core comparison and measuring tape spread between the components as a reference for length..... 83

Figure 4.8: Stratigraphic log for CS1..... 84

Figure 4.9: Image of three open cut core sections from CS3. Colour wheel present as a reference for cross-core comparison and measuring tape spread between the components as a reference for length..... 87

Figure 4.10: Stratigraphic log for CS2..... 88

Figure 4.11: Image of three open cut core sections from CS3. Colour wheel present as a reference for cross-core comparison and measuring tape spread between the components as a reference for length..... 90

Figure 4.12 Stratigraphic log for CS3..... 91

Figure 4.13: Image of three open cut core sections from CS4. Colour wheel present as a reference for cross-core comparison and measuring tape spread between the components as a reference for length..... 93

Figure 4.14: Stratigraphic log for CS4..... 94

Figure 4.15: Image of two open cut core sections from CS5. Colour wheel present as a reference for cross-core comparison and measuring tape spread between the components as a reference for length..... 96

Figure 4.16: Stratigraphic log for CS5..... 97

Figure 5.1: Evolution of the Matakana Barrier Island. (a)6,000 Cal BP, (b)4,000 Cal BP, (c)1,750 Cal BP, and (D) 600 Cal BP. From Shepherd et al (1997)..... 104

Figure 5.2: Anoxic units seen in CS5 in the upper 20 cm. These units rapidly oxidised once the core was opened..... 105

Figure 5.3: Radium concentration through the harbour overlain on a map from Google Earth. Radium concentrations are provided from (Stewart, 2016). The solid black line marks the projected orientation of FS2 where the fault trace is known from the Seismic, and the dashed line marks the fault trace of FS3, where seismic did not directly mark the location of a fault trace and is so more speculative. Additionally, a solid yellow line marks evidence of a fault to the east of FS1, with no Radium hotspots identified at the location of FS1 itself. ..... 113

Figure 5.4: Parallel fracturing forming as stress builds up in the subsurface due to doming. ..... 114

# List of Tables

Table 2.1. New Zealand estuary types and their definitions according to the EEC (NIWA, 2013) ..... 7

Table 2.2: Average modelled residence times of sub-estuaries in the southern basin of Tauranga Harbour. Sc. = Scenario. Sc. 0 = Base case, Sc. 1 = No wind conditions, Sc. 2 = Storm winds 11 m s-1 from 100o in winter, Sc. 3 = Storm winds 11 m s-1 from 100o in summer, Sc. 4 = Storm winds 11 m s-1 from 230o in winter, Sc. 5 = Storm winds 11 m s-1 from 230o in summer, and Sc. 6 = high freshwater discharge from Wairoa River 540 m3 s-1. Bolded sub-estuaries mark those exposed to central channels while unbolded estuaries have more constricted entrances. Data adapted from Tay et al. (2013). ..... 19

Table 2.3: THSS subestuary and subcatchment identification. Adapted from Hume et al. (2009). ..... 25

Table 2.4: Summary statistics of catchment sediment supply to the Tauranga Harbour. Adapted from Hume et al. (2009) ..... 27

Table 2.5: Sedimentation rates calculated at Waimapu, Waikareo Estuary, Te Hopai, and Hunters Creek by the THSS. Rate of sedimentation is presented along with the time period over which the rate was estimated (years). Estimated rates originally presented in Hancock et al. (2009). ..... 29

Table 2.6: Estimated scarp retreat and volumes for identified failure events. From Moon et al. (2015) ..... 30

Table 4.1: Grainsize composition with horizon change through CS1 ..... 83

Table 4.2: Grainsize composition with horizon change through CS2 ..... 87

Table 4.3: Grainsize composition with horizon change through CS3 ..... 90

Table 4.4: Grainsize composition with horizon change through CS4 ..... 93

Table 4.5: Grainsize composition with horizon change through CS5 ..... 96

Table 5.1: Correlation of Core Site and Core Group facies, to one of three categories; Fluvial Holocene Deposits, Tsunami Holocene Deposits, or Pre-Holocene Deposits ..... 101

# CHAPTER 1

# INTRODUCTION

## 1.1 Background

Tauranga Harbour is situated on the north-eastern coastline of the North Island and covers an area of 851 $km^2$. It extends 35 km along the coastline with an average width of 5 km (*Figure 1.1*). It is one of only two coastal inlets on the eastern New Zealand coastline where a dual inlet system is featured (Hume et al., 1992), with the Katikati Inlet found to the north and the Tauranga Inlet found to the south. Both inlets feature a Holocene barrier tombolo (Bowentown at north side of the Katikati Inlet and Mt Manganui at the south side the Tauranga Inlet) that provide positional stability, while Matakana Island acts as a barrier to the open ocean (Hume et al., 1992; Kruger and Healy, 2006). The Tauranga Harbour can be divided into two basins: the Katikati Basin in the north; and the Tauranga Basin in the south. The two basins are separated by extensive shallow intertidal flats and can so be considered hydrodynamically independent. (Tay et al., 2013).

Consistent with coastal embayments worldwide, Tauranga Harbour naturally infills with sediment over time. Rates of infill for coastal embayments can be highly variable, depending on a range of factors including but not limited to: size, shape, rate of sediment supply, sediment composition, and anthropic influences (Barnett, 1985). The southern Tauranga Basin is a mesotidal lagoon with a spring tidal range of 2.2 m, a spring tidal prism of $165 \times 10^6$ $m^3$, and features a well-developed tidal inlet and delta complex at its mouth. A number of catchments empty into the harbour, of which the Wairoa River is the most important discharge, although its influence is minimal with respect to the tidal prism (Davies-Colley et al., 1978; Davies & Healy, 1993).

The Tauranga Basin has high socio-economic and ecological value, experiencing high amounts of recreational use, and boasts many unique flora and fauna, so the preservation of the harbour is of the upmost importance. Additionally, the harbour also contains within it the Port of Tauranga, New Zealand's largest port with 12.6 million tonnes of cargo passing through annually. Dredging has been carried out since 1968 from the inlet to the port, in the southeast of the southern basin. After

capital dredging in 1991/92, the shipping channel was maintained at 14.1 m below sea level, involving 110,500 $m^3$ of sediment being removed annually. Further capital dredging occurred between October 2015 and August 2016, with minor additional expansion of the channels planned for the future. Despite the dredging, the southern basin continues to infill with sediment. (Kruger and Healy, 2006; Brannigan, 2009).


***Figure 1.1: Satellite image of the Tauranga Harbour with an image of New Zealand in the top right corner for reference (orange dot marks the location of Tauranga Harbour).***

Various sedimentation studies have been undertaken within the Tauranga Harbour since the 1970s to better understand the sediment dynamics. The existing research has identified patterns of sedimentation occurring around catchment sources into the harbour, and sediment dynamics around the tidal inlet. However, the sediment dynamics through the middle to upper Western Channel of the harbour remains unknown (*Figure 1.2*). Furthermore, the sources of sediment infilling the harbour are also not well known. Catchment sources have been identified as contributing primarily silts to the harbour, most of which appear to be exported out of the

harbour. Meanwhile, mapping of the harbour has identified that accretion predominantly involves sand-sized sediment, with minor biogenic gravels. The presence of eroding cliffs through the harbour has led to suggestion that these may be a significant source of sediment for the harbour.

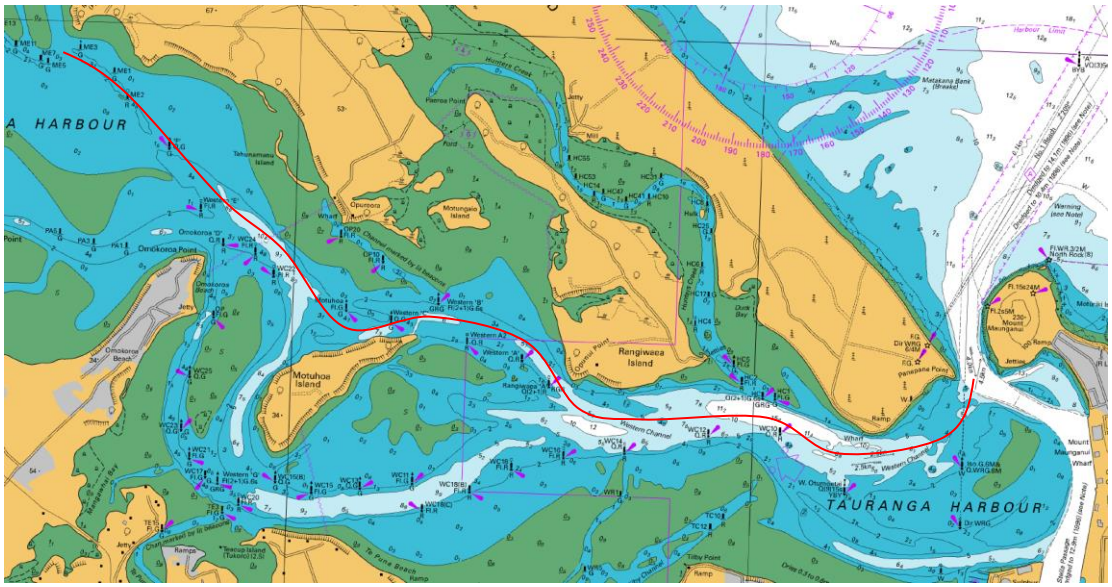


***Figure 1.2: Hydrographic chart of the southern Tauranga Basin. Western Channel marked with a solid red line. From LINZ (2016)***

## 1.2 Thesis Aim and Objectives

The aim of this thesis is to investigate the Holocene evolution of the Upper Western Channel within Tauranga Harbour. The specific research objectives are:

*(I)* Mapping of the Western Channel utilizing seismic survey reflection, to identify: (a) patterns of sedimentation, and (b) areas of active faulting.

*(II)* Sediment coring of the Western Channel to observe how local sedimentary structure varies through the harbour and with depth, and identify the presence of faults

*(III)* To identify: (a) patterns of sedimentation along the Upper Western Channel, (b) sedimentary variations with depth, (c) the sources of sediment, and (d) approximate rates of sedimentation.

*(IV)* To interpret the structural integrity of the Western Channel.

## 1.3 Thesis Structure

***Chapter 2. Literature Review***

This chapter summarizes the background literature for the Tauranga Harbour including estuarine morphology, regional geology, sediment- and hydro-dynamics, and past sedimentation studies.

***Chapter 3. Seismic Survey Interpretation***

This chapter introduces seismic mapping, describes field and laboratory analytical methods, and provides an interpretation of the seismic results.

***Chapter 4. Sediment Coring Interpretation***

This chapter introduces the vibracoring technique, describes field and laboratory methods analytical, and provides an interpretation of the core results.

***Chapter 5. Discussion***

This chapter synthesizes the Seismic Mapping and Sediment Coring chapters, along with relevant literature to discuss the evolution of the Upper Western Channel.

***Chapter 6. Conclusions***

This chapter will summarize the key findings of this study and outline recommendations for future research.

# CHAPTER 2

# LITERATURE REVIEW

## 2.1. Introduction

Sedimentation is a natural phenomenon occurring in all estuarine environments. Estuaries themselves are environments that can be considered "born to die". Essentially, over time due to the addition of sediment, an estuary will evolve from a marine environment to a terrestrial environment. The rate of infilling is highly variable and is controlled by a range of factors (e.g. geology, hydrodynamics, sediment contributions, inlet stability and shape, estuarine stability and shape, anthropogenic influences etc.); though these can be simplified to two governing process (Barnett, 1985) summarised below:

I. The long-term sediment supply from terrestrial and marine sources and the long-term sediment transport patterns.

Sediment contributions can come from terrestrial and marine sources, with the sediment composition being highly variable depending on the source. The shape and maturity of the estuary dictates the hydrodynamics of an estuary. A younger estuary will be predominantly flood dominant and infill with marine sediment throughout the harbour, while a more mature estuary will have expansive tidal flat where sedimentation is active, although the tidal channels will be deeper and display ebb dominance whereby terrestrial sediment may be exported offshore (Parker, 1991).

II. Abrupt Changes to the estuarine morphology as a consequence of storm surges and engineering works.

Abrupt changes function in a way that they can either cause mass erosion or relative sea level rise, resulting in resetting the estuary to an environment earlier in its history, or can be associated with rapid deposition or relative sea level fall, which can accelerate the rate of infilling. These changes can be a consequence of natural events such as: storm surges and tsunamis, both of which can be associated with

mass erosion and deposition (Bourgeois, 2009), or earthquakes, which can alter the morphology and hydrodynamics of a coastal body (Hull, 1986; Hughes et al., 2015); or anthropogenic influences such as: dredging, or structures that can alter the hydrodynamics of an estuary at site specific or estuary wide scales (Herbst et al., 2002).

This chapter will provide an overview on the relevant literature concerning the evolution of the Tauranga Harbour. The chapter is divided into the following subsections; **2.2.Estuaries** – A definition and classification system of estuaries in New Zealand, **2.3. Regional Geology** – Covering the setting and known evolution of the Tauranga Region, **2.4. Hydrodynamics** – A look into the processes which mobilise sediments and how they operate through the Tauranga Harbour, **2.5. Evolution of the Tauranga Harbour** – Covering the more recent observed changes which have occurred in the harbour, **2.6. Sedimentation Studies** – A summary of the sedimentation studies identifying sources and sinks of sediment in the harbour and **2.7. Summary** – where the key points of the chapter will be summarised.

## 2.2. Estuaries

Pritchard (1967) defined an estuary as "*a semi-enclosed coastal body of water which has a free connection with the open sea and within which sea water is measurably diluted with fresh water derived from land drainage*". However, while this is useful in a general sense, definitions of estuaries vary between researchers at both global and local scales depending on their specific applications. A classification system developed by the National Institute of Water and Atmospheric Research (NIWA) for the purpose of managing New Zealand estuaries, defines an estuary as "*a partially enclosed coastal body of water that is either permanently or periodically open to the sea in which the aquatic ecosystem is affected by the physical and chemical characteristics of both runoff from the land and inflow from the sea"* (Hume et al. 2007).

This definition forms the basis of the NIWA Estuary Environment Classification System, which classifies estuaries into one of eight classes based on the (i) shape and volume of the water body, (ii) quantity of river flow entering the estuary, and

(iii) quantity of exchange of seawater between the estuary and ocean (NIWA, 2013). The classes in the EEC are defined from estuarine characteristics discussed in a range of research papers including Pritchard (1967), Day (1981), Healy et al. (1982), Hume et al. (1988), Hume et al. (1993), and Hume et al. (2007).

New Zealand is surrounded entirely by water, with all boundaries being coastal environments. The coastline of New Zealand stretches some 14,000 km, and is extremely diverse with highly variable geology and marine processes. Along the coastline, there are a number of embayments that are considered estuaries by the EEC, including drowned river valleys, river mouth estuaries, barrier enclosed estuaries, and more. The eight estuarine classes identified by the EEC are presented in *Table 2.1*. Stretches of contiguous coastline will for the most part feature similar estuarine types across their lengths. Thus for the North Island, it is found that the northwest coast features mostly Type A and Type B estuaries, where the volume of river water is greater than the volume of tidal water, the northeast coast features primarily Types D, E and F where river influence is less and the estuaries are relatively shallow, and the remaining North Island coasts are effectively Type B estuaries. The Tauranga Harbour, on the North East coastline of New Zealand, is classed as a Type F estuary in the EEC, otherwise known as a barrier-enclosed mesotidal estuarine lagoon (Davies-Colley et al., 1978).

***Table 2.1. New Zealand estuary types and their definitions according to the EEC (NIWA, 2013)***

| Estuary Type | Definition |
|---|---|
| ***Type A - Coastal Lakes*** | *Very shallow basins (several metres depth). They are often elongated and run parallel to the shore. Feature zero tidal area, are poorly flushed, and wave suspension of sediments.* |
| ***Type B - Tidal River Mouths*** | *Elongated basins of simple shape and several to ten metres depth. Majority subtidal. River-dominated flow, well flushed, bars at ocean side of estuary, minor wind fetch and small wave,* |

| | |
|---|---|
| | *muddy sediments in areas of high tidal flows.* |
| ***Type C - Tidal River Lagoons*** | *Occur where the mouth of a main river channel connects shallow lagoons. Significant intertidal area, river-dominated flows, well-flushed river channel and poorly-flushed lagoon, minor wind fetch, and wave resuspension.* |
| ***Type D - Coastal Embayments*** | *Shallow, circular or slightly elongated basins with simple shorelines and wide entrances that are open to the ocean. Subtidal with intertidal areas restricted to sheltered areas, little river influence, ocean forced circulation, wave-driven sedimentation, and a sandy substrate.* |
| ***Type E - Tidal Lagoons or Barrier Enclosed Lagoons*** | *Shallow circular elongated basins with simple shorelines, an extensive intertidal area and ebb and flood tidal deltas at the mouth on littoral drift shores. Ocean forced circulation, strong flushing and win mixing, and a sandy substrate.* |
| ***Type F - Barrier Enclosed Lagoons or Drowned Valleys*** | *Similar to Type E, featuring shallow basins with deep channels leading off the main basin, tide dominated, and narrow mouths usually formed by a spit and sand barrier. Mixing and wave resuspension less pronounced than in Type E, featuring sandy substrate with a transition to muddy in the upper* |

| | |
|---|---|
| | *portions of the arms which are characterised by salt wedges and stratification.* |
| ***Type G - Fjords or Sounds*** | *Very deep (up to 100s of metres), narrow, elongated basins which are largely subtidal. Characterised by sills at the mouth, thermohaline forcing, and poor flushing.* |
| ***Type H - Drowned Valleys, Rias or Fjords*** | *Deep (10s of metres), narrow, elongated basins which are largely subtidal with the estuary bed lower than the low tide mark. Feature thermohaline forcing, and a longitudinal gradient with riverine forcing and stratification in the headwaters and ocean forcing and vertical mixing at the entrance, poor flushing and fine sand or mud substrate.* |

## 2.3. Regional Geology

The Tauranga region is formed up of six physiographic units: Kaimai Range, Whakamarama Plateau, Tauranga Basin, Mamaku Plateau, Papamoa Range, and a group of volcanic domes. The Tauranga Harbour lies within the Tauranga Basin, a Pleistocene fluvial/estuarine basin, which infilled following subsidence associated with the eruption and emplacement of the Waiteraiki Ignimbrite. Subsequent infills include estuarine and terrestrial volcanoclastic sediments, and ignimbrite and airfall tephras. The Tauranga Basin covers 570 $km^2$, with the Tauranga Harbour occupying ~200 $km^2$ (Briggs, 1996)

### *2.3.1.* Volcanism

Briggs et al. (1996) provided a description on the geology of the Tauranga Region. The deposits within this area (from both primary and secondary volcanic origin) are made up of basaltic-rhyolitic lavas and dacitic-rhyolitic ignimbrites and tephras, sourced from the Taupo Volcanic Zone (TVZ) and the Coromandel Volcanic Zone (CVZ). Some of the units were reworked through fluvial/lacustrine/estuarine process and redeposited in interbedded sequences within primary deposits. The stratigraphy of the region is shown in *Figure 2.1* while Figure *2.2* shows the exposed formations of the Tauranga Basin. Of importance to this study are the Waiteraiki Ignimbrite, Matakana Basalt, Matua Subgroup, and Late Pleistocene and Holocene Tephras, described below. With the exception of older materials (i.e. Otawa Volcanics and Matakana Basalt), recent materials are predominantly of rhyolitic composition (Briggs et al., 2005)

#### *2.3.1.1. Waiteraiki Ignimbrite*

The Waiteraiki Ignimbrite overlies the Aongatete Ignimbrite, and together they form the Whakamarama Plateau. The Plateau was deposited prior to the uplift of the Kaimai Ranges, and now is tilted gently north-eastwards (3-5$^{o}$), and also displaced by the Hauraki and Okauia Faults. K-Ar dating of the Waiteraiki Ignimbrite indicated ages of 2.18±0.15 Ma and 2.13±0.17 Ma, suggesting that it was sourced from the Kaimai Volcanic Centre (Briggs et al., 2005; Jorat et al., 2016). The Waiteraiki Ignimbrite itself forms the local basement of the Tauranga Basin, where it is overlain by a series of volcanic and sedimentary deposits (Briggs, 1996).

#### *2.3.1.2. Matakana Basalt*

The Matakana Basalt is a solitary basalt lava outcrop with pseudo-pillow structures, 30 m offshore of Matakana Island, on the harbour side. It is the only occurrence of a basalt in the Tauranga Region. The Matakana Basalt has been dated by K-Ar at 2.7 $^{+}$/- 0.1 Ma, indicating that it pre-dates the Minden Rhyolite and post-dates the Otawa Volcanics (Briggs, 1996; Briggs et al., 2005).

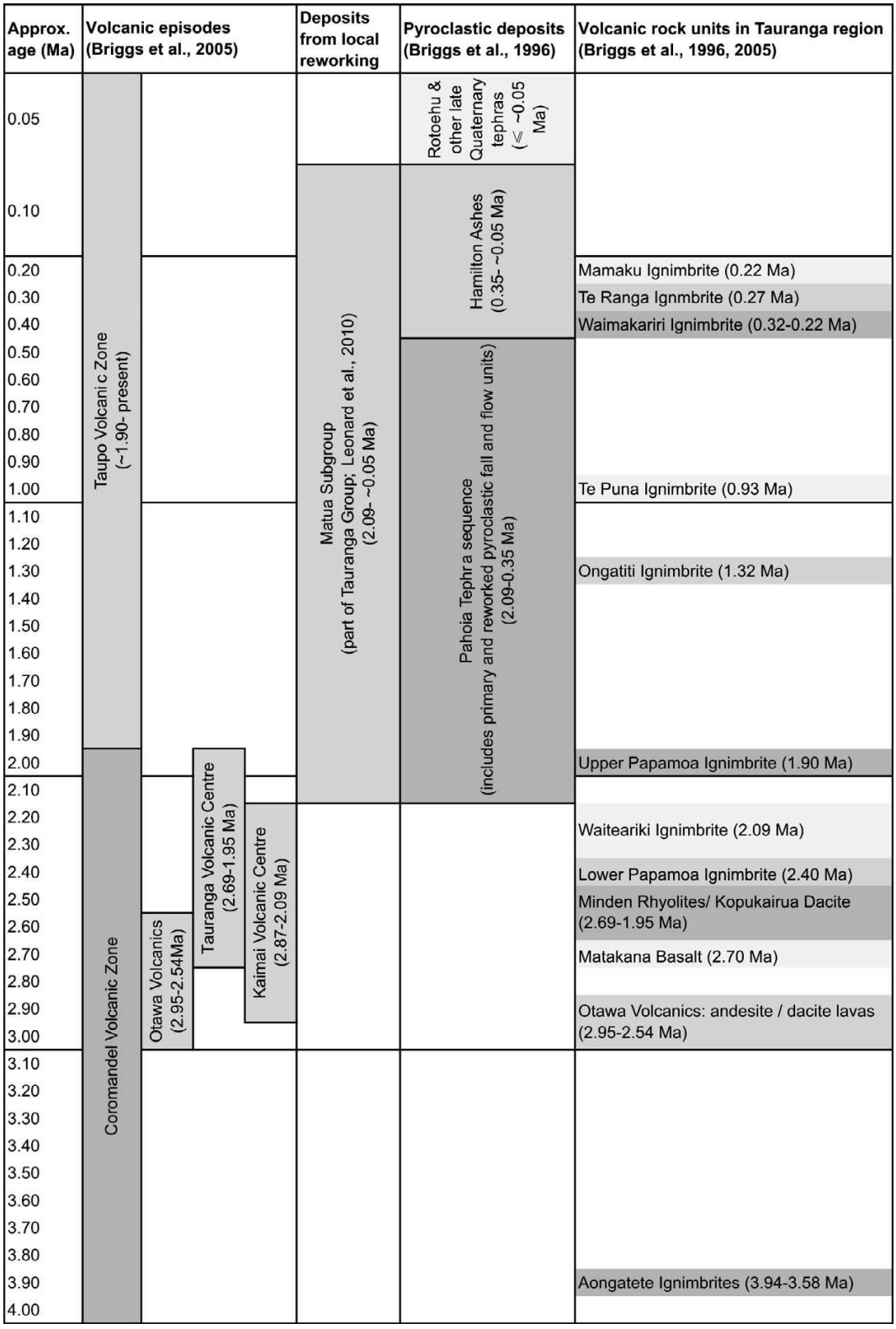


***Figure 2.1: Stratigraphy of the Tauranga Region (From Jorat et al., 2016)***

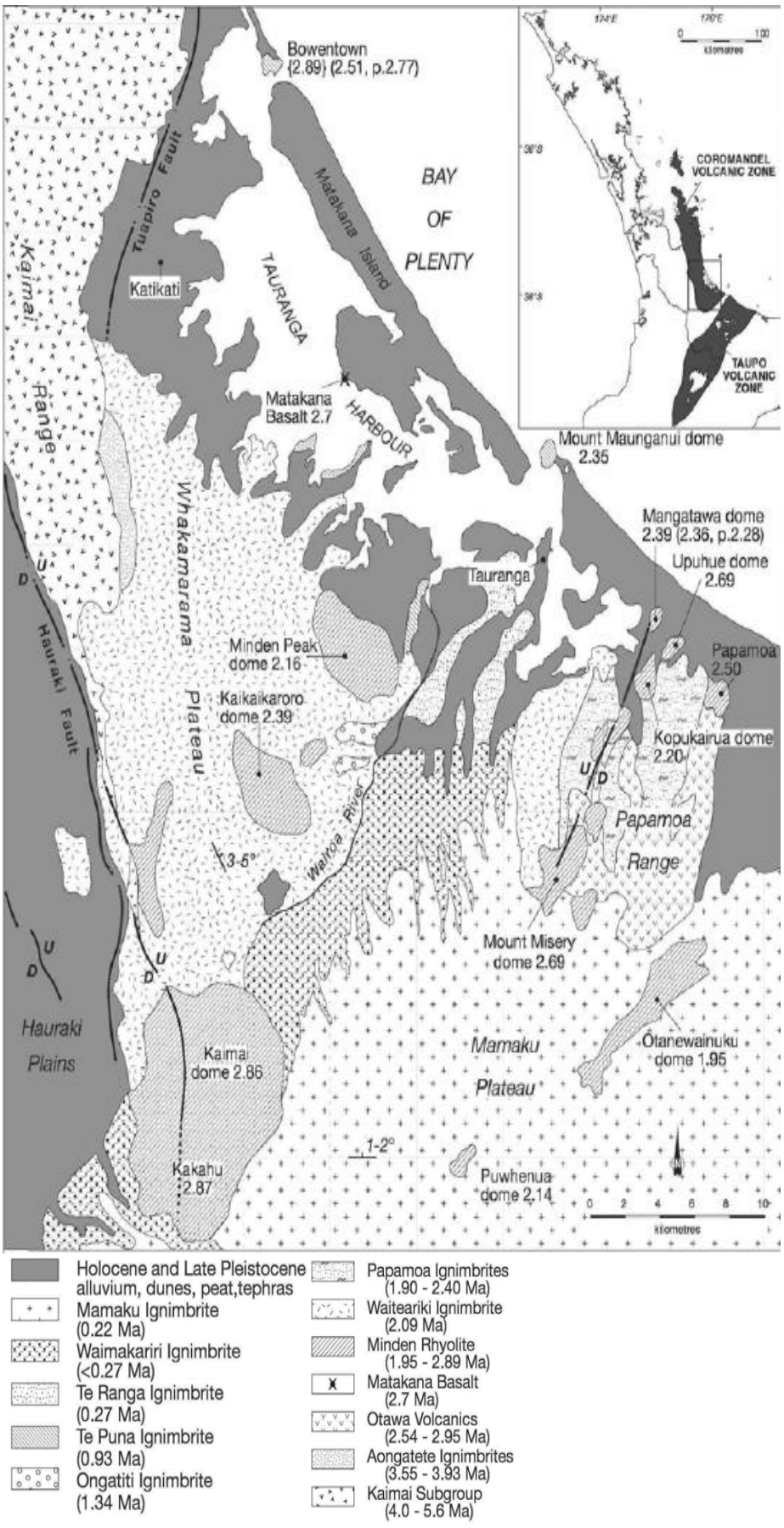


***Figure 2.2: Geological map of the Tauranga area and Southern Kaimai Range showing the major units and their ages where known (from Briggs et al., 2005)***

#### *2.3.1.3. Matua Subgroup*

The Matua Subgroup is formed up of fluvial pumiceous and rhyolitic silts, sands and gravels, lacustrine and estuarine diatomaceous muds, and lignites and peats, intercalated with two distal ignimbrites, the Te Puna Ignimbrite and the Te Ranga Ignimbrite (Whitbread-Edwards, 1994), and the Pahoia Tephras.

**Pahoia Tephras**: Poorly defined unit of weathered primary and reworked rhyolitic volcanoclastic materials, ranging in age from 2.18 to 0.35 Ma. Pahoia Tephras include all tephras older than the Hamilton Ash within the Tauranga Basin. Pahoia Tephras are observed exposed in coastal sections of the Greertion, Maungatapu, Matapihi terraces, the base of Mt Manganui, Matua, on the Omokoroa and Pahoia Peninsulas, and on Matakana and Motuhoa Islands (Briggs, 1996; Briggs et al., 2005).

**Te Puna Ignimbrite**: A hornblende bearing, pumice-rich, crystal-rich, non-welded to partially-welded ignimbrite. Reversed primary magnetisation suggests the deposit is older than 0.78 Ma, while lithic fragments dated at 1.21±0.04 Ma provide a maximum age. The deposit is exposed next to the Wairoa River, in coastal sections at Omokoroa and Pahoia Point, and on the harbour side of Matakana Island (Briggs, 1996; Briggs et al., 2005).

**Te Ranga Ignimbrite**: A variably pumice rich to pumice poor, crystal rich, non-welded, sandy textured ignimbrite. The deposit is distributed over a 30 $km^2$ area, covering most of the area between Maungatapu and the Wairoa River, including segments of Matakana and Motuhoa Islands (Briggs, 1996; Briggs et al., 2005).

#### *2.3.1.4. Late Pleistocene and Holocene Tephras*

A collection of Late Pleistocene and Holocene tephras blanket the entire region. Notable amongst these is the Rotoehu Ash, a product of the second largest eruption of the Taupo Volcanic Zone (TVZ) in the last 230 ka (second only to the 26.5 ka Oruanui Eruption), which acts as an important marker bed for much of the North Island (Lowe, 2011). The Rotoehu Ash has been dated at >50 ka based on $^{40}Ar/^{39}Ar$

relationships (Briggs et al., 2005), 61±1.4 ka by K-Ar dating of lavas (Wilson et al., 2007), and at 45 ka by $^{14}C$ and (U-TR)/He ages of Rotoiti pyroclastics (Danisik et al., 2012).

### *2.3.2.* Faulting in the Tauranga Harbour

No faults have been actively traced through the harbour, with minimal faulting suspected post the emplacement of the Waiteraiki Ignimbrite. However, Briggs (1996) envisioned a series of NNE orientated, deep seated faults. The evidence of faults is geomorphology with the NNE orientation of major rivers and terraces that strike into the Tauranga Harbour. However, a gentle 1-2$^{o}$ dipping of some terraces may indicate late stage rejuvenation of the faults, associated with minor lifting.
Christophers (2015) provided evidence of a fault through the Omokoroa Peninsula where the Te Puna ignimbrite is observed in the western side of the peninsula, while no such outcrops can be observed on the eastern side. This feature has previously been noted and mapped (Briggs et al., 2005) (*Figure 2.2*), and corresponds to the suggestion of NNE orientated faults aligned with terraces (Briggs, 1996).

## 2.4. Holocene Evolution of the Tauranga Harbour

During the last glaciation, sea level was at its global minimum ~21 ka; at which stage extensive glaciers could be found on most continents. The Holocene transgression started as these glacier began to melt ~12 ka, and sea level subsequently rose at rates up to 20 mm/yr. The transgression culminated around 7 – 7.75 ka, whereby modern global sea levels were achieved, though fluctuations of ±2 m persisted (Pluet and Pizzaroli, 1991).

Research of prehistoric sea levels for the New Zealand coastline has provided similar dates for the achievement of the modern sea level. de Lange et al. (2015) estimated a date of 7.2 cal ky BP, while Clement et al. (2010) estimated a date of 7.55 cal ky BP for the Manawatu. Regarding the Tauranga Harbour, Christophers (2015) dated peats overlain by estuarine sands at the Omokoroa Peninsula to 6.6 cal ky BP, with sea levels predicted to be slightly higher to present.

### *2.4.1.* Sedimentary Evolution

Paleogeographic reconstructions split the Holocene evolution in two phases. Firstly, from 8100 $^{+}$/- 80 yr BP to the post-glacial transgression stillstand, when modern sea levels were achieved, late Pleistocene fluvial and fan deposits were overlain by shelly mud as sea level rose. The oldest Holocene deposits within Tauranga Harbour can be dated to 8.1 cal y BP (Davies & Healy 1993; de Lange et al., 2015). Subsequently, with the establishment of modern sea level, the barrier island Matakana domed while Bowentown and Mt Manganui became connected to the headland by progradational dunes ridges, comprised of a combination of fixed and moving dune sands (Davies & Healy 1993). Concurrently, low lying terraces formed through fluvial incision into the accumulation of river and stream alluvium and peat deposits (Briggs et al., 1996).

#### *2.4.1.1. Formation of Matakana Island and Tidal Deltas*

Development of the Tauranga Harbour began with establishment of the modern sea level. Relatively stable sea level allowed fluvial conditions to equilibrate, along with considerable levels of sediment reworking, allowing both Matakana Island and the spit connecting Mt Manganui to the mainland to accrete through onshore and longshore transport of eroded volcanoclastic sediment (Davies & Healy 1993). Up until ~4 cal ky BP, Matakana Island is believed to have been a sequence of barrier and eroding Pleistocene islands, subject to episodic storm and washover events, producing extensive backbarrier washover slopes (Shepherd et al., 1997).

Due to the absence of key marker mid- and late- Holocene tephra units at two locations along Matakana Island, inlets are inferred to have been present near Hunters Creek and Blue Gum Bay (*Figure 2.3*). Ongoing sedimentation and changes to tidal currents eventually culminated in the closure of Hunters Creek (5.2 ka) and Blue Gum Bay (~3.5 ka), and the formation of modern Matakana Island (Shepherd et al., 1997). It is unknown whether the present day tidal inlets at either end of Matakana Island were already in place or formed subsequently. Most recently, extensive ebb and flood tidal deltas have formed at the northwestern and southeastern entrances of Tauranga Harbour. The oldest sediment within the ebb tidal delta at the Tauranga Harbour Entrance has been dated to 3.4 cal BP indicating

either timing of the formation of the delta or a period of extensive accretion (de Lange et al., 2015).

## 2.5. Hydrodynamics

Estuaries represent a coastal environment that act as a transitional zone between land and sea, and transport and trap marine and terrestrially derived nutrients, sediments, contaminants, and pollutants, through a combination of freshwater flows, winds, waves, and tides. Understanding the hydrodynamics operating within an estuary provides insight into the fate of inputs and exchanges of nutrients, sediment, contaminants, and pollutants, between the estuary and coastal zone (Tay et al., 2013).

The Tauranga Harbour is a barrier enclosed meso-tidal lagoon. Other examples of this type of estuary found along the New Zealand coast are commonly shallow with extensive mudflats, and are vertically well mixed and well flushed (Healy and Kirk 1982). The harbour has an area of 201 $km^{2,}$ with a tidal range from 1.2 – 1.9 m. The catchment of the southern basin covers an area of 1200 $km^2$ and contributions a mean annual inflow 30.5 $m^3$ $s^{-1}$, of which 17.6 $m^3$ $s^{-1}$ is derived from the Wairoa River (Santos et al., 2014). The average annual rainfall is 1100 mm (Chappell, 2013). In total, freshwater input is only 0.5% of the tidal prism volume, and 66% of the harbour is intertidal flats (Santos et al., 2014). The hydrodynamic processes operating within the Tauranga Harbour include: tidal currents, which dominate the harbour hydrodynamics; wind waves, which are important for entraining sediment over the intertidal flats; and storm surges, which have a reduced impact on the hydrodynamics (Davies-Colley and Healy, 1978).

### *2.5.1.* Tidal Currents

The observed tidal currents correspond closely to a standing tidal wave within the harbour. Peak currents are observed soon after the mid tides during both the flood and ebb. Overall, tidal currents in the southern basin have been proved to be more ebb dominant (Davies-Colley and Healy 1978). Tidal amplitude is quite consistent through the harbour, attenuating slightly within the inner harbour channel through the entrance, before amplifying slightly up harbour past Motuhoa Island (Tay et al.,

2013). Tidal currents have also been shown to increase in strength on windy days, more-so in shallower waters (<1 m). An increase of 10 cm $s^{-1}$ in tidal currents was recorded on a windy day (40 km $h^{-1}$), in a water depth of 60 cm (Davies-Colley and Healy, 1978).

Five tidal constituents dominate the tidal currents: M2 (Principal Lunar Semidiurnal), S2 (Principal Solar Semidiurnal), N2 (Larger Lunar Elliptic Semidiurnal), K1 (Lunar Diurnal) and O1 (Lunar Diurnal). The M2 tide is the most dominant, contributing an amplitude of 0.69 m, the S2 and N2 are approximately the same at 0.05 m, the K1 is 0.03 m, and the O1 is 0.015 m. The other constituents are much smaller and so have very minimal influence on the tidal wave propagation (Tay et al., 2013).

### *2.5.2.* Wind Waves

The dominant winds within the Tauranga Harbour are westerlies in terms of both strength and frequency. The east-west fetch is the longest in the basin and so the largest wind waves are generated on the eastern harbour shore. However, winds are relatively small, exceeding 45 cm only 2% of the time, though waves as high as 1 m have been noted on the eastern end of the Western Channel. Considering the impact wind waves have, orbital velocities are only sufficient to entrain sediment in shallow water (e.g. shallower than 1 – 1.5 m). Thus, the effect of wind waves is highly dependent on the tidal phase, and they only play a significant role on the intertidal flats or along shorelines (Davies-Colley and Healy, 1978).

### *2.5.3.* Storm Surge

Surges are often the result of storms as a consequence of a combination in change to air pressure and wind set-up. In the Bay of Plenty, storm surges are generated by the clockwise revolving storms (Hay et al., 1991) and can occur as positive surges (occur when a there is a fall in atmospheric pressure and onshore or longshore winds that keep coast on their left are present) or negative surges (occur where there is an increase in atmospheric pressure and offshore or longshore winds that keep the coast on their right are present). Variability in storm surges has been partially linked to the seasonal El Nino-Southern Oscillation (ENSO) and the Inter-Decadal Pacific

Oscillation (IPO) (de Lange and Gibb, 2000). It is notable that storm surges along New Zealand are not considered a major hazard, and those generated are often several magnitudes smaller than storm surges that occur in the Tropics where atmospheric fluctuations are much greater (Heath, 1979).

### *2.5.4.* Residence Times, Salinity and Temperature

#### *2.5.4.1. Residence Times*

Residence Time can be defined as the amount of time a parcel of water spends within a specified location before departing. Studies have found that the harbour is well flushed, with residence times of 2 to 4 days found near the harbour mouth and within the Western Channel (*Table 2.2*). Moving away from the harbour mouth, residence times increase, with much higher residence times found in sub-estuaries with constricted entrances. The highest residence times identified were at Rangataua and Welcome Bays, where residence times up to 7.8 and 8.2 days were identified respectively. Residence times are controlled strongly by the residual circulation patterns in the Tauranga Harbour, which was found to be highly channelized with the strongest currents occurring at the harbour mouth, and can be affected by strong winds during storm events (Tay et al., 2013).

#### *2.5.4.2. Salinity Gradient*

A salinity gradient can be identified through the harbour, with three distinct regions identified: just inside the harbour entrance: Western Channel to the Omokoroa Peninsula; and above the Omokoroa Peninsula. During a flood tide, marine water flows over the intertidal flats, and subsequently during the early ebb tide, water drains from the area. In the later stages of ebb and early stages of the flood, water is confined to the channels, and thus the highest salinities are observed within the channels when averaged over a tidal period (Tay et al., 2013). Stratification can occur with an increased freshwater discharge from the Wairoa River. The maximum salinity gradient is found to occur around 3 km from the river mouth, while a reduction in salinity can be noted up to 5 km from the river mouth. Following high discharge events, the harbour takes three to five tidal cycles to mix the freshwater into the estuary and return to the average salinity gradient (Tay et al., 2013).

***Table.2.2: Average modelled residence times of sub-estuaries in the southern basin of Tauranga Harbour. Sc. = Scenario. Sc. 0 = Base case, Sc. 1 = No wind conditions, Sc. 2 = Storm winds 11 m s-1 from 100o in winter, Sc. 3 = Storm winds 11 m s-1 from 100o in summer, Sc. 4 = Storm winds 11 m s-1 from 230o in winter, Sc. 5 = Storm winds 11 m s-1 from 230o in summer, and Sc. 6 = high freshwater discharge from Wairoa River 540 m3 s-1. Bolded sub-estuaries mark those exposed to central channels while unbolded estuaries have more constricted entrances. Data adapted from Tay et al. (2013).***

| | **Average Residence Times (Day)** | | | | | |
|---|---|---|---|---|---|---|
| **Sub-Estuary** | **Sc. 0** | **Sc. 1** | **Sc. 2** | **Sc. 3** | **Sc. 4** | **Sc. 5** |
| ***Waipu Bay*** | ***4.8*** | ***4.3*** | ***2.8*** | ***3.2*** | ***3.1*** | ***3.7*** |
| Rangataua Bay | 7.8 | 7.1 | 3.6 | 4.1 | 4.1 | 5.2 |
| Welcome Bay | 8.2 | 7.4 | 3.5 | 4.1 | 4.0 | 5.2 |
| Waimapu Estuary | 6.4 | 6.1 | 4.0 | 4.8 | 4.0 | 4.9 |
| Waikareao Estuary | 6.3 | 5.9 | 4.6 | 5.7 | 4.4 | 5.4 |
| ***Wairoa River Mouth*** | ***4.7*** | ***4.3*** | ***2.4*** | ***3.1*** | ***2.6*** | ***3.8*** |
| Te Puna Estuary | 7.4 | 7.3 | 6.1 | 7.9 | 5.1 | 6.5 |
| Waikaraka Estuary | 7.2 | 7.0 | 5.4 | 6.8 | 4.6 | 5.7 |
| ***Deep Channel South*** | ***3.1*** | ***2.9*** | ***1.7*** | ***1.9*** | ***2.0*** | ***2.4*** |

#### *2.5.4.3. Temperature*

Temperature within the harbour, unlike salinity is highly sensitive to solar flux and wind mixing throughout the harbour as opposed to the state of the tides, and varies diurnally. Under calm conditions, water temperatures is generally >22 $^{o}$C, while under windy conditions water temperature ranges 18 – 22 $^{o}$C. Winds lower water temperature through either heat transfer at the surface due to radiative transfer, and evaporative and sensible heat loss, or enhanced mixing, increasing surface current speed and cause a more effective change in heat. Diurnal temperature differences have been identified at Omokoroa with higher water temperatures identified with the ebb tide. Higher temperature may be due to the water heating of shallow tidal flats with the heated water then passing the Peninsula with the ebb tide. Finally, the Wairoa River subestuary has also been found to change temperature during large flood events, similar to how the salinity regime altered. Essentially, the freshwater plume was on average 4 $^{o}$C colder than the average harbour conditions (Tay et al., 2013).

## 2.6. Sedimentation Studies

Previous research into sedimentation patterns through the Tauranga Harbour has been quite limited. Existing research can be categorised into: (a) research focused on sedimentation around the Tauranga Harbour Inlet, (b) research looking at the yields and distribution of catchment derived sediment, and (c) research into alternate sources of sediment such as cliff erosion.

### *2.6.1.* Tauranga Harbour Inlet

The recent evolution of the Tauranga Harbour inlet can be evaluated by comparing hydrographic charts starting with the first available chart of the Tauranga harbour entrance dated 1852 (Brannigan, 2009), as seen in *Figure 2.3*. In 1852, the inlet is shown to be both wider and shallower relative to today. By 1879, the inlet has deepened by 6 m, though no change in the width is observed. However, by 1954, the inlet has narrowed significantly (~300 m) and the flood tidal delta has increased in size and shoaled considerably (de Lange et al., 2015).

Dredging of the harbour entrance was first undertaken in 1968, with a further capital dredging to enlarge the channels in 1992. Since 1992 the main shipping channel has been maintained at 14.1 m below chart datum (Kruger et al., 2006). Overall, it is difficult to distinguish the effects dredging has had on the ebb tidal delta from the natural channel migration and associated erosion and accretion that has occurred since 1852. Most evidently, a weakening of the ebb jet has been noted since 1968 reducing the tidal flow and increasing ocean driven wave processes. The weakening ebb jet has caused accretion along the Matakana Island shoreline, where it had previously been spread over the western platform of the ebb tidal delta (de Lange et al., 2015).

*Figure 2.4* shows the grain size composition of sediment sampled around the Tauranga Harbour Inlet. Most of the sites are unimodal, though four sites (III, IV, VII, 17) indicate bimodality, all of which occur within deeper tidal channels. All the sites show sands as the dominant grain size, though the bimodal sites also contain the second mode as gravel, attributed to shells and a small proportion of pumices and rhyolitic fragments (Davies-Colley et al., 1978). A contour map of the mean grainsize distribution (*Figure 2.5a*) shows that the coarsest material is found

at the channel entrance. Moving away from the inlet, both inside and outside the harbour a decrease in the mean grainsize is observed. Correspondingly, sorting (*Figure 2.5b*) is the poorest within the inlet channel and improves away from the inlet. Thus a correlation can be drawn between the grainsize and sorting around the tidal inlet (Davies-Colley et al., 1978).

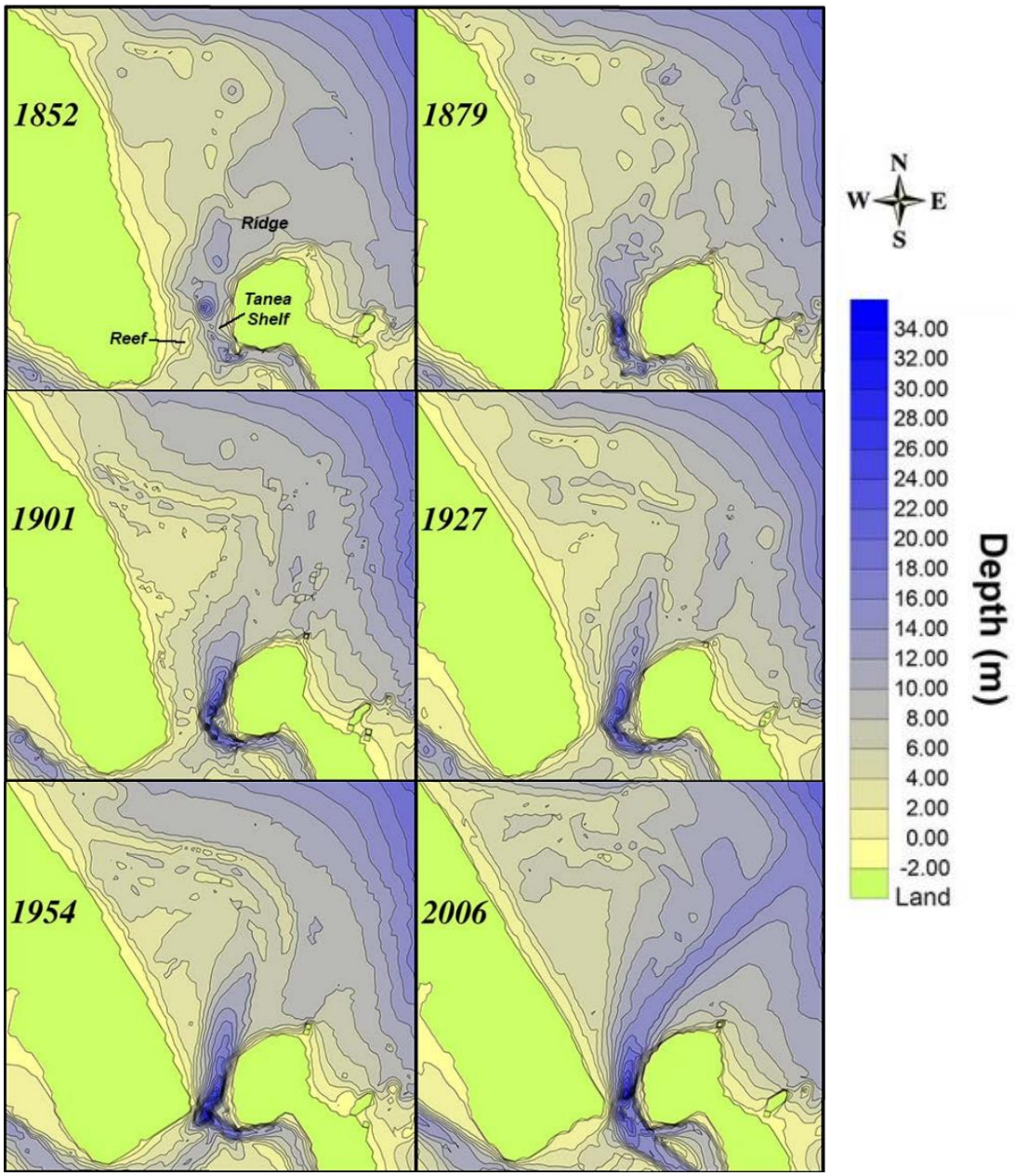


***Figure.2.3: Bathymetry of the ebb tidal delta and the tidal inlet. The data show the progressive narrowing and deepening of the tidal inlet associated with the progradation of Panapane Pt, and the changing morphology of the ebb tidal delta between 1852 and 1954. From de Lange et al., 2015***

Additionally, extensive sampling of the harbour was undertaken as part of the Tauranga Harbour Study (Healy, 1985). Sampling covered the tidal inlet, the main shipping channel, and the Western Channel as far as western Rangiwaea Island. Ultimately, nine depositional facies were identified. Of particular note were the active sediment pathways, and shell lagged areas, which were found to correlate with strong currents and scouring action.

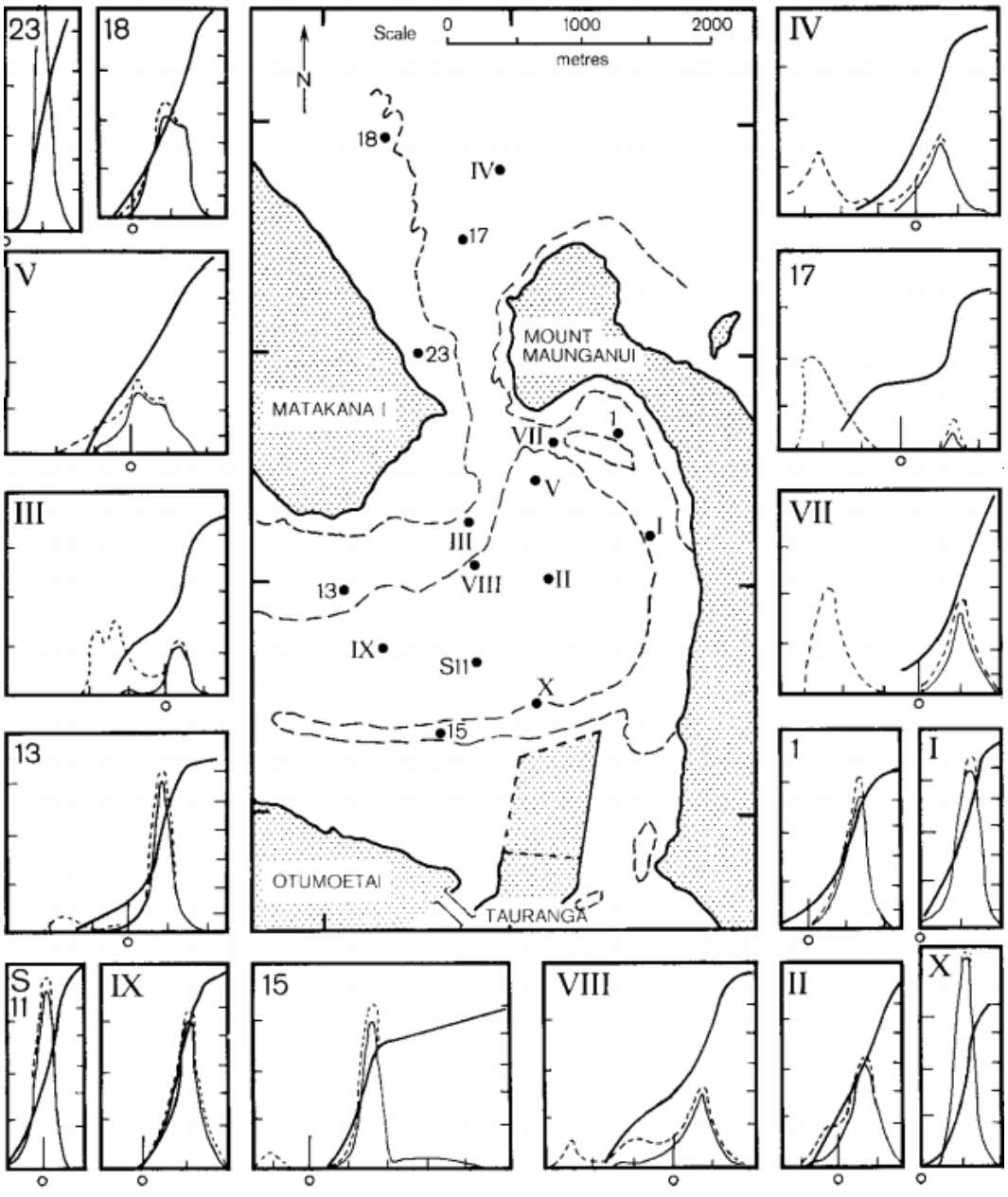


***Figure 02.4: Representative frequency grain size frequency curves around the Tauranga Basin Inlet. Three curves given for each site with (i) the dashed line showing percent by weight frequency curve for the total sample, (ii) the solid line showing frequency for the acid insoluble fraction, and (iii) the cumulative line showing cumulative percent by weight frequency curve for the acid-insoluble fraction. Taken from Davies-Colley et al. (1978)***

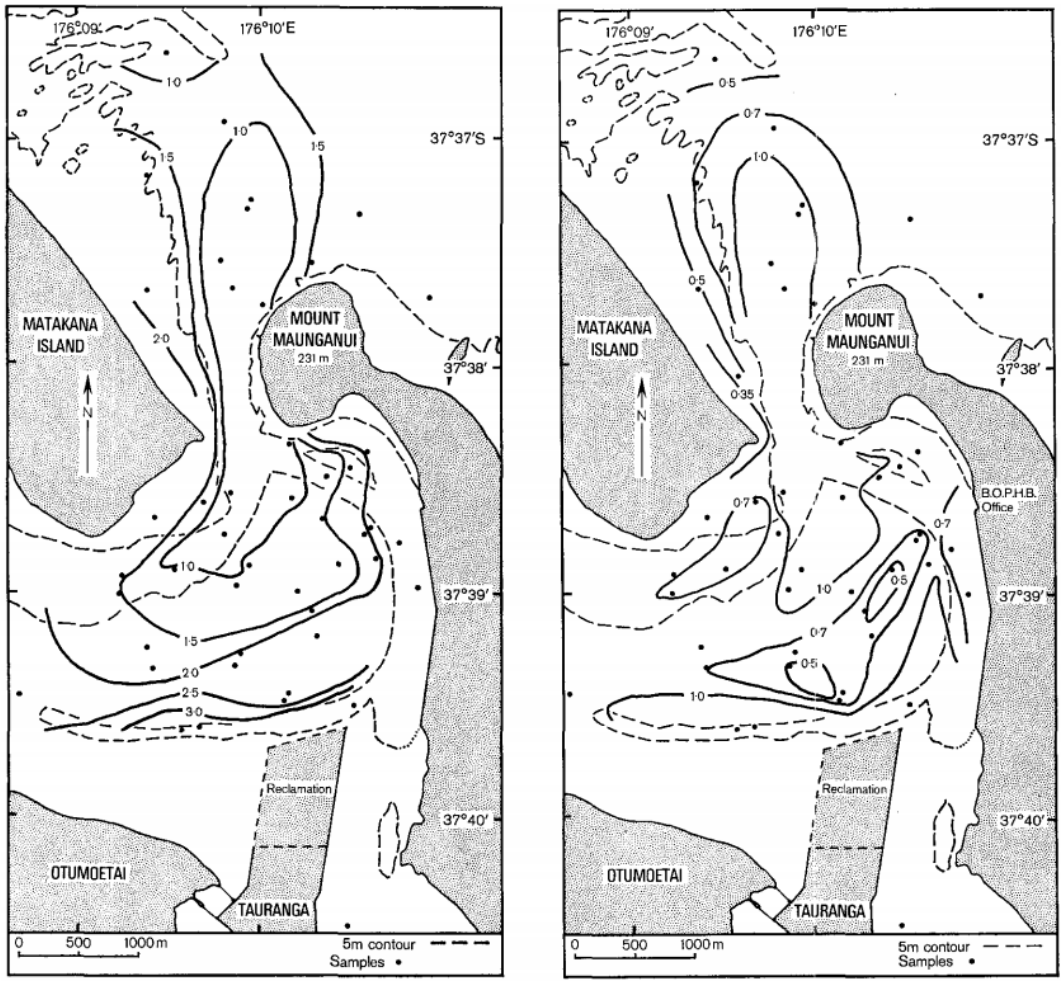


***Figure 2.5: Contour map of (a) mean grain size and (b) sorting of non-carbonate materials. From Davies-Colley et al. (1978)***

### *2.6.2.* Catchment Sediment Studies

Catchment studies have received the greatest amount of attention in sedimentation studies focusing on the Tauranga Harbour. Notably, these include a Tauranga Harbour Sediment Source Survey published in 1999 (Surman et al., 1999), and a NIWA led project Tauranga Harbour Sediment Study (THSS) published in 2009. While the Surman et al. (1999) study looked at the sediment yield of 23 catchments flowing into the Tauranga Harbour, the THSS covered a much greater scope, published into six modules: **Module A (Specification of Scenarios)** – establishing land use and weather information for models (Parshotam et al., 2008), **Module B (Catchment Sediment Modelling)** – modelling catchment runoff under present and future scenarios, and providing sediment yields into the harbour (Parshotam et al., 2009; Elliot et al., 2009), **Module C (Harbour Bed Sediments)** – a look into

grainsize compositions in the harbour and sedimentation rates over the last 50 years (Hancock et al., 2009), **Module D (Harbour Modelling)** – modelling the dispersal and deposition of sediment though the harbour (Pritchard and Gorman, 2009), **Module E: USC-3 Model** – linking sediment catchment sources with sediment estuarine sinks, (Green, 2009a; Green 2009b), and **Module F (Assessment of Predictions For Management)** – a synthesis on the modelling results (Hume et al., 2009).

### *2.6.2.1. Study Comparisons*

The THSS involved separating the Harbour into subcatchments and subestuaries (*Figure 2.6 and Table 2.3*). On a 1:50,000 scale, 73 streams have been mapped that discharge into the Tauranga Harbour. The Surman et al. (1999) study looked at 15 catchments flowing into the southern basin, while the THSS looked at 17 catchments. While there are many catchments that did not appear in either study, eleven were measured in both (Waitoa, Katemako, Waimapu, Kopurereua, Wairoa, Te Puna, Mangawhai, Waipapa, Apata, Wainui, Aongatete.). The importance of these catchments is that all have significant sediment yields, each contributing over 1,000 t/yr of sediment, and collectively constitute 94% of the catchment area.

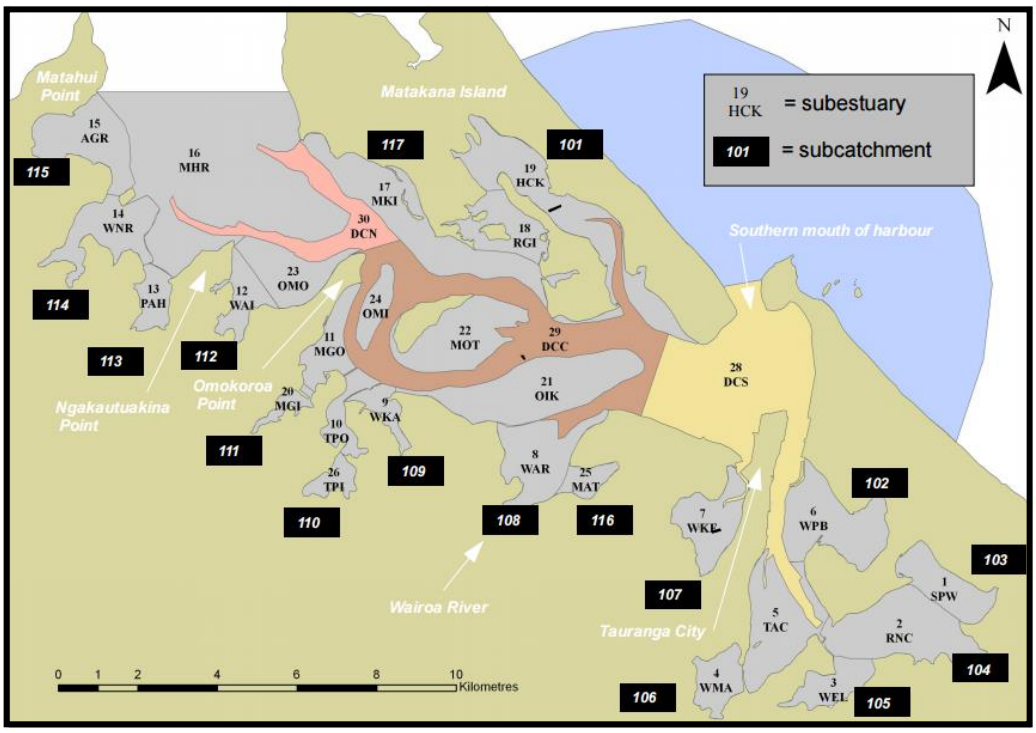


***Figure 02.6: Subdivision of the southern Tauranga Harbour into subestuaries and the association of subcatchments with subestuaries. The black numbers mark subestuaries. The white numbers in the black boxes mark subcatchments. From Hume et al. (2009).***

***Table 2.3: THSS subestuary and subcatchment identification. Adapted from Hume et al. (2009).***

| . Code | Subestuary | Code | Subcatchment |
|---|---|---|---|
| 1 | *Speedway* | 101 | *Matakana 1* |
| 2 | *Rangataua* | 102 | *Mount Manganui* |
| 3 | *Welcome Bay* | 103 | *Papamoa* |
| 4 | *Waimapu* | 104 | *Waitao* |
| 5 | *Tauranga City Foreshore* | 105 | *Kaitemako* |
| 6 | *Waipu Bay* | 106 | *Waimapu* |
| 7 | *Waikareao* | 107 | *Kopurererua* |
| 8 | *Mouth of Wairoa River* | 108 | *Wairoa* |
| 9 | *Waikaraka River* | 109 | *Oturu* |
| 10 | *Te Puna (outer)* | 110 | *Te Puna* |
| 11 | *Mangawhai Bay (outer)* | 111 | *Mangawhai* |
| 12 | *Mouth of Waipapa River* | 112 | *Waipapa* |
| 13 | *Pahoia Beach Road* | 113 | *Apata* |
| 14 | *Mouth of Wainui River* | 114 | *Wainui* |
| 15 | *Mouth of Aongatete River* | 115 | *Aongatete* |
| 16 | *Middle Harbour Sandbanks* | 116 | *Matua* |
| 17 | *Matakana Island* | 117 | *Matakana 2* |
| 18 | *Rangiwaea Island* | | |
| 19 | *Hunters Creek* | | |
| 20 | *Mangawhai Bay (inner)* | | |
| 21 | *Okimoke Point* | | |
| 22 | *Sandbank east of Motuhoa Island* | | |
| 23 | *Matua* | | |
| 24 | *West of Omokoroa Peninsula* | | |
| 25 | *Matua* | | |
| 26 | *Te Puna (inner)* | | |
| 27 | *Ocean* | | |
| 28 | *Deep Channel South* | | |
| 29 | *Deep Channel Central* | | |
| 30 | *Deep Channel North* | | |

#### *2.6.2.2. Sediment Distribution*

The sediment yield of each sub catchment was calculated and the distribution of sediment from each catchment was modelled (*Figure 2.8 and Table 2.4*). The THSS identified two sedimentation patterns:

(I) *Sediment contributing to active sedimentation is more-or-less confined to where it enters the harbour*. The only exceptions to this are the Wairoa, Waimapu, and Matakana 2 catchments, which have a much broader distribution of sediment. The Wairoa catchment has the highest discharge into the estuary and so the sediment is deposited much farther into the harbour and so redistributed by channel currents. The Matakana 2 catchment meanwhile deposits into an exposed subestuary and so tidal currents easily redistribute sediment. Finally, Waimapu is the second largest catchment interacting with the Tauranga Harbour and thus, similar to Wairoa has a broad distribution in the enclosed bay in the southeast where it provides sediment to all the subcatchments present.

(I) *Most of the sediment entering the central portion of the estuary is exported out to sea*. Ten of the subcatchments have <50% of sediment deposited out to sea, while 7 have >50% sediment deposit out to sea. Those which have a high percentage taken out to sea fit one of two criteria. They either have a high discharge that transports sediment into the centre of the harbour where wave and current reworking mobilizes the sediment and transports it out (Waitoa, Kopurereua, Wairoa, Waipapa), or the subestuaries are sufficiently open and exposed so that easily mobilized by waves and tidal currents and then transported out by the ebb tide (Mount Manganui, Matua, Matakana 2)

*Table 2.4: Summary statistics of catchment sediment supply to the Tauranga Harbour. Adapted from Hume et al. (2009)*

| Subcatchment Number | Subcatchment Name | Relative Catchment Area (%) | Sediment Yield (t/yr) | Relative Sediment Yields (%) | Fine Sediment that reaches ocean (%) |
|---|---|---|---|---|---|
| 101 | Matakana 1 | 1.42 | 53.14 | 0.05 | 42 |
| 102 | Mount Manganui | 1.31 | 329.69 | 0.34 | 87 |
| 103 | Papamoa | 1.119 | 275.05 | 0.28 | 15 |
| 104 | Waitoa | 4.36 | 7160.30 | 7.38 | 67 |
| 105 | Katemako | 2 | 1776.82 | 1.83 | 23 |
| 106 | Waimapu | 11.9 | 14649.81 | 15.11 | 42 |
| 107 | Kopurereua | 7.93 | 7302.39 | 7.53 | 80 |
| 108 | Wairoa | 46.83 | 44783.56 | 45.56 | 95 |
| 109 | Oturu | 1.17 | 390.13 | 0.40 | 26 |
| 110 | Te Puna | 2.82 | 3819.76 | 3.94 | 26 |
| 111 | Mangawhai | 1.97 | 1123.50 | 1.16 | 41 |
| 112 | Waipapa | 3.7 | 4228.39 | 4.36 | 53 |
| 113 | Apata | 1.25 | 2682.53 | 2.77 | 41 |
| 114 | Wainui | 3.54 | 4433.31 | 4.57 | 32 |
| 115 | Aongatete | 7.9 | 4068.93 | 4.20 | 40 |
| 116 | Matua | 0.96 | 225.35 | 0.23 | 64 |
| 117 | Matakana 2 | 0.75 | 278.71 | 0.29 | 88 |

### *2.6.2.3. Rate of Sedimentation*

The THSS calculated rates of sedimentation at four sites through the harbour (*Table 2.5*). The range of sedimentation rates they calculated was 0.75 – 1.57 mm/yr. Two factors were found that correlated with the rates of sedimentation: firstly, how exposed the location was to the open channel currents; and secondly what the dominant grain size was (*Figure 2.7*). Two sites with sedimentation rates <1 mm/yr are found in relatively sheltered bays and accrete with primarily fine sediment. Conversely, the two sites with greater rates of sedimentation (>1.3 mm/yr) are found in exposed subestuaries, and a much coarser grain size is present. Specifically, the Te Hopai subestuary is found on the edge of a channel and experiences the greatest calculated rates of sedimentation. The phenomenon can be attributed to flood dominance at the tidal flats. The channel effectively deposits sand at the site, while a reducing silt composition marks increasing fine sediment resuspension through wind waves and export with the ebb currents.

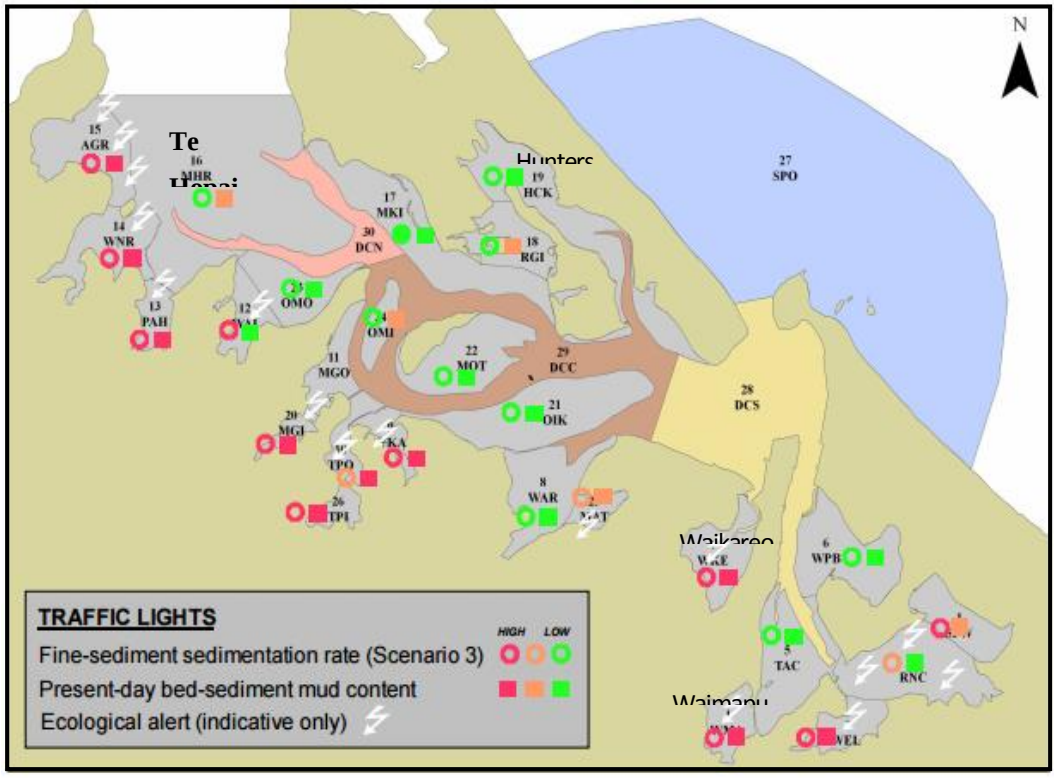


***Figure 2.7: Fine sedimentation rates and composition at each subestuary. From Hume et al. (2009).***

***Table 2.5: Sedimentation rates calculated at Waimapu, Waikareo Estuary, Te Hopai, and Hunters Creek by the THSS. Rate of sedimentation is presented along with the time period over which the rate was estimated (years). Estimated rates originally presented in Hancock et al. (2009).***

| Subestuary | Site Number | mm/yr | Years |
|---|---|---|---|
| Waimapu | 4 | 0.75 | 90 |
| Waikareo Estuary | 7 | 0.90 | 58 |
| Te Hopai | 16 | 1.57 | 45 |
| Hunters Creek | 19 | 1.33 | 23 |

### *2.6.3.* Sand Sedimentation

Sedimentation through the central region of the harbour has been found to be accreting predominantly with sand sediments. The THSS found that terrestrial contribution of sediment to the harbour is silt dominated. However, examples have also shown that low sand yields can effectively fuel rapid coastal sedimentation. The Waipoa River, where the sand contribution is ~1% of the total sediment yield, supplies sufficient sand for the rapid accretion of the Poverty Bay shoreline (Kuehl et al., 2016). Other sources of sand sedimentation for the Tauranga Harbour have been suggested as driven by local erosion occurring within the harbour (Davies-Colley, 1978; MacGibbon et al. 2011). Evidence of erosion is observed throughout the harbour including via storm overwash of Matakana Island (Shepherd et al., 1997), cliff erosion with evidence from numerous coastal collapses including the Omokoroa Peninsula (Moon et al., 2015) and the Maungataupu Peninsula (Oliver, 1979), and episodic tsunami events. Furthermore, the presence of over 1000 erosion protection works throughout the harbour by 1992 showed a variety of attempts to protect sections of coastline from erosion (Herbst et al., 2002).

#### *2.6.3.1. Omokoroa Peninsula*

While a number of landslides have occurred within the Tauranga Harbour in recent times, extensive research has been conducted on the Bramley Drive landslide at the Omokoroa Peninsula, most recently by the University of Waikato. Monitoring rates of retreat has been ongoing since the major failure of 2011 (Garae, 2015; Moon et al., 2015), and attempts have been made to quantify the contribution of the landslide to sedimentation in the harbour existing. Retreat of the cliff face since the 1979

landslide (*Table 2.6*) found that between large scale events at 1979 and 2011, the cliff was stable and experienced minimal erosion, even developing an extensive vegetative cover. However, since 2011 significant rates of erosion have been occurring at the landslide.

***Table 2.6: Estimated scarp retreat and volumes for identified failure events. From Moon et al. (2015)***

| Date | Scarp Retreat (m) | Width (m) | Height (m) | Volume ($m^3$) | Recurrence Interval (Years) | Annual Exceedance Probability |
|---|---|---|---|---|---|---|
| August 1979 | 20 | 60 | 25 | 30,000 | 36 | 0.028 |
| Pre-March 2010 | 2 | 9 | 25 | 450 | 7.2 | 0.139 |
| 11 May 2011 | 6 | 45 | 25 | 6,750 | 12 | 0.083 |
| 26 April 2012 | 1.5 | 45 | 25 | 1,750 | 18 | 0.056 |
| 24 June 2012 | 1.5 | 45 | 25 | 1,750 | 9 | 0.111 |
| 24 June 2014 | 0.5 | 2 | 25 | 27 | 6 | 0.167 |

Christophers (2015) calculated sedimentation rates around the Omokoroa Peninsula through coring. The rates of sedimentation calculated varied from 0.00111 – 0.455mm/yr (*Figure 2.8)*, and two trends were discovered:

(I) Sedimentation rates are greater on the eastern side of the Peninsula

(II) Since AD 1970, rates have increased significantly in the northern portion of the Omokoroa domain.

Rates of sedimentation through the Holocene for the western side of the Peninsula ranged from 0.0011 – 0.00319 mm/yr, and on the eastern side of the Peninsula from 0.00445 – 0.0524, with the exception of the northern section accreting at 0.455 mm/yr. A grainsize analysis found that the coarsest sediment is found around the high tide mark and increasingly finer sediments are present heading offshore across the tidal flats. Sediment transport patterns for the western Peninsula indicate minimal sediment movement. The coincidence between the Bramley Drive Landslide and sand accretion occurring on the western side of the Peninsula, points to locally sourced sediment from the landslide. Along the eastern Peninsula, sediment transport pathways indicate a longterm southward transport, and sediment

composition again points to locally sourced sediment from marine erosion and mass wasting of cliffs.

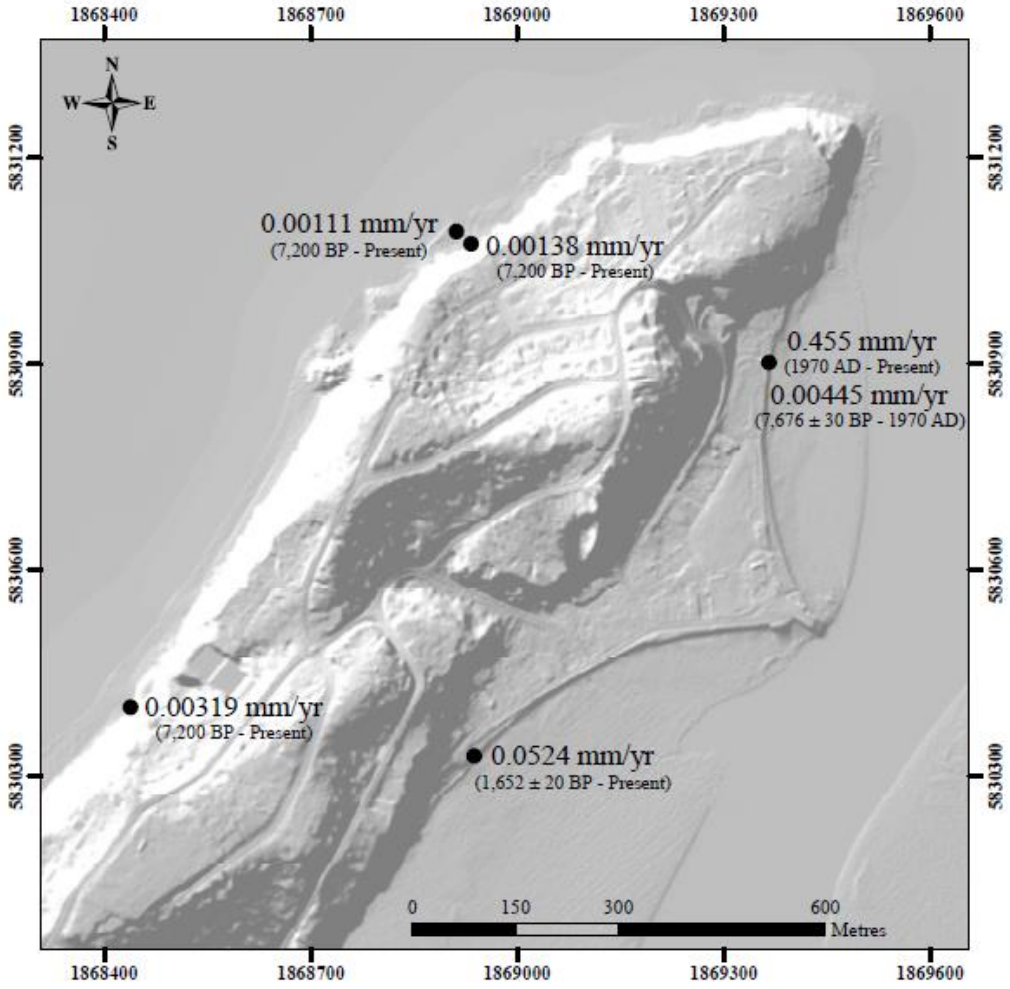


***Figure 2.8: Sedimentation rates calculated based on radiometric dates and inferred Holocene – Pleistocene Boundary. From Christophers (2015).***

### *2.6.3.2. Tsunami Erosion*

Tsunamis are a somewhat common event around New Zealand, with 12 to 13 >1 m events occurring every century around New Zealand. In the Bay of Plenty, there have been twelve tsunamis known to have affected the coastline since 1840 (Bell et al., 2004).

Evidence of two palaeo-tsunamis with major regional impacts, and four localised events occurring within the last 4000 years has been found. The two major events occurred 582 ± 66 cal y BP and at ~2.5 ka years BP. The more recent one is believed to have been caused by a submarine volcanic eruption (Mt Healy) and subsequent

caldera collapse, with the Loisels Pumice marking the deposit, in addition to truncated coastlines along of Matakana Island at the Purakau Shoreline (*Figure 2.9*), and three truncated coastlines on the western end (Bell et al., 2004; de Lange et al., 2015). Deposits for the older of the two events were found at Waihi Beach (Bell et al., 2004), and may correlate with deposits at Omokoroa dated at 1652 ± 20 cal y BP (Christophers, 2015) and next to the Wairoa River (Bell et al., 2004). The tsunami appears to have been confined within the Bay of Plenty and may be associated with a locally generated earthquake (de Lange et al., 2015). In addition to the large events, several smaller localised tsunami events have been identified through the Bay of Plenty including at; 2900-3000 years BP at Ohiwa Harbour, 1600-1700 years BP at eastern Papamoa, AD 1200 – AD 1300 at Waiotahi, and AD 1600 – AD 1700 at Kohika associated with a local subsidence event (Goff, 2002; Bell et al., 2004).

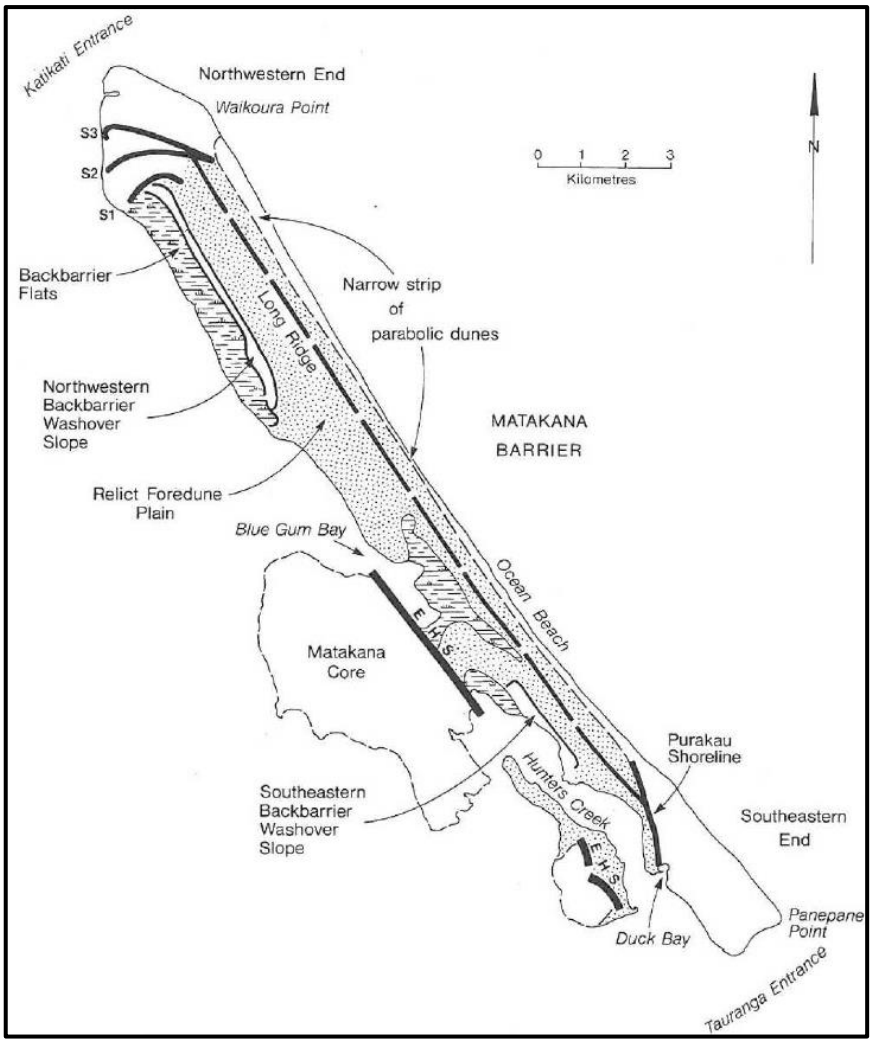


***Figure 2.9: Map of Matakana Barrier Island showing former landforms and shorelines. EHS = Early Holocene Shoreline, S1 and S2 = former eroded shorelines, S3 – Kaharoa Shoreline. From Shepherd et al., 1997***

de Lange et al. (2015) suggests that the rapid sedimentation changes that occurred at the Tauranga Harbour entrance between 1852 and 1879, may be partially a product of two Chilean Tsunami events in 1868 and 1877. While no contemporary evidence of scour from these events is found at the Tauranga Inlet, various estuaries around New Zealand provide evidence of scour from these events, as does evidence around Sulphur Point within the harbour.

## 2.7. Summary

- The Tauranga Harbour is a barrier enclosed meso-tidal lagoon found on the northeast coastline of New Zealand, confined by two Holocene tombolos and a barrier island. The Harbour is effectively split into two hydrodynamically independent basins by a shoal between Matahui and Tirohanga Points. Both basins of the harbour are actively infilling.
- Geologically, the Tauranga Harbour is found within the Tauranga Basin. The local basement is formed by the Waiteraiki Ignimbrite, which slopes northeastwards from the Kaimai Ranges into the harbour. The ignimbrite is overlain by a series of intercalated volcanic and sedimentary deposits. No faults have been previously identified through the harbour, but the northeast orientation of peninsulas and rivers suggest a series of deep-seated northeast-orientated faults.
- The Tauranga Harbour formed in the Holocene following the last glaciation and marine transgression. Upon modern day sea level establishment (7-7.75 ka), Matakana Island and the tidal inlet and delta systems developed.
- The hydrodynamics of the harbour are dominated by tidal currents and wind waves, with a tidal range of 1.2 – 1.9 m. The Wairoa River is the largest catchment draining into the harbour, though the total catchment freshwater input is minimal, comprising only 0.5% of the total tidal prism.
- Sedimentation research of the harbour has been minimal despite evidence of active infilling. Previous research has looked at inlet sedimentation, catchment input, and erosion around the shorelines.
    - Inlet studies have found active sedimentation in the form of sand, with smaller contributions of mostly biogenic gravel. The Tauranga

inlet has narrowed significantly between 1852 and the present, and the associated flood delta has shoaled considerably. Dredging of the main shipping channels has been ongoing since 1968 though the effects of dredging have been difficult to discern from the natural channel migration, and erosion and accretion patterns.

- Extensive research by NIWA on catchment sediment yields and distribution found terrestrial derived sediment to be either be deposited the harbour or transported out to sea depending on the sediment size and the processes operating with the subestuaries linked to each catchment. In contradiction to the expected impact of these factors, the calculated rates of sedimentation indicated that higher energy open subestuaries were accreting the fastest, while also containing higher sand compositions than low energy restricted subestuaries.
- Erosion is known to be actively operating around the shorelines of the harbour and has been suggested as a significant source of sediment. Erosional sources that have been suggested include storm overwash of the Matakana Island Barrier, erosion of coastal cliffs found throughout the Tauranga Harbour, and tsunami events, of which several impacting the Tauranga Harbour have been identified within the Holocene.

# CHAPTER 3
# SEISMIC SURVEY INTERPRETATION

## 3.1. Introduction

A seismic reflection survey was carried out in the Tauranga Harbour through the western channel to identify key stratigraphic formations at the sea floor and within the subsurface. This chapter is subdivided into; **3.2. Seismic Reflection** – an explanation of seismic mapping theory, **3.3. Methods** – covering the field seismic mapping procedure and subsequent laboratory interpretation, **3.4. Sedimentation Patterns** – a description of phenomenon marking variable sedimentation patterns, and an interpretation of where such phenomenon are observed through the Western Channel in the seismic, **3.5. Faulting Interpretation** – an interpretation of structural features indicating faulting through the western channel in the seismic, and **3.6. Summary** – where the key points of the chapter will be summarized.

## 3.2. Seismic Reflection

Seismic reflection utilizes a sound source that produces an acoustic pulse of a set frequency, power, and duration. The acoustic pulse travels through the water column and penetrates the sea floor. Some of the acoustic signal is reflected at the seafloor, while the remainder penetrates it. Beneath the surface, different layers have variable levels of acoustic impedance, Z, dependent on the wet bulk density, p, and the compressional velocity, c (*Equation 3.1*). Thus, at each layer met, part of the acoustic signal is reflected

$$Z = pc \qquad \textit{Equation 3.1}$$

The returning sound waves are recorded by an acoustic receiver (variable types of receivers depending on the type of system used). The receiver resolves the pulses of energy with signals from sallower reflections arriving first, thus forming a profile. The product is a continuous, real-time displayed, record of the bathymetry and the boundaries of subsurface strata (Penrose et al., 2005).

## 3.3. Methods

### *3.3.1.* Field Methods

A Knudsen Pinger Sub-Bottom Profiler was used to conduct the shallow seismic reflection for this research, operating on a chirp sonar system. Chirp sonar functions by generating wide band, frequency modulated pulses. These effectively allow the system to sweep through a band of frequencies, with the central band of the Knudsen Pinger Sub-Bottom Profiler at 3.5 kHz (*Figure 3.1*). With each returning band, an algorithm estimates attenuation of the sub-bottom reflections, by waveform matching with a theoretically attenuated waveform. The result is a continuous, real time displayed, record of the bathymetry and subsurface strata. Chirp systems are highly effective in soft sediments, capable of producing high resolution profiles, with resolutions down to ~5 cm (Schock et al., 1989; Penrose et al., 2005). The information was saved in individual 5 – 10 min long segments to simplify the analysis procedure. All results were processed through standard Knudsen software.

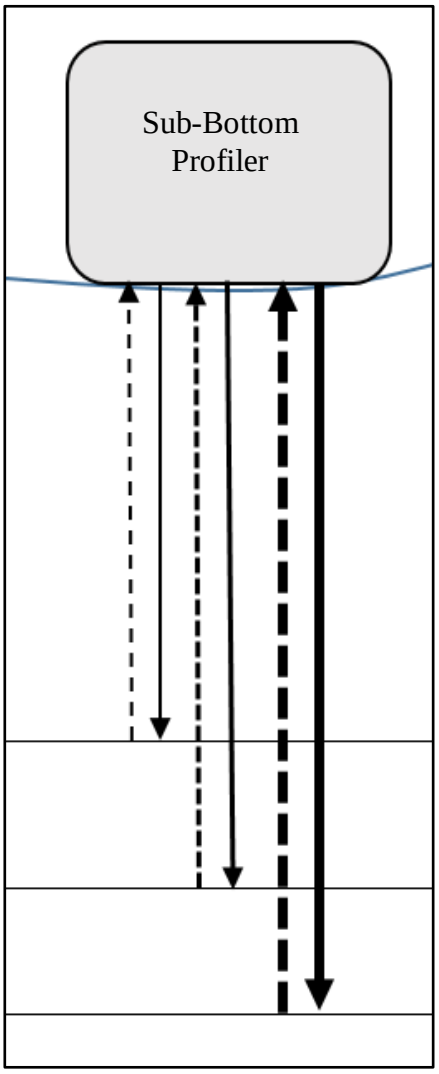


***Figure 3.1: Example of Seismic Reflection utilizing a chirp sonar system. Solid lines are emitted waves. and dashed are reflected***

The area of interest, the Western Channel of the Tauranga Harbour (*Figure 3.2*), was mapped from just south of Rangiwaea Island towards the northwest, approaching the tidal flats connecting Matakana Island to the mainland. A reverse route was also taken through the Western Channel from the northwest corner down to Rangiwaea Island, and then continued further to the southernmost tip of Matakana Island. A detour was taken midway through the reverse route around the eastern and western sides of the Omokoroa Peninsula, to obtain seismic data for a separate project.

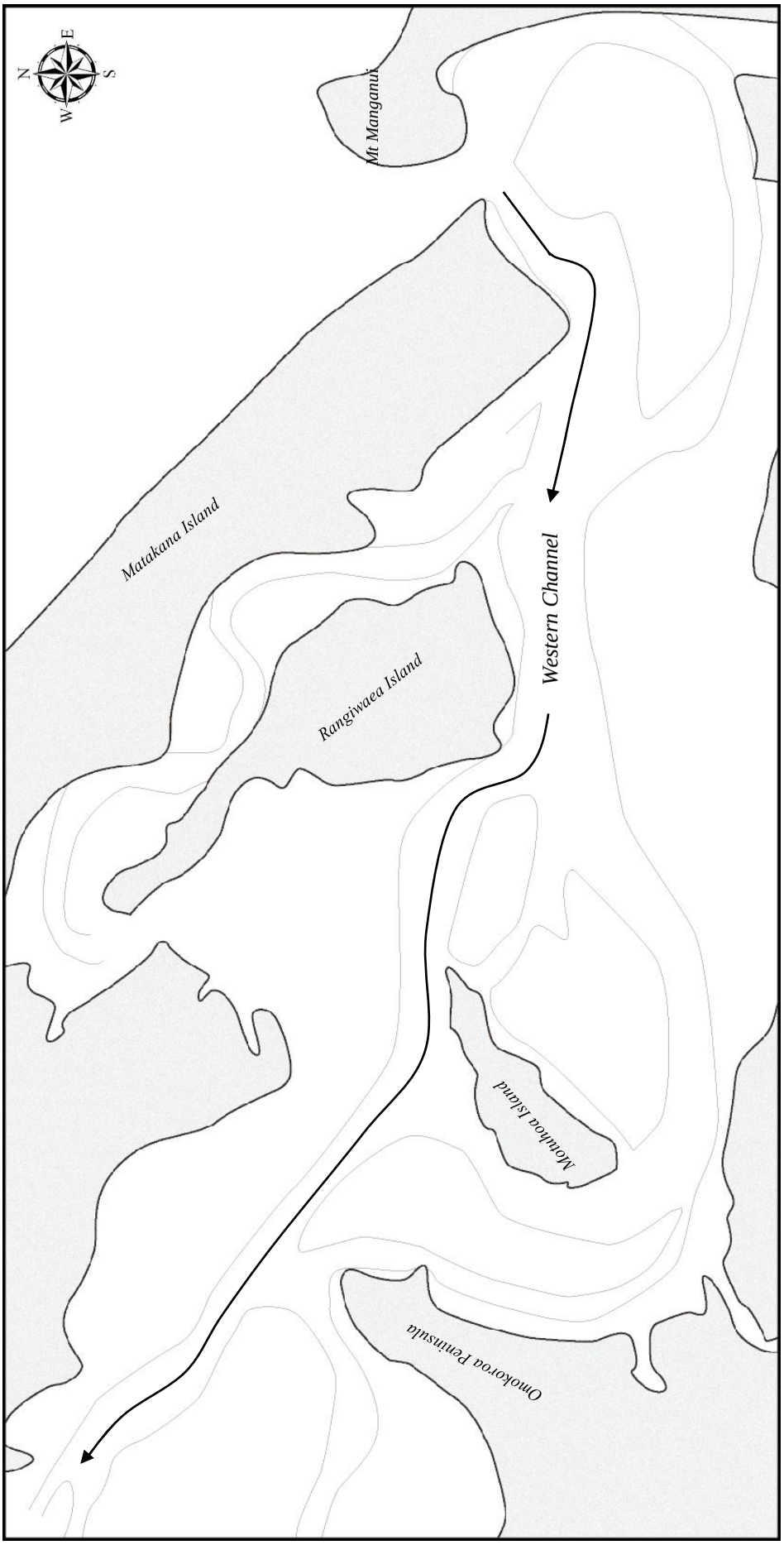


***Figure 3.2: Map of the field area. Matakana, Rangiwaea and Motuhoa Islands, and Omokoroa Peninsula are all labelled. The Western Channel is marked by a solid black line from the inlet and approaching the tidal flats***

### *3.3.2.* Laboratory Interpretation

The seismic data were stored as Knudsen KEB files and generic SGY files, and analysed using Knudsen PostSurvey software. Seismic data were obtained in continuous segments ranging from <100 m to ~1500 m in length. GPS tracking of the vessel allowed for the location of each ping to be recorded. These positions were used to plot the seismic segments within Google Earth. Analysis of the seismic segments involved identifying surface structures (e.g. changes to the general trend) and subsurface structures (e.g. variable trends to surface patterns), incorporating both digital and physical methods.

The seismic survey was split into three continuous segments of data. Transect I involved the initial route taken from the Rangiwaea Island to Matakana Point in the northwest (*Figure 3.3*), Transect II involved the first half of the reverse route from Matakana Point to the Omokoroa Peninsula (*Figure 3.4*), and Transect III involved the final route from Omokoroa Peninsula to the south tip of Matakana Island (*Figure 3.5*). A secondary analysis involved the transfer of surface and subsurface structures onto tracing paper, into continuous segments correlating to the three transects. Here the data could be analysed without the noise present in the raw data. Parallel transects were compared with one another (e.g. First half Transect I = Transect III, Second half Transect I = Transect II) to confirm phenomenon identified in one or the other transect.

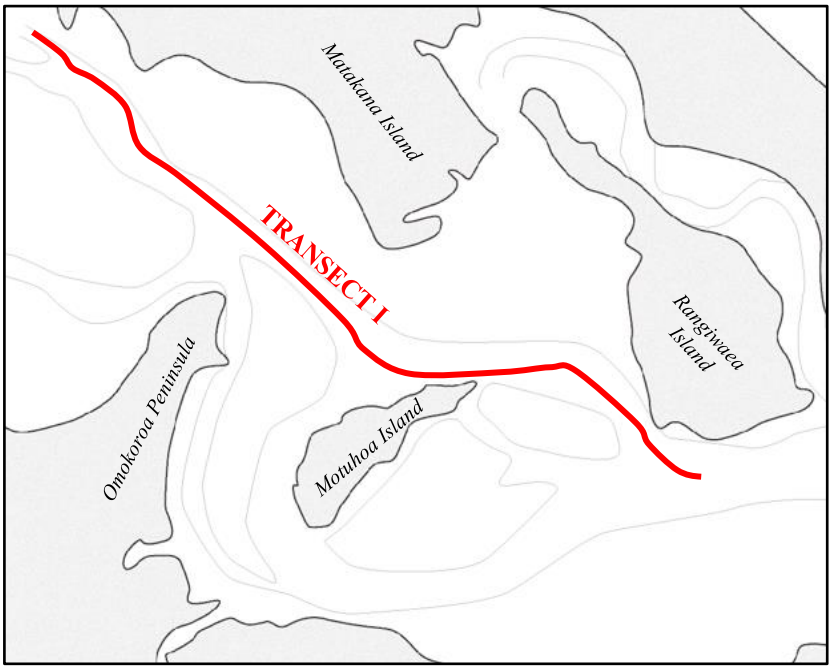


***Figure 3.3: Transect I of the seismic data consisting of the initial route from Rangiwaea Island to Matakana Point***

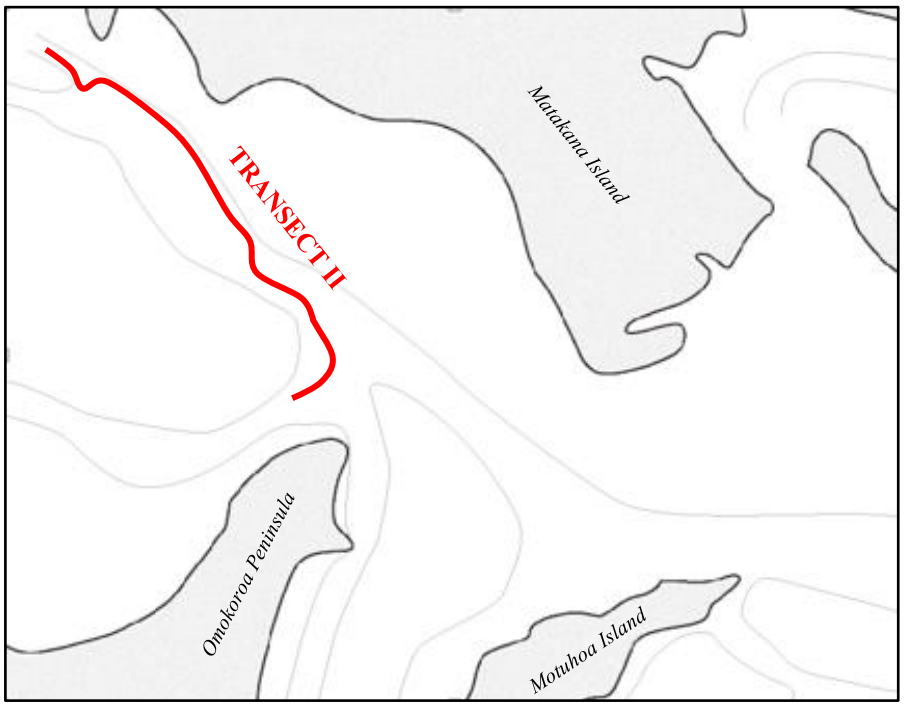


***Figure 3.4: Transect II of the seismic data, consisting of the first section of the reverse route from Matakana Point to just north of the Omokoroa Peninsula***

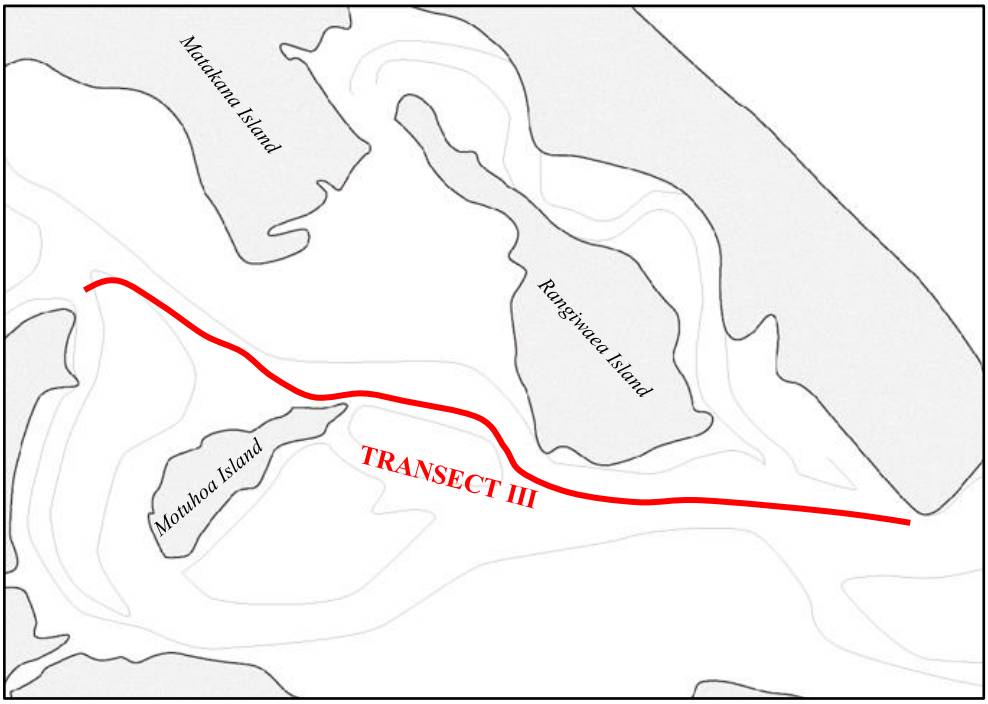


***Figure 3.5: Transect III of the seismic data, consisting of the second section of the reverse route from the Omokoroa Peninsula to the southernmost tip of Matakana Island***

## 3.4. Sedimentation Patterns

The first component of the seismic analysis concentrated on identifying sedimentation patterns found through the field area. This subsection will cover sandwaves, a phenomenon indicative of variable sedimentation patterns, where they can be found in the field area, and a brief interpretation on their occurrence through the field area.

### *3.4.1.* Sandwaves

Sediment transport within the Tauranga Harbour is dominated by tidal currents and transport occurs with both flood and ebb tide. As such, large bedforms are required to discern the net sedimentary transport pathways. Take for example that sediment moves with both the flood and ebb tidal currents and that small scale formations are caused as a consequence of this transport (Allen, 1980). However, when taking into account tidal asymmetry over the long term, formations created are more or less independent of the individual tides, and instead form consequently of net tidal difference and the fluctuations of wind and gravity induced currents (Bokuniewicz et al., 1977; Terwindt and Brouwer, 1986).

Sandwaves are large, flow traverse bedforms that form consequently of reversing tidal currents, and are a prime example of net sedimentary transport. They are frequently found in high energy environments where there are high levels of mobile sediment, and can be easily observed in seismic data (Bokuniewicz et al., 1977).

#### *3.4.1.1. Formation*

Individual sedimentary grains become mobilized when the flow velocity exceeds a critical threshold. Quantifying sediment mobility comes down to two key factors, the currents acting at a site, and the sedimentary composition:

(I) **Currents:** There are two types of currents that commonly mobilize sediments in estuaries; these are tidal currents and wind induced waves. Tidally generated residual currents are the main factor influencing sand sediment transport in estuaries. Residual currents themselves are primarily generated by the dominant tide. On the other hand, fine (mud)

sediment transport is controlled directly by tidal asymmetry (Liu and Aubrey, 1993; van de Kreeke and Hibma, 2004; Fiechter et al., 2006). Wind-waves meanwhile influence the hydrodynamics in shallow water environments where they can control the near surface shear. Waves mobilise sediments though orbital velocities, which decay exponentially with depth and so in deeper water waves will have minimal impact. However, in sufficiently shallow waters, wind-waves can have a significant influence on sedimentary transport (Soulsby, 1997, Hunt et al., 2015).

(II) **Sedimentary Composition:** Sandwaves have been shown to abruptly form or cease where no changes in the hydraulic regime are observed. Both excess levels (>15%) of coarse sediment (gravels) or fine sediments (silts) can inhibit sandwave formation. Coarser sediments require stronger currents to mobilise sediment due to a higher critical shear stress, so without a change to the hydrological regime, sediment is less likely to mobilise going up in grade size (Bokuniewicz et al., 1977). Fine sediments are meanwhile more complex, though the lack of sandwaves may be explained by (a) more sediment moving in suspension which doesn't contribute to sandwave formation (McCave, 1971), or (b) an increased cohesion of sands caused by the addition of fine sediments, thus featuring a higher critical shear stress and requiring stronger currents to be mobilised (Bokuniewicz et al., 1977).

#### *3.4.1.2. Morphology*

The key morphological features of a sandwave (*Figure 3.6*) include the wavelength $L$ (distance between troughs), the wave height $H$ (difference in elevation between trough and crest), $a$ (the long length of $L$ from trough to crest) and $\alpha$ (the corresponding angle from trough to crest), $b$ (the short length of $L$ from crest to trough) and $\beta$ (the corresponding angle between trough and crest). The steeper face of a sandwave indicates the direction of net sedimentary transport (e.g. a steeper eastern face indicates net transport east) (Terwindt, 1971; Ludwick, 1975; Bokuniewicz et al., 1977; Allen 1980).

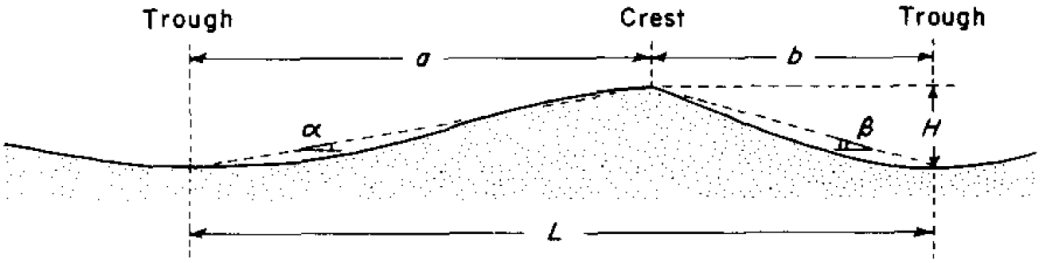


***Figure 3.6: Sandwave profile with principal morphological features and measurements labelled. From Allen (1980)***

Sediment supply will often determine the extent of the morphological features. An increased sediment supply results in longer and slightly sinuous crests, while a more a restricted sediment supply will commonly result in the formation of short and strongly angled sandwaves (Allen, 1980). Additionally, sandwave symmetry can be controlled by the tidal asymmetry, where a reduced tidal asymmetry will reduce net transport and form highly symmetrical sandwaves (McCave, 1971).

### *3.4.2.* Sandwaves Identified

Five sites were identified along the seismic profiles where sandwaves were observed (*Figure 3.7*). The locations are distributed through the western channel between Rangiwaea Island and Matakana Point. Sandwave Site 1 (SS1) occurs south of Rangiwaea Island, SS2 is northeast of Motuhoa Island, SS3 and SS4 are northeast and northwest of the Omokoroa Peninsula respectively, and SS5 is found just south of Matakana Point approaching the tidal flats. Three are located close to eroding cliffs (SS1, SS2, & SS5), and four are located at channel junctions (SS1, SS2, SS3 & SS4). Sandwave positions are then compared with modelled residual currents in *Figures 3.8* and *3.9*.

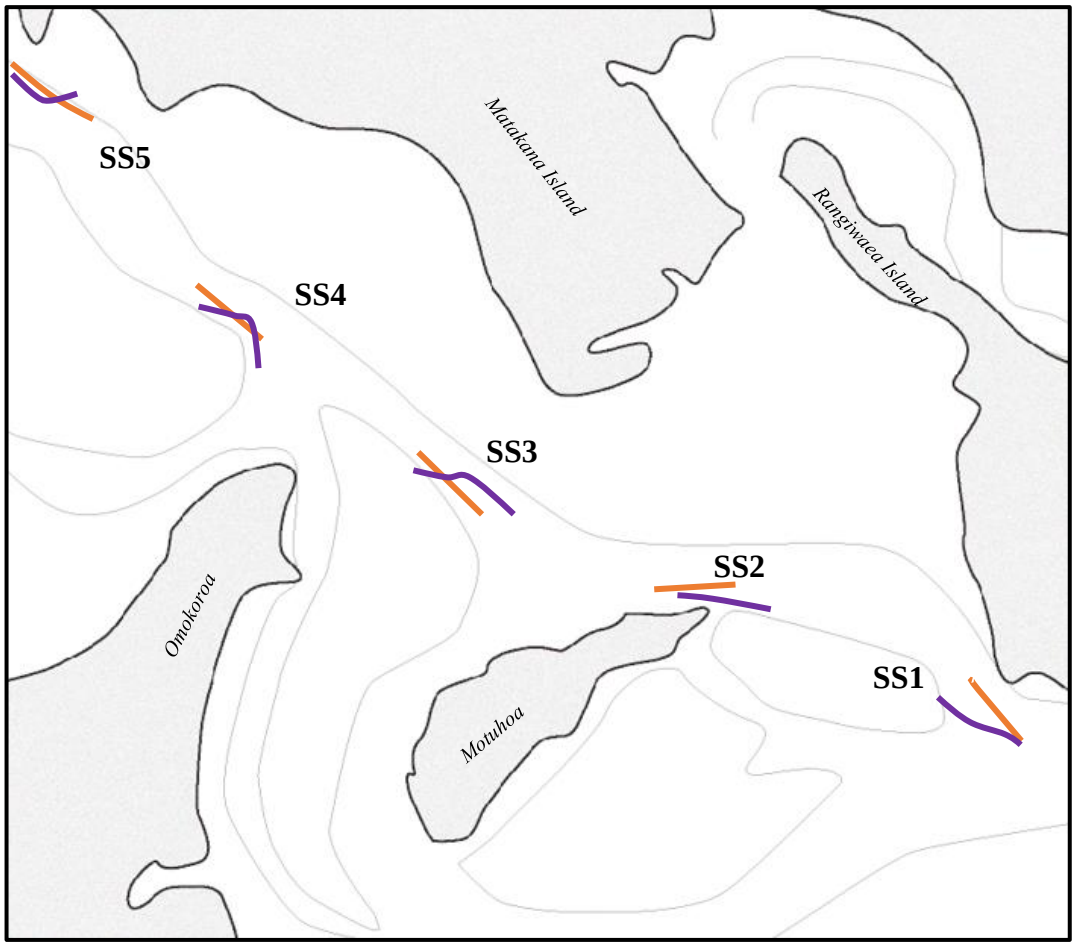


***Figure 3.7: Locations through the harbour where sandwaves have been identified in the seismic interpretation with the bold numbers marking the sites. The lines mark the respective profile length of each sandwave length, with the colours corresponding to the transects that the profiles are derived from; Orange = Transect I, Purple – Transects II & III.***

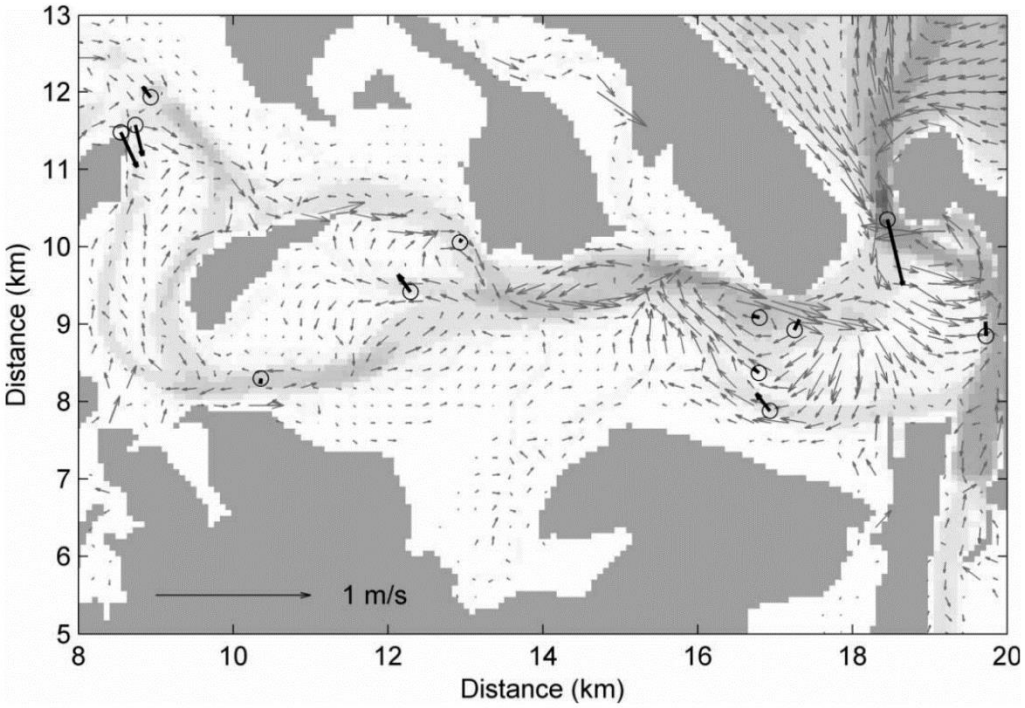


***Figure 3.8: Modelled residual current speed and direction calculated over a 28 day period. Black arrows with circles are the observed residual currents. From Tay et al. (2013).***

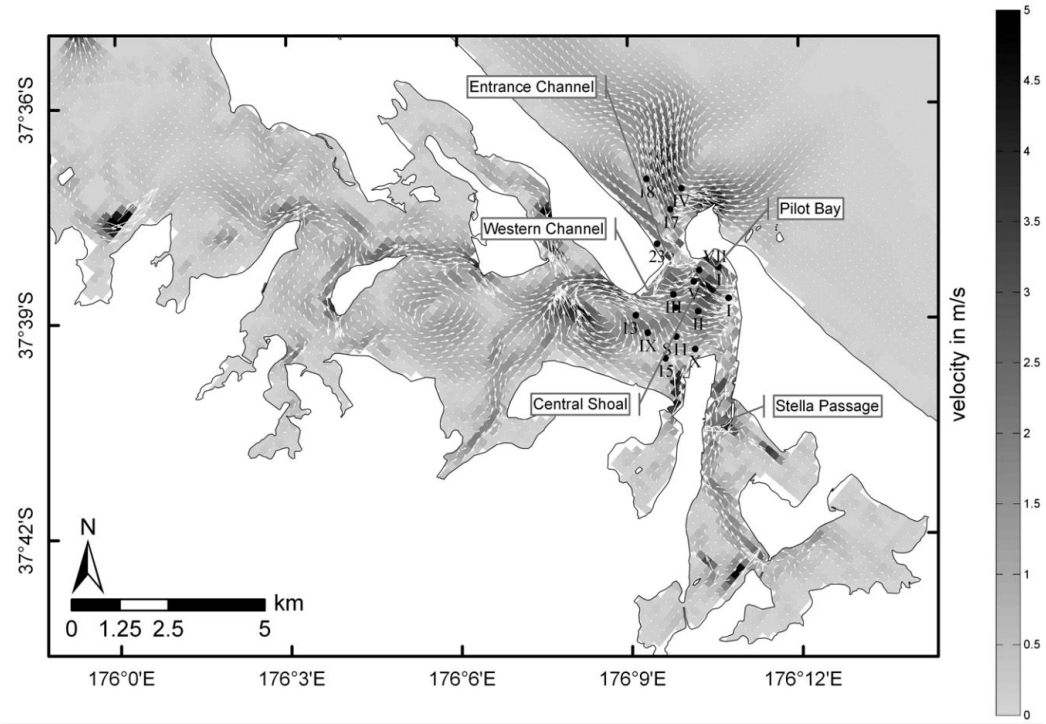


***Figure 3.9:Modelled residual velocity over two representative tidal cycles. The greyscale indicates velocity magnitude (m/s). Sample locations are indicated by black dots. From Kwoll and Winter (2011).***

**Sandwave Site 1**

SS1 occurs in the southeast corner of the field area, just south of the southernmost tip of Rangiwaea Island. The locale coincides with a fork in the Western Channel, where travelling up harbour sees the channel split into a west/northwest component (the continuation of the Western Channel and the field area) and a smaller south/southwest flowing component.

The seismic profiles for the site are derived from Transect I and Transect III, observed in *Figure 3.10*. Of the two profiles, slightly different routes are taken as Transect I passes by closer to Rangiwaea Island and the centre of the channel, while Transect III is found closer to the southern channel bank. Despite the small separation between transects, the slightly different routes exhibit entirely different sedimentation patterns. Mapped residual currents for the locations show a variable patterns operating within the channel (*Figures 3.7* and *3.8*).

***Sandwaves***

- Distinct differences are noted between the two profiles. While Transect I displays extensive sandwaves throughout the length of the profile, no sandwaves whatsoever are observed in Transect III. The variable sandwave pattern can be attributed to different flow patterns at the location, either side of the channel. The sandwaves present range in height from 3 m in the southeast to <1 m in the northwest. They are well defined, highly symmetrical structures, with a steeper southeastern face. Modelled residual currents show dominance to the southeast for the location, consistent with the observations. The seismic data indicate that the sandwaves occur in a deposit formed above a relatively flat resistant layer containing sub-parallel reflectors.

***Water Depth***

- Again, the two profiles show distinctly different patterns, with Transect I being deeper with greater vertical relief. The average water depth in Transect I is ~10.5 m, although the surface fluctuates throughout between 9 – 11.5 m. There appears to be a gradual shallowing from southeast to northwest in the profile. Transect III features an average water depth around 9.5 m, although the surface evidently deepens from southeast to northwest. An initial water depth of ~9 m in the southeast and ~10.5 m in the northwest depicts a reverse trend to that observed in Transect I.

(a)

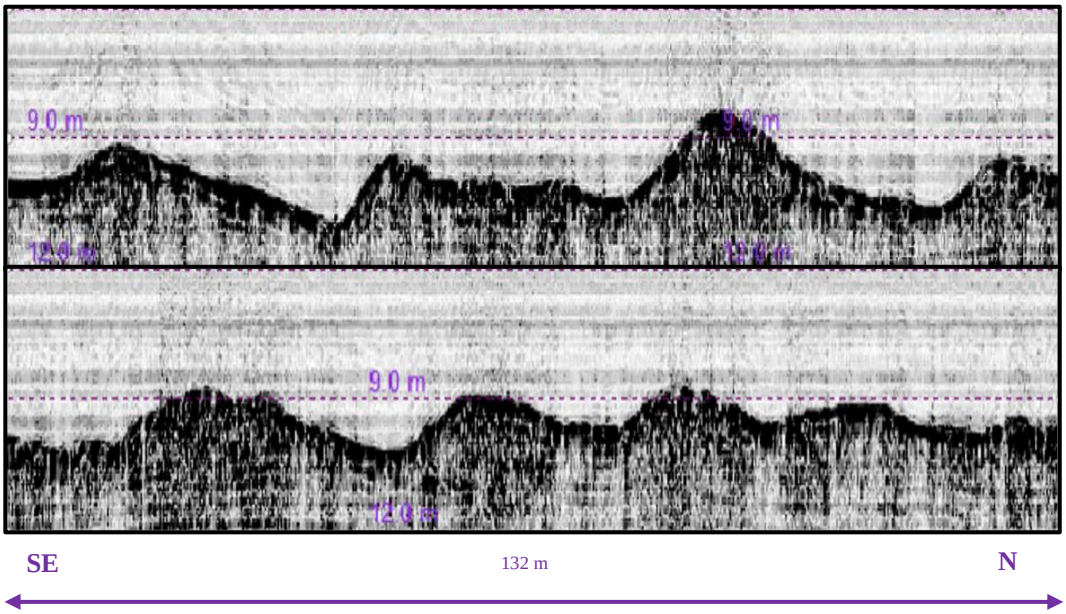


(b)

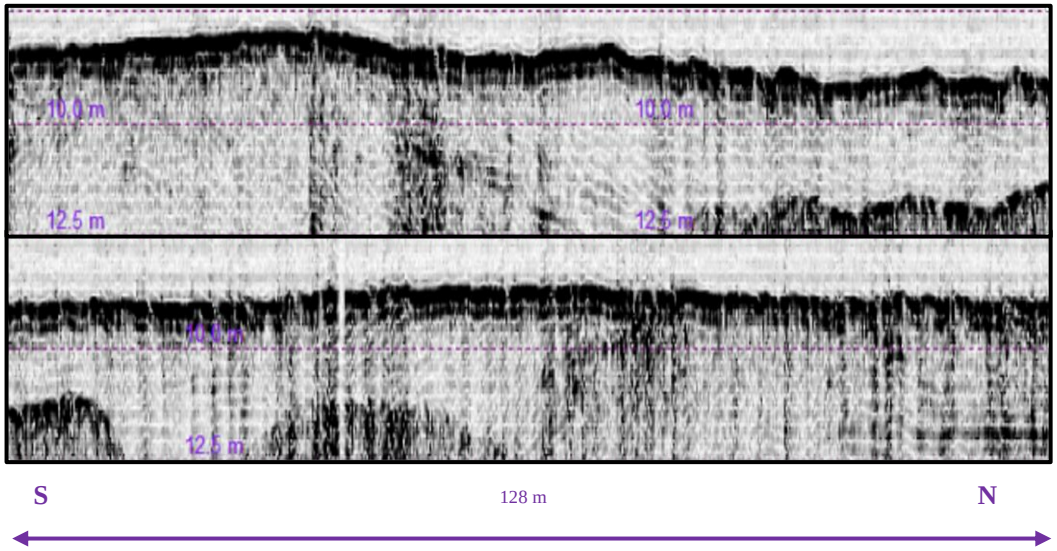


***Figure 3.10: Two seismic profiles taken at SS1. Both profiles are split into two halves, with the lower half continuing on the right of the upper half. For both profiles the left marks the southeastern side and the right the northwestern. (a) is sourced from Transect I with a total length of 264 m, (b) is sourced from Transect III with a total length of 255 m***

## Sandwave Site 2

SS2 is located north of Motuhoa Island where there is another observable fork in the Western Channel. Splitting into three channels, as two channels pass by either side of Motuhoa Island, while the largest component remains the westward flowing Western Channel.

The seismic profiles for the site (*Figure 3.11*) are derived from Transect I and Transect III. The two profiles take highly similar pathways through the channel, though Transect III passes slightly closer to Motuhoa Island. Modelled residual currents (*Figures 3.7* and *3.8*) show a dominant eastward flow, moving with the ebb tide

### *Sandwaves*

- Unlike SS1, both profiles show evidence of sandwaves although the sandwaves here are not as well defined as at SS1. Instead, they feature a small yet sharp rise, followed by a long gentle slope, with steeper eastern faces. The most pronounced sandwaves occur through the first half of Transect I. The sandwave orientations match with the modelled residual currents, suggesting net sedimentary transport with the ebb tide.

### *Water Depth*

- The water depth between the two profiles is noticeably different. In the top profile (i.e. Transect I) the water depth fluctuates around 6 m, while in the bottom profile the fluctuations occur around a 7.5 m depth. The difference in water depth is attributed to the positioning of the two profiles in the channel.

(a)

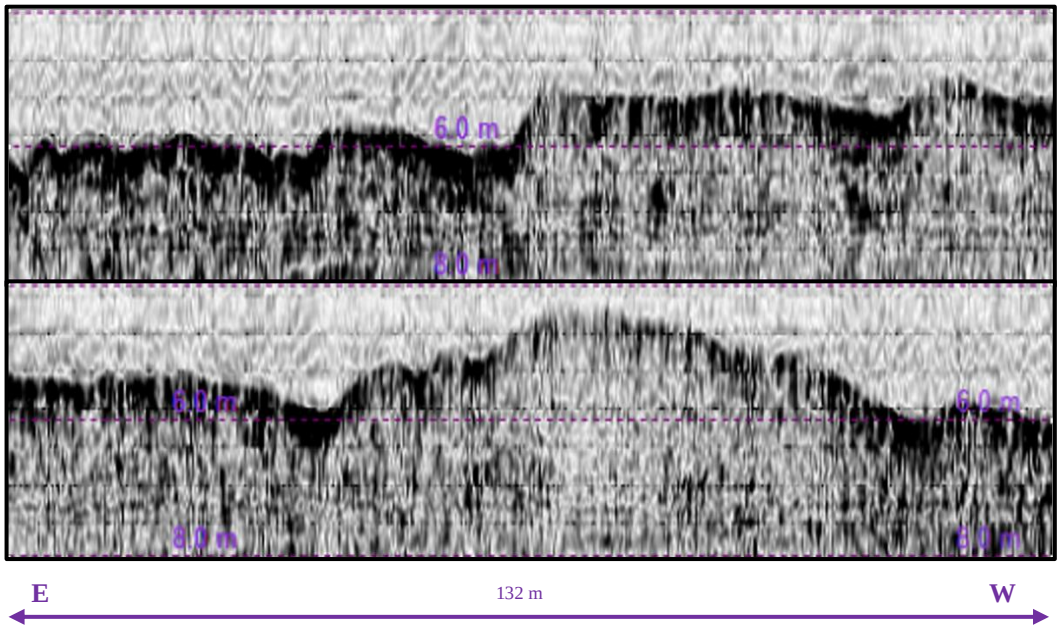


(b)

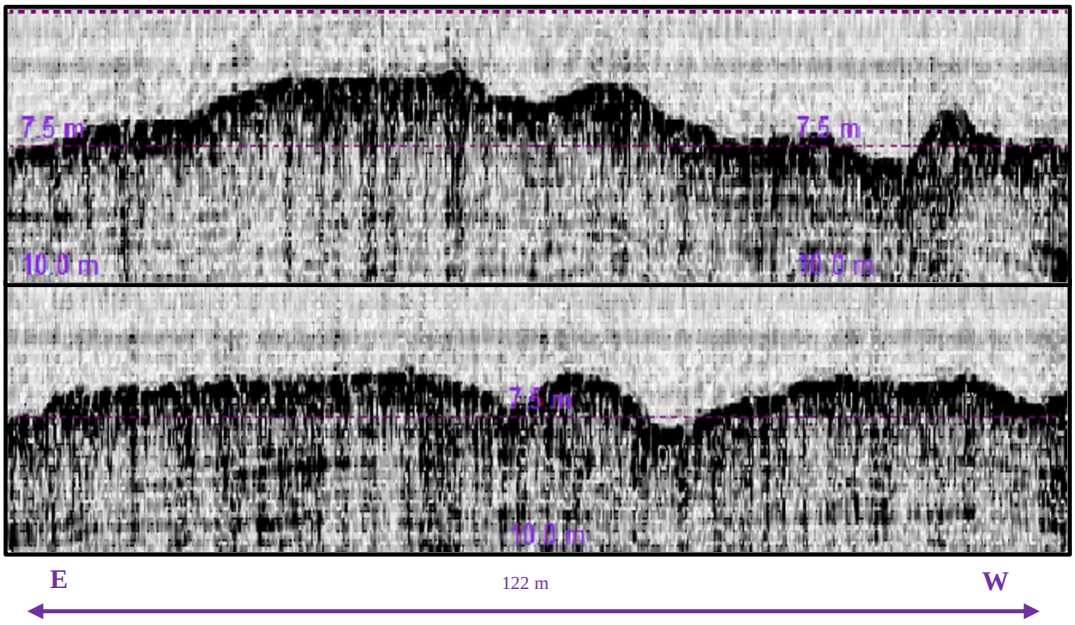


***Figure 3.11: Two seismic profiles taken at SS2. Both profiles are split into two halves, with the lower half continuing on the right of the upper half. For both profiles the left marks the eastern side and the right the western. (a) is sourced from Transect I with a total length of 265 m, (b) is sourced from Transect III with a total length of 245m***

## Sandwave Site 3

SS3 is found northeast of the Omokoroa Peninsula at a fork in the Western Channel, which divides it into southwest and northwest channels. Similar to the previous two sites.

The seismic profiles for the site (*Figure 3.12*) are derived from Transect I and Transect III. The two transects took different routes as Transect I remained within the central Western Channel entirely, while Transect III started out in the centre of the channel and headed towards the southern bank. Through the section, the residual currents (*Figures 3.7* and *3.8*) display net movement towards the southeast, with the ebb tide, with residual currents appearing more pronounced on the southern banks of the channel than the northern.

***Sandwaves***

- Both profiles display the presence of sandwaves to some degree. Throughout the length of Transect I, sandwaves are present ranging in size from <1 m to 2 m. In the southeastern side of the profile, the sandwaves appear taller though narrower, while in the northwest they are shorter but wider. In comparison, Transect III is largely lacking the presence of sandwaves through the central section, while smaller sandwaves (relative to Transect I) can be noted at both the southeast and the northwest sides of the profile. A steeper southeast face in both Transects marks net sedimentary movement with the ebb, matching with modelled residual currents.

***Water Depth***

- The water depth lies between 10 – 11 m in both profiles, with a slight shallowing trend occurring in the northwest of Transect III. It is also notable that both profiles display a dip in the surface elevation to their immediate southeast.

(a)

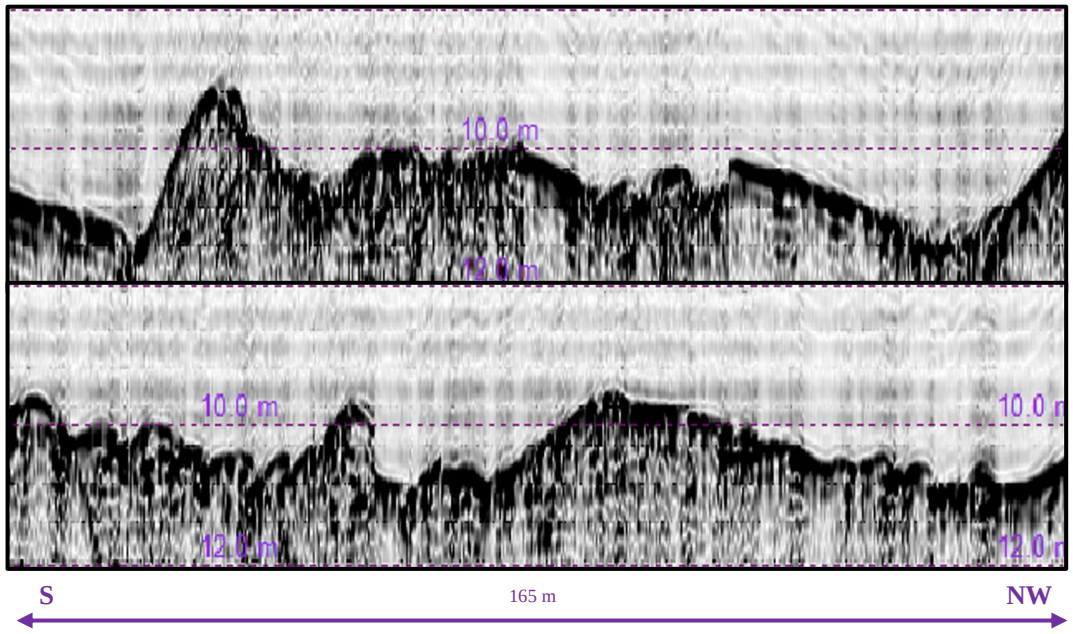


(b)

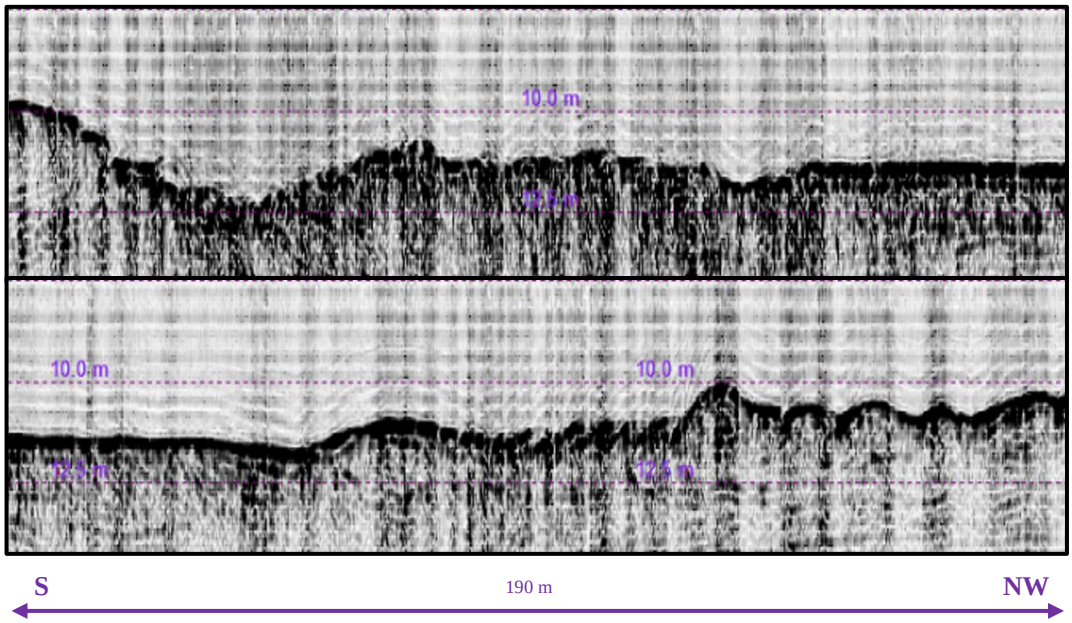


***Figure 3.12: Two seismic profiles taken at SS3. Both profiles are split into two halves, with the lower half continuing on the right of the upper half. For both profiles the left marks the southeastern side and the right the northwestern. (a) is sourced from Transect I with a total length of 330 m, (b) is sourced from Transect III with a total length of 380 m***

## Sandwave Site 4

SS4 occurs north/northwest of the Omokoroa Peninsula. While very close to SS3, different channel dynamics occur here, with the fork from SS3 found to the south. Instead, a channel travelling north along the eastern coastline of the Omokoroa Peninsula appears to be the main influence on local hydrodynamics.

The seismic profiles (*Figure 3.13*) at this site show both obvious similarities and differences between one another. The top profile once again comes from Transect I while the bottom profile is from Transect II. Transect I occurred more centrally within the Western Channel, and Transect II closer to the banks. The modelled residual currents are only available for one site (*Figure 8*), with currents appearing much weaker and more difficult to identify, though still seemingly displaying a slight ebb dominance.

***Sandwaves***

- Sandwaves are evident throughout both profiles. In the southeastern side, the sandwaves appear longer and gradually get narrower towards the northwest in both profiles. Additionally, at both sites, the steeper faces of the sandwaves are facing the northwest, which indicates a migration in the same direction. Therefore, the sandwaves forming appears in contrast to the modelled residual currents.

***Water Depth***

- The water depth of the two profiles differ from one another. While the top profile (i.e. Transect I) shows a shallowing environment, the bottom profile (i.e. Transect II) shows a deepening one. Both the profiles show a depth at their respective ends of ~5 m at the shallow side, and ~6 m at the deeper side. The contrasting water depths are attributed to Transect I remaining within the western channel entirely, while Transect II was initially very close to the channel banks before moving towards the centre of the channel.

(a)

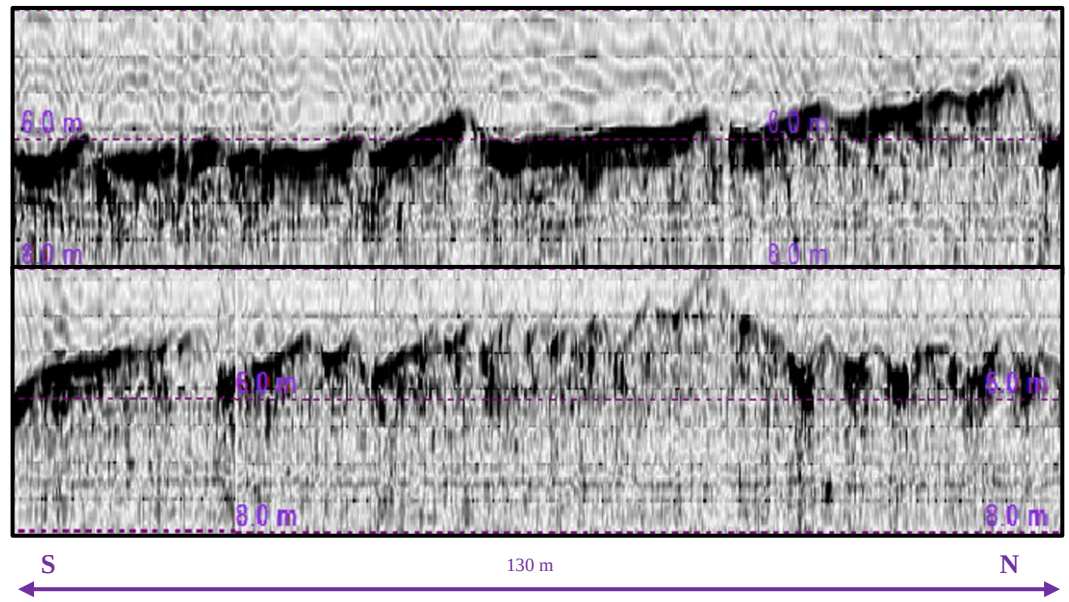


(b)

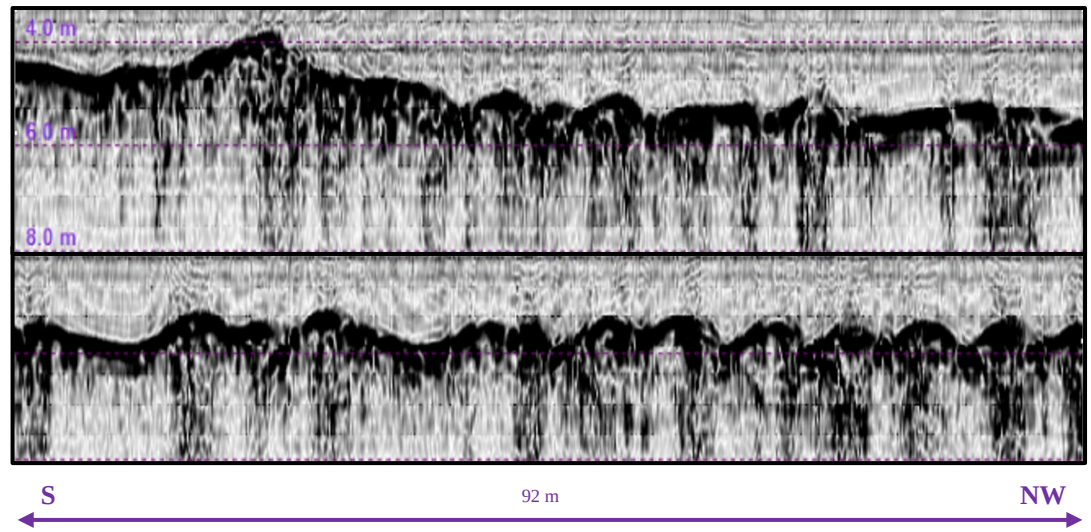


***Figure 3.13: Two seismic profiles taken at SS4. Both profiles are split into two halves, with the lower half continuing on the right of the upper half. For both profiles the left marks the southeastern side and the right the northwestern. (a) is sourced from Transect I with a total length of 260 m, (b) is sourced from Transect II with a total length of 185 m***

## Sandwave Site 5

The final site is located in northwestern most portion of the field area, south of Matakana Point. In contrast to the previous sites, there is a lack of any channel merging or splits occurring in the vicinity. Instead, the site is close to the tidal flats that separate the two hydrodynamically independent halves of the Tauranga Harbour. The site is also close to an area of eroding cliffs at Matakana (Flax) Point. Very similar phenomena are observed in the seismic profiles of the two transects (*Figure 3.14*). Like the previous site, the top profile is Transect I while the bottom profile is Transect II. Residual currents are again only available from the on source (*Figure 8*), with the ebb currents appearing stronger over the first part of the profile, while no dominance is observed in the later.

***Sandwaves***

- Both profiles exhibit the presence of sandwaves throughout their lengths. The heights of the sandwaves are similar between the two profiles, although those in Transect II are longer wavelength. Both profiles also show that towards the northwest the sandwaves become gradually longer. All the sandwaves feature a steeper northwestern face, which indicate sandwave migration towards the northwest with the flood currents. Again, the sandwave migration appears to counter to the modelled ebb currents which depict net movement with the ebb.

***Water Depth***

- The transects are similar to one another, with both profiles shallowing towards the northwest. However, the water depth is slightly variable between the two. Transect I is initially at ~5 m in the southeast but shallows to ~3 m in the northwest. Transect II meanwhile is at ~4 m in the southeast and shallows to ~3 m in the northwest.

(a)

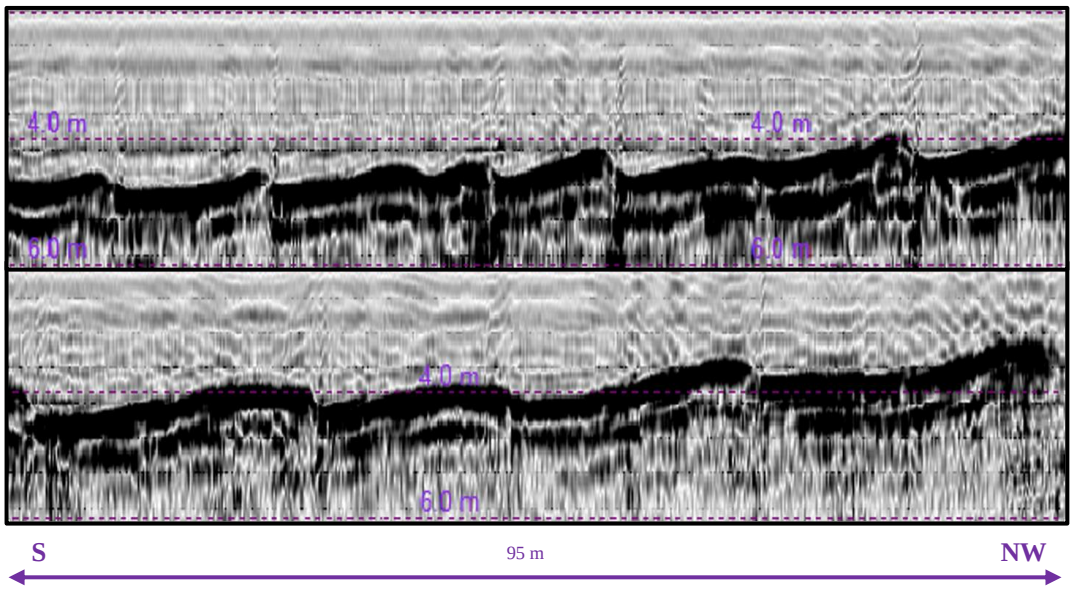


(b)

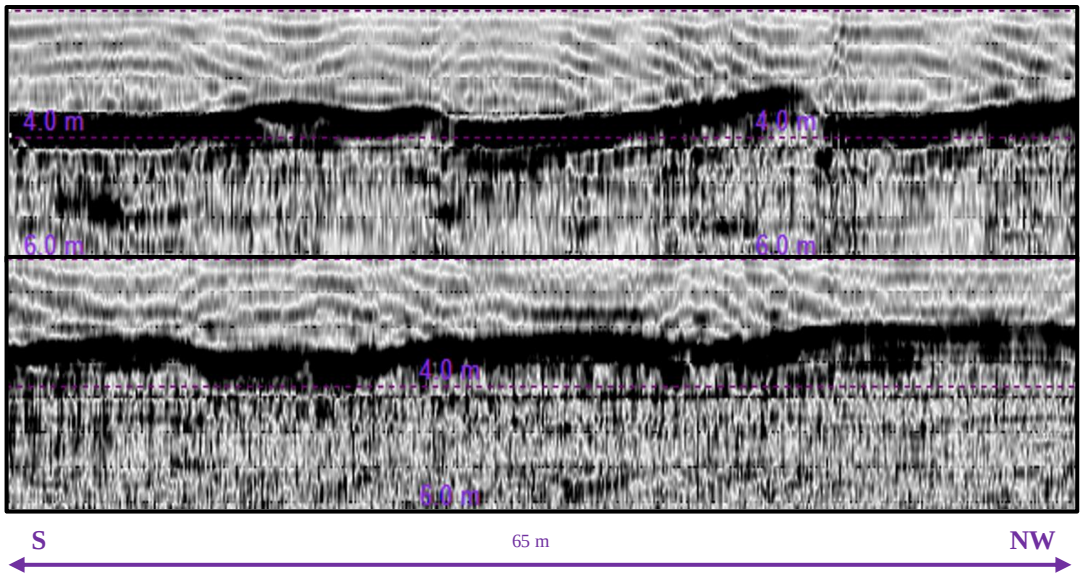


***Figure 03.14: Two seismic profiles taken at SS1. Both profiles are split into two halves, with the lower half continuing the right of the upper half. For both profiles the left marks the southeastern side and the right the northwestern. (a) is sourced from Transect I with a total length of 195 m, (b) is sourced from Transect II with a total length of 128 m***

### *3.4.3.* Discussion

Consistent features appear to control the distribution of sandwaves through the upper Western Channel within the harbour. Mainly, sandwaves occurrence correlates to dynamic changes of the hydrodynamics through the Western Channel. Notably, these hydrodynamic changes occur at locations where multiple channels merge or where water depth changes rapidly. The location of the sandwaves also appears to correlate to a local source of sediment from cliff erosion.

#### *3.4.3.1. Channel Merging*

Four of the sandwave sites identified coincide with two or more channels merging at a location (SS1, SS2, SS3 and SS4). Furthermore, these sites occur at all the locations through the Western Channel where there are channels merging. The reason for the sandwaves being at such locations is that when two or more channels merge, the energy output of each channel combines to produce a new, higher energy output at the location of the merge. Thus, with a greater energy output, there is more potential for sedimentary transport to occur and for sandwaves to be formed (Bokuniewicz et al., 1977; Allen 1980).

Further evidence to support this hypothesis is that the larger the merging channels, the larger the sandwaves formed. SS1 and SS3 both feature sandwaves that reach up to 3 m in height, while the other locations rarely had sandwaves >1 m. Channel patterns indicate that at both SS1 and SS3, all existing channels are restricted to a narrow path, accelerating the flow. Conversely at SS2 and SS4, while both experience hydrodynamic changes due to the merging of channels, parallel channels are maintained. Therefore, the energy output experienced at SS1 and SS3 is much greater than that experienced at SS2 and SS4 and hence the sandwaves formed are more pronounced.

#### *3.4.3.2. Tidal Flats*

The other hydrodynamic mechanisms controlling sedimentation is a rapidly shallowing environment, such as is experienced at SS5 approaching the tidal flats. Peak tidal currents occur at just after mid-tide during both flood and ebb. In a shallow environment, channels flood with the flood tide and stronger currents are

able to penetrate further into the environment, while maintaining high energy. Conversely, with the ebb tide shallow environments will drain before strong currents are established. Thus, in shallow environments such as SS5, net sedimentary transport occurs as stronger flood currents transport sediment farther up through the channel, where the ebb currents lack sufficient energy to mobilise the sediment with the reversing tide (Le Hir et al., 2000; Friedrichs; 2011).

#### *3.4.3.3. Tidal Dominance*

Considering the role of residual currents in controlling sand transport, these patterns can explain the orientation of sandwaves at three of the sites. SS1, SS2 and SS3 all display ebb dominant sandwaves, with net sedimentary transport southeast towards the tidal inlet. Similarly, the residual tidal patterns modelled show dominant residual currents moving in the same directions.

However SS4 and SS5, feature sandwaves that appear in contrast to modelled residuals. The difference is associated with model limitations associated with a lack of calibration points taken in the upper Tauranga Harbour. The formation of the flood dominant sandwaves can be explained by:

(I) SS4 is controlled by the merging of two channels. A smaller channel travelling up the eastern Omokoroa Peninsula enters the Western Channel just southeast of SS4. The merging occurs with the flood tide, while with the ebb tide the Western Channel splits and energy dissipates. Thus, the evidence suggests flood dominance at the location.

(II) The tidal dynamics of SS5 are dictated by the tidal flats to the northwest. Considering the flood dominance of tidal flats (Le Hir et al., 2000; Friedrichs; 2011), and the proximity of the rapidly shallowing SS5 to the tidal flats, the location is also believed to be flood dominant.

Thus, both SS4 and SS5 may be considered flood dominant systems. Given that residual currents are primarily generated by the dominant tide, sandwave migration to the northwest would be expected on the basis of the tidal patterns.

At three of five locations through the Western Channel where sandwaves are evident, their morphologies are consistent with the residual tidal currents,

complementing the theory that dominant tidal flow controls the net direction of sedimentary transport and sandwave migration. The two sites in contrast to modelled currents, are considered model limitations toward the upper harbour, where flood dominance begins.

#### *3.4.3.4. Sandwave Asymmetry*

Two sandwave locations display highly symmetric sandwaves (SS1 and SS3) whilst three display highly asymmetric sandwaves (SS2, SS4 and SS5). Sandwave asymmetry can also be considered a product of the tidal asymmetry.

The symmetry of sandwaves correlates to the magnitude of tidal currents. Where similar magnitude ebb and flood currents occur, symmetrical sandwaves are produced. Conversely, where the flood and ebb currents have a significant difference to their magnitudes, more asymmetric structures will occur (McCave, 1971).

#### *3.4.3.5. Channel Location*

Sandwave patterns appear to be controlled relative to their positioning in the channel. They were found to be more pronounced in the central portions of the channel than towards the edges. Strictly put, the centre of the channel will be the deepest portion of the channel, which follows the thalweg, and so currents will be strongest there. Stronger currents mean a greater proportion of mobile sediment. This phenomenon is best observed at SS1 and SS3. At both these sites, the seismic profile of Transect I was taken more centrally within the Western Channel. Similarly at both sites, extensive sandwaves are observed in the Transect I profile whilst they are entirely absent from Transect III at SS1, and greatly reduced on Transect III at SS3.

#### *3.4.3.6. Sedimentary Source*

Finally, for sandwaves to form, there must also be a source of sediment available. All the sandwave sites are notable for featuring an erosional surface nearby. Starting from the from the inlet side of the harbour, and moving towards the tidal flats, the following sources are identified: SS1 – Erosion of the Pleistocene Rangiwaea

Island; SS2 – Erosion of the Motuhoa Island; SS3 – Erosion of an uplifted fault surface occur to the east; SS4 – Erosion of an uplifted fault surface to the south; SS5 – Erosion at Matakana and Flax Points occurs

## 3.5. Structural Interpretation

Post the emplacement of the Waiteraiki Ignimbrite (2 Ma), tectonic activity in the Tauranga Region has been minimal (Briggs, 1996). However, a dominant (north) northeast orientation of peninsulas striking into the harbour, and a similar orientation of catchments in the region, has led to postulation of a series of deep seated faults. The faults have subsequently been covered by the Waiteraiki Ignimbrite and subsequent deposits (Briggs, 1996). Postulated faults have been suggested at:

(I) Two faults in the Papamoa Ranges based on a north-northeast alignment of rhyolite domes (Briggs, 1996)

(II) At the rhyolite domes of Kaikaiaroro, Manawata, Minden Peak based on their north-northeast alignment (Whitbread-Edwards, 1994; Briggs, 1996)

(III) Omokoroa Peninsula (Christophers, 2015)

The following subsection will provide evidence from the seismic profiles that may indicate active faulting through distortions of surface and/or subsurface formations. *Figure 3.15* shows three locations of interest where varying degrees of fault evidence are present in the seismic reflection data.

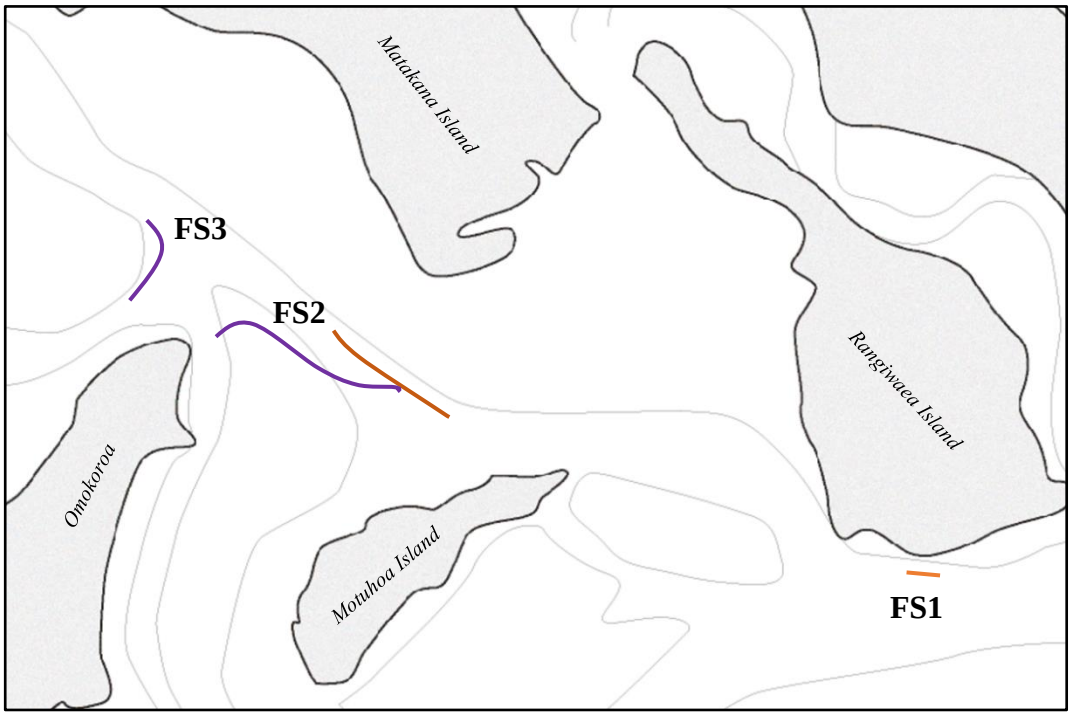


***Figure 3.15: Locations where faults have been identified in the seismic interpretations with the bold numbers marking the site. The lines mark the respective seismic profile lengths for each fault site. The colours correspond to the transects the profiles are derived from, Orange = Transect I, Purple – Transect II & III***

## Fault Site 1

FS1 occurs just south of Rangiwaea Island. The seismic profile (*Figure 3.16*) is taken from the east (inlet side) to the west (tidal flat side), with the fault running perpendicular to the profile.

### *Surface Evidence*

- A sudden change in the surface elevation is clearly noted from east to west. The eastern side of the profile sits initially at 10 m featuring a flat horizontal surface. Midway through the profile, the surface suddenly shallows to a depth of ~7 m. Subsequently, similar to the eastern half of the profile, a flat horizontal surface is also observed on the western half.

### *Subsurface Evidence*

- Similar phenomenon can be observed at ~2 m below the surface. A horizontal layer can be traced from the east at ~12 m depth, before rising rapidly to a depth of ~9 m, maintaining the same thickness throughout the profile and in essence mirroring the surface.

The main evidence of faulting at the location is that a sudden change in the surface elevation is observed within the channel. While there is no evidence of the fault breaking a plane here, there is a noticeable degree of deformation occurring. This suggests a monoclinal structure that may very well coincide with a deeper fault.

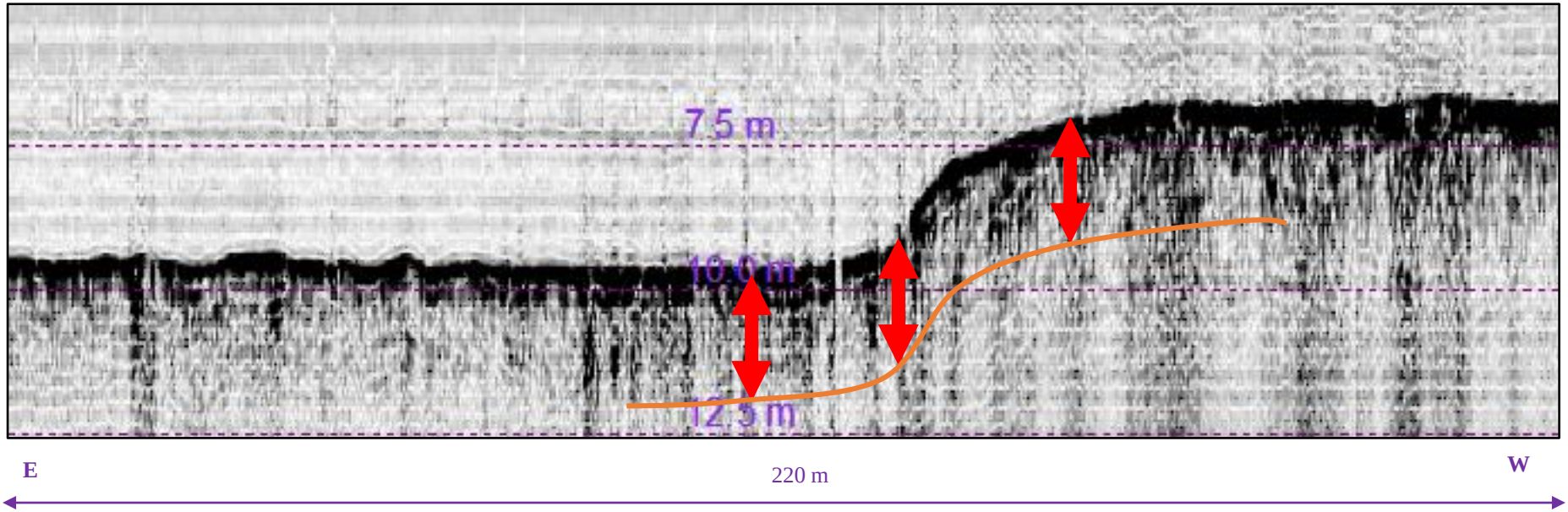


***Figure 3.16: Seismic profile of FS1 from Transect III. The solid orange line marks the bottom of a layer identified under the surface. The arrows display a constant thickness with the subsurface layer.***

## Fault Site 2

FS2 is located within the Western Channel, between Motuhoa Island and the Omokoroa Peninsula. Two seismic profiles show evidence of the fault, *Figure 3.17* from Transect I, and *Figure 3.18* from Transect III. The location also coincides with SS4, with the profiles from SS4 comprising the north-western halves of *Figures 3.17* and *3.18*. Both profiles are taken from southeast (inlet side) to northwest (tidal flat side).

### *Surface Evidence*

- A drop in elevation can be observed from southeast to northwest, followed by the presence of sandwaves. The elevation change is not as sudden as at FS1, with sandwaves also masking the sharpness of the elevation change. In contrast, the change is more observable in Transect III, where the sandwaves are less extensive, than within Transect I.

### *Subsurface Evidence*

- To the southeast of the inferred fault within both profiles, a subsurface reflector sloping towards the northwest is found. The feature is most clear in the first half of Transect I, and evident throughout Transect III. The subsurface reflector appears independent of the surface, with the surface dipping towards the northwest (e.g. the reverse of the subsurface layers), for both Transects. To the northwest of the inferred fault, the surface rises gently towards the northwest in Transect III (e.g. the same as the subsurface layers).

- Several subsurface layers ($X_1$, $X_2$, $X_3$) identified in Transect III provide further reinforcement of a fault presence. Essentially, the layer $X_1$ is observed on the southeastern side of the fault and suddenly ends around the fault trace with no further indication on the northwest. Similarly, $X_2$ and $X_3$ are first identified at the fault trace on the northwestern side, sloping up towards the northwest, with no indication of the layers on the southeast of the incidence.

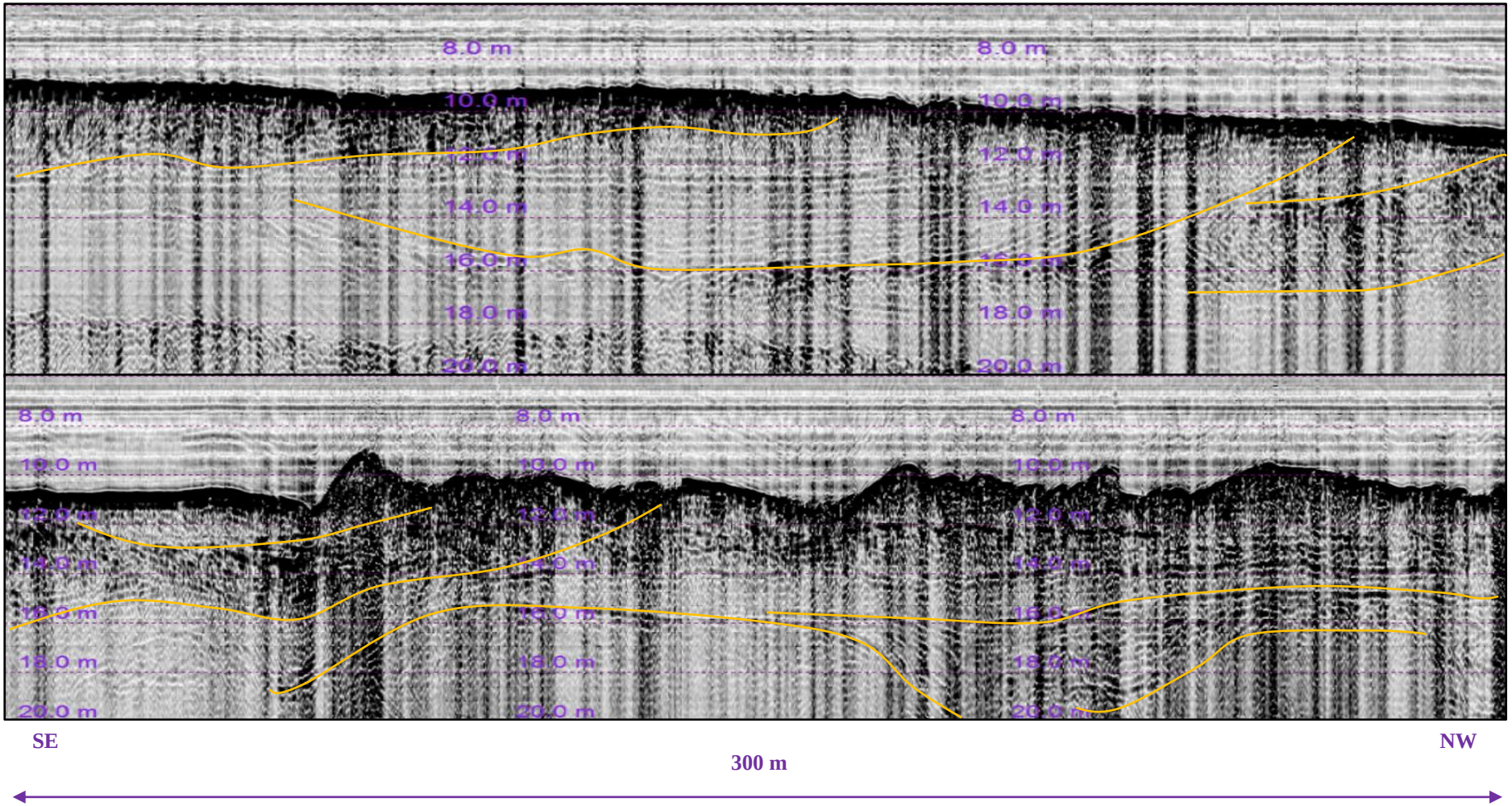


*Figure 3.17: Seismic profile of FS2 from Transect I. The total length of the profile is 600 m with the lower image continuing from the right of the upper image. The left side marks the southeast (inlet side of the harbour) and the right the northwest (tidal flat side of the harbour). Solid yellow lines mark the boundaries of subsurface layers.*

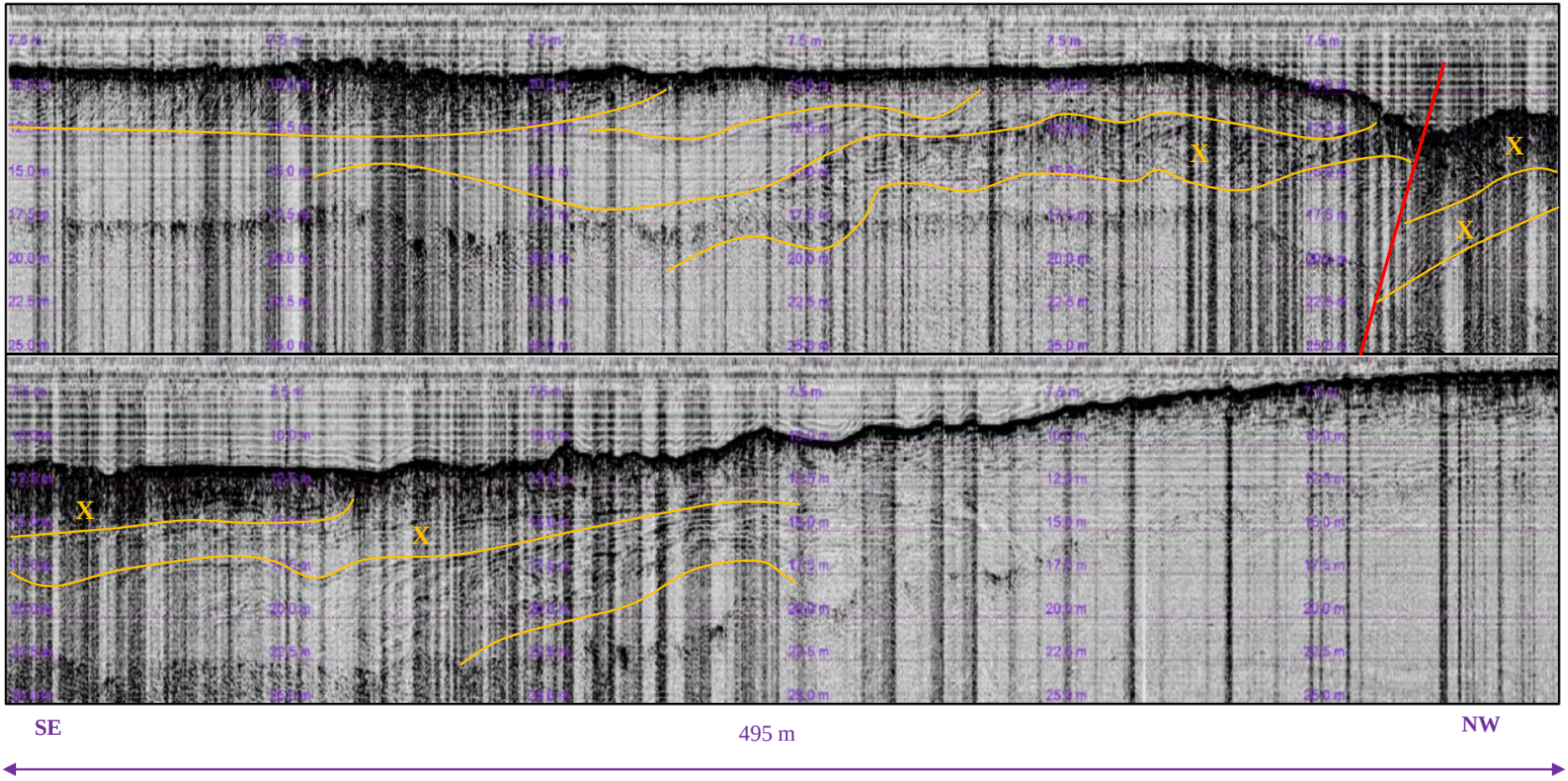


*Figure 3.18: Seismic profile of FS2 from Transect III. The total length of the profile is 990 m with the lower image continuing from the right of the upper image. The left side marks the southeast (inlet side of the harbour) and the right the northwest (tidal flat side of the harbour). Solid yellow lines mark the boundaries of subsurface layers. The solid red line marks the presumed fault location*

## Fault Site 3

FS3 occurs northwest of the Omokoroa Peninsula, at the final fork of the Western Channel, with the seismic profile taken from south to north (the tidal inlet is east). A solitary seismic profile (*Figure 3.19*) is available for the site, derived from Transect III. The profile is also taken from directly southeast of SS4.

### *Surface Evidence*

- Unlike the previous two sites, no sudden change in surface elevation is observed here. A gently sloping surface is evidenced from south to north, with similar sloping having been observed at FS2. Additionally, sandwaves occur to the north of the northern elevated surface.

### *Subsurface Evidence*

- The subsurface evidence displays strongly sloping layers in the reverse direction of the surface (e.g. down towards the north). Essentially, the surface gently slopes up towards the north, while the subsurface strongly slopes down towards the north.

Unlike FS1 and FS2, no clear fault traces are identified at this location. However, the surface and more notably the subsurface, have marked evidence of being altered post deposition with an erosional surface truncating the beds.

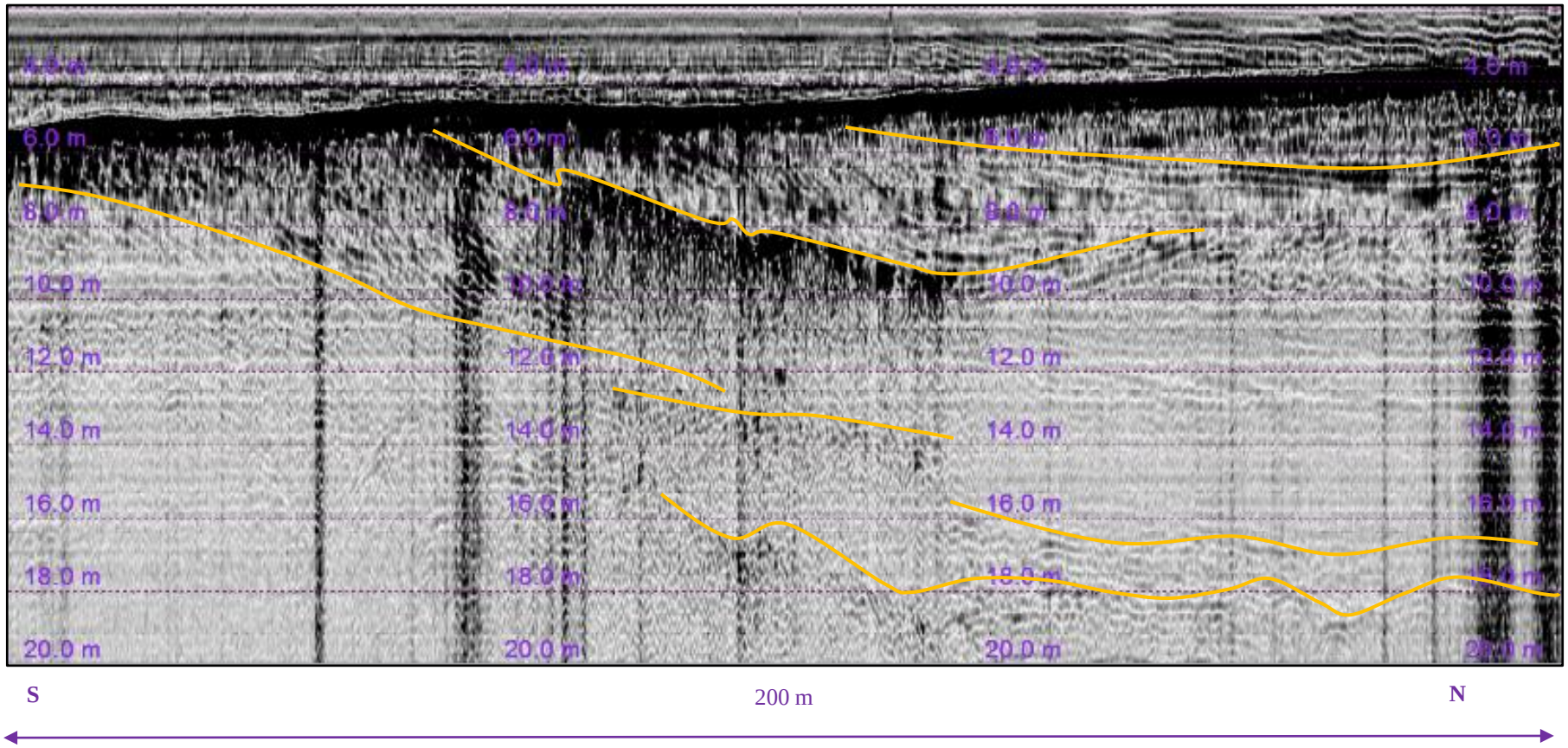


***Figure 3.19: Seismic profile of FS3 from Transect II. The total length of the profile is 200 m. The left side marks the south and the right the north, which coincides with a fork in the Western Channel with both directions leading towards tidal flats. Solid yellow lines mark the boundaries of subsurface layers.***

### *3.5.1.* Faulting Discussion

Three locations have been identified in the seismic analysis that may be indicative of faults intersecting the Western Channel. The faulting exhibited at the sites varies in fracture type, and the strength of evidence. FS1 depicts folding with no evidence of a fracture, FS2 depicts what appears to be a fault breaking the surface, and FS3 does not display any potential fault trace though hints at one nearby.

#### *3.5.1.1. FS1*

At FS1, evidence from the seismic clearly depicts the surface elevation changing very rapidly. Additionally, with the subsurface largely mirroring the surface, direct evidence of a fault associated fracture is not observed. However, folding is exhibited instead. Thus, it is theorized that the fold present is associated with a fault occurring at depth. Fault propagated folds can been defined as "deformation that takes place just in front of the propagating fault surface" (Suppe, 1985; Erslev, 1991). Examples of fold propagated folding are shown in *Figure 3.20*, with the examples exhibiting similar phenomenon to those observed in the seismic of FS1, and in particular, example *D*. Therefore, it is suggested that the phenomenon observed at FS1 is a fault propagated fold.

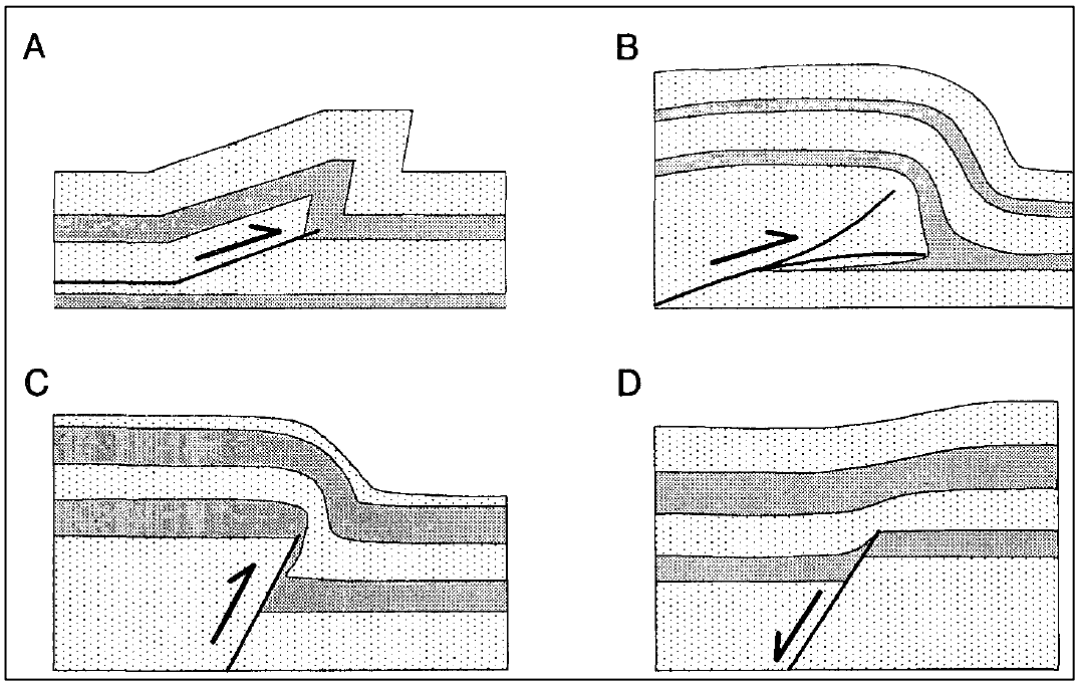


***Figure 3.20: Models of fault propagation folds. (A) Geometric kick-band model. (B), (C), (D) Analog experimental models of folds above (B) thrust, (C) reverse, (D) normal faults. From Erslev (1991)***

#### *3.5.1.2. FS2*

At FS2, there appears to be clear evidence of a fault fracturing the surface: with an observed change in surface elevation; the sloping of the subsurface layers to the northwest; and subsurface layers evident on one side of the fault trace and not on the other. *Figure 3.21* depicts the sequence associated with a reverse fault subject to surface erosion (Fossen, 2016), which appears similar to the observations at FS2.

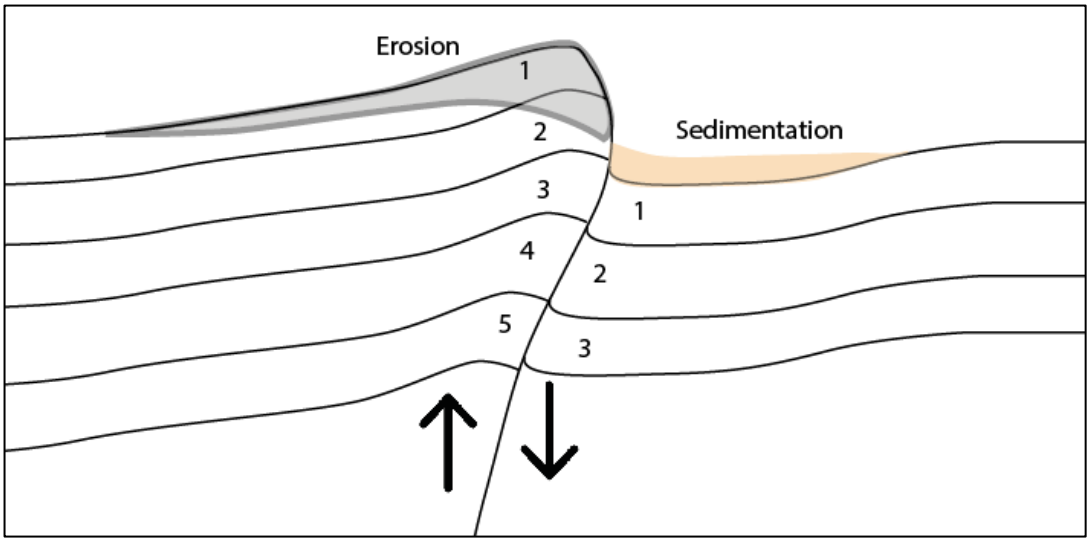


***Figure 3.21: Example of the reverse fault fracture presumed at FS2***

**Surface elevation**: a change in surface elevation, from southeast to northwest, suggests the southeast side has been uplifted and the northwest down-thrown. Sandwaves occurring on the down-thrown side form as sediment transport is enhanced, as a consequence of erosion occurring on the uplifted side of the fault.

**Subsurface Sloping**: On the southeastern, uplifted side of the fault trace, the subsurface structures are seen sloping upwards towards the northwest. Considering maximum movement occurs at the fault, the upward slope towards the fault is expected. Additionally, several of the subsurface layers on the southeastern side end at the surface, which provides evidence of active erosion occurring, reinforcing the observed enhanced sedimentation to the northwest. On the down-thrown side of the fault, the subsurface layers display the reverse trend of the uplifted side, with sloping occurring down towards the fault. This can once again be attributed to the same cause and effect with maximum movement occurring at the fault.

**Layers $X_1$, $X_2$ and $X_3$**: The three layers marked $X_1$, $X_2$ and $X_3$ in *Figure 3.17* are notable for appearing to abruptly begin/end at the fault trace. $X_1$ can be traced on the southeastern uplifted side of the fault sloping upwards, before suddenly ending. $X_2$ and $X_3$ are the reverse, with no indication of their presence on the southeastern side of the fault, but easily traceable on the northwest. Thus, the perception of brittle deformation here is further emphasized with $X_1$, indicating the oldest layer of the three, which has been uplifted from depth.

#### *3.5.1.3. FS3*

The third fault site is a lot more ambiguous than the first two. No direct fault trace has been mapped here, however, the evidence points for a fault in the nearby vicinity as opposed to being identified directly in the seismic. The subsurface sloping depicts similar formations to those observed around the FS2 fault, along with a truncated surface. Additionally, the sandwave cover to the north also points to greater rates of mobile sediment that has been found to correlate with faulting at FS2, due to increased erosion of the uplifted surfaces.

## 3.6. Summary

- Seismic mapping was undertaken through the Western Channel of the Tauranga Harbour utilizing a Knudsen sub-bottom profiler. The seismic data were processed by Knudsen PostSurvey software and the locations of the surveys plotted in Google Earth. The purpose of the seismic mapping was to identify sedimentation patterns through the harbour and provide evidence of faulting.
- Sandwaves were used to identify variation in sedimentation patterns. Sandwaves themselves are large traverse bedforms that form consequence of net sedimentary transport. They have been identified at five locations through the harbour, varying in both size and shape.
    - Sandwaves occurred at four sites where two or more channels merged (SS1, SS2, SS3, SS4), and at one site approaching the tidal flats where water depth rapidly shallows (SS5).

  - Three locations depicted net sedimentary transport with the ebb tide (SS1, SS2, SS3), and two with the flood tide (SS4, SS5). The flood dominant sites are in the upper harbour whilst the ebb are found in the middle-lower harbour.
  - The symmetry of sandwaves can be correlated to the tidal dominance. Two sites depict highly symmetrical sandwaves in locations where residual ebb currents are slightly greater than the flood (SS1, SS3). The remaining sites featured highly asymmetrical sandwaves with a clear ebb (SS2) or flood (SS4, SS5) dominance.
  - Finally, sandwaves were more pronounced in the central portions of the channel than closer to the banks. Where parallel transect took slightly different routes through the same channel, the phenomenon was evident (SS1, SS3).
- Three potential fault sites were identified through the harbour
  - FS1 shows a sharp surface elevation though no evidence of a fault breaking the surface. It is thus theorized a fault propagated fold.
  - FS2 displays a fault breaking the surface in the form of a reverse fault. Evidence of the fracture is observed in both the surface and subsurface.
  - FS3 is the most ambiguous with no potential fault traces identified. However, the surface and subsurface features are similar to FS2 indicate the potential for a fault nearby.

# CHAPTER 4
# SEDIMENT CORING INTERPETATION

## 4.1. Introduction

Sediment cores were taken at five sites through the Western Channel utilising vibracoring techniques. Core locations were chosen based on the seismic survey interpretation covered in the previous chapter. This chapter is subdivided into the following sections: **4.2. Vibracoring**– an overview on the theory, development, and use of vibracoring, **4.3. Core Sites** – covering where the core sites are located and how they were chosen, **4.4. Field Methods** – describing the equipment used, the coring procedure, core storage, and core splitting, **4.5. Analytical Methods** – describing the core logging and laser sizing procedures, **4.6. Stratigraphic Logs** – a description of the stratigraphy at each core site, **4.7. Facies Interpretation** – analysing how the facies vary; through the harbour, with depth, and postulated ages of deposits, **4.8. Sediment Sources** – an interpretation of sources of sediment, **4.9. Faulting Interpretation** – where the evidence for faulting will be discussed, and **4.10. Summary** – where the key points of the chapter will be summarized.

## 4.2. Vibracoring

VIbracoring is a method of attaining sequence cores, based on the principle of thixotropy, where "*A viscous fluid occurring under static conditions, upon experiencing a mechanical force such as shaking will become thinner and less viscous*". Thixotropy essentially sees physically bound water in soil transform into free water, or from a sol to a gel (Gumenksi and Komarov, 1961; Barnes, 1997). Vibracoring operates by sending pulsations from a vibrator, through a drill rod to the drill tip, and then onto the surrounding soil. These high frequency oscillations subsequently decrease the shear resistance of the soil and so, under its own weight and that of the vibrator, the drill penetrates the soil (*Figure 4.1*). Once the required drilling depth is met, the drill is raised (Gumenksi and Komarov, 1961).

Vibracoring is operable at any angle, and is applicable in a variety of environments including; semi- to un-consolidated sedimentary deposits in marine, coastal, estuarine, fluvial, and terrestrial environments. However, vibracoring operates most

effectively on unconsolidated, waterlogged, heterogeneous sediments, where vibrations allow displacement of grains within the liquid spaces of the matrix. Where vibracoring is applicable, it is preferred to traditional coring methods, where large amplitude and low frequency driving of cores, increases friction along the core and causes displacement of sediment. In contrast vibracoring yields relatively undisturbed cores (Barrow, 1995).

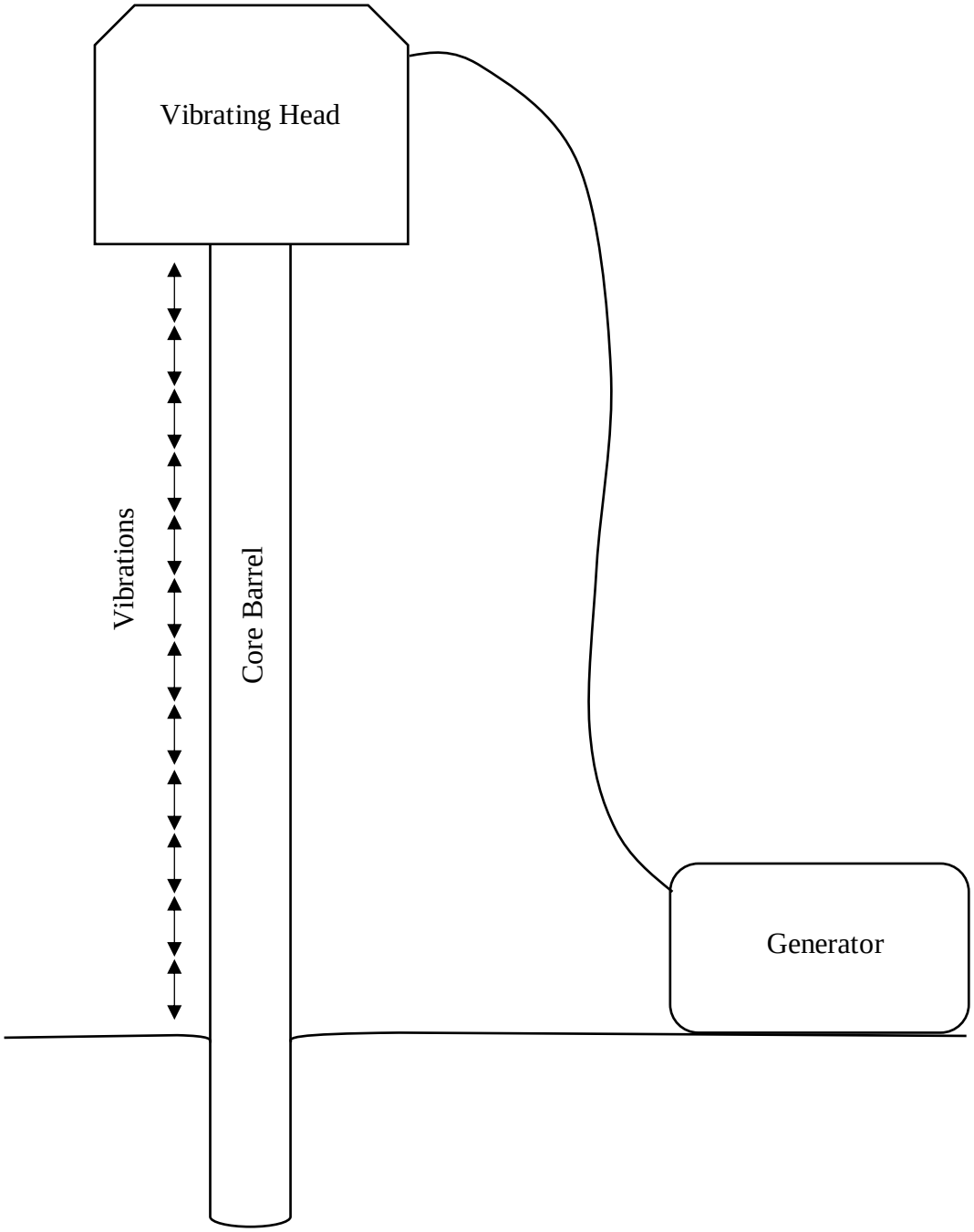


***Figure 4.1: Example of a vibracore setup. A generator powers a vibrating head, sending a vibrations through the core barrel and allowing penetrations of the surface under the weight of the unit.***

## 4.3. Core Sites

Five core sites (CS1, CS2, CS3, CS4, and CS5, *Figure 4.2*) were sampled through the Western Channel utilising the vibracoring method. These sites were chosen following the seismic survey interpretation in **Chapter 3**. The purpose of the coring was to obtain ground truth data for the seismic survey in order to understand sedimentation patterns and identify faulting. Cores had to be sampled through all reaches of the Western Channel, to observe how sedimentation patterns (e.g. rates and sediment composition) varied through the harbour. Fault identification required sampling of cores either side of fault traces identified in seismic profiles, in hopes of identifying discontinuities in sedimentary composition with depth. As such, the five core sites were put into three core groups: CG1 = CS1 and CS2; CG2 = CS3 and CS4; and CG3 = CS5.

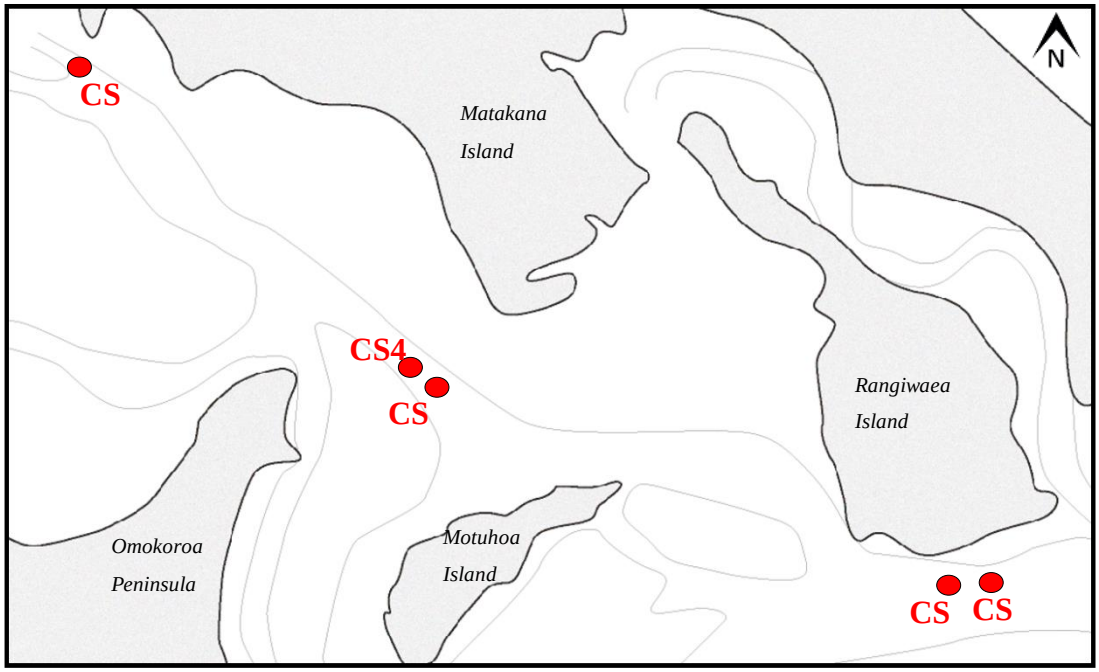


***Figure 4.2: Locations of core sites through the harbour. CS = Core Site. Tidal inlet is found southeast of Rangiwaea Island. Tidal flats occur northwest of CS5***

### *4.3.1.* Core Group 1

CG1 consists of two cores taken at the southeast extent of the field area, just south of Rangiwaea Island. The cores were taken at the following coordinates: CS1 (*37°38'35.45"S, 176°07'06.51"E*) and CS2 (*37°38'35.29"S, 176°06'58.56"E*).

These core sites correspond to FS1 from ***Chapter 3***. CS1 was taken on the down-thrown side of the fault and CS2 was taken on the uplifted side. Additionally, CS2 was taken near SS1 from Chapter 3. Thus, the purpose of coring at CG1 was:

(I) To describe local sedimentation patterns

(II) To compare the sedimentation pattern occurring at the southeast extent of the field area with the other core sites through the harbour

(III) To provide further evidence of a fault identified in seismic analysis

### *4.3.2.* Core Group 2

CG2 consists of two cores taken mid-way through the field area, between Motuhoa Island and the Omokoroa Peninsula. The two cores forming the group are CS3 (*37°37'39.5"S, 176°04'02.1"E*) and CS4 (*37°37'37.4"S, 176°03'58.67"E*). They correspond to SS3 and FS2 in **Chapter 3**. Similarly to CG1, a core was sampled both sides of the predicted fault, with CS3 on the uplifted side, and CS4 on the down-thrown side. Additionally, CS4 was located in a region of extensive sand waves. Thus, CG2 shares the same three goals from sampling as CG1:

(I) To describe local sedimentation patterns

(II) To compare the sedimentation pattern occurring at the central portion of the field area with the other sites across the harbour

(III) To provide further evidence of a fault identified in seismic analysis

### *4.3.3.* Core Group 3

Unlike the other two core groups, CG1 is composed of only one core site, CS5 (*37°36'08.27"S, 176°01'55.77"E*) due to time and budgetary constraints. The core was sampled at the northwestern extent of the field area, just south of Matakana Point. The site corresponds to SS5 in **Chapter 3**. Unlike the other core groups, which hope to provide evidence of faulting, there are only two goals for this core site:

(I) To describe the local sedimentation pattern

(II) To compare the sedimentation pattern occurring at the northeast extent of the field area, with the other core sites through the harbour

## 4.4. Field Methods

### *4.4.1.* Equipment

#### *4.4.1.1. Vibracorer QR 300*

For core sampling, the Vibracorer QR 300, manufactured by Quaternary Resources PTY Limited, was used. This model is designed to collect cores using standard aluminium pipes of 76 mm diameter or PVC pipes of 80 mm diameter, in lengths of up to 6 m, and is capable of sampling at water depths up to 300 m. It is operable in marine, coastal, estuarine, fluvial, and terrestrial environments. Deployment of the vibracorer employs a coordinated operation of a drilling vessel, equipped with winches and rope/strap, and a lifting capacity of at least 1.5 tonnes, for lifting the vibracorer during deployment and recovery. The vibracorer can be split into four components with a combined weight of ~250 kg. These include (1) a 6.8 m tall demountable tower, (2) a vibrating head, (3) a power supply, and (4) a core barrel (Quaternary Resources PTY Limited, 2016). The height of the tower can be adjusted by removing 1.5 m sections.

#### *4.4.1.2. Core Barrel*

PVC (polyvinyl chloride) core barrels were used for the sampling procedure. The cores were of an 80 mm internal diameter, greater than the standard 76 mm diameter of aluminium core barrels, providing a slightly greater volume of collected data for analysis. PVC core barrels also reduces the potential for metal contamination if the heavy metal content of the sediment needs to be measured.

#### *4.4.1.3. Barge*

The coring was undertaken aboard the self-propelled barge *Quest* operated by Bay Marine Works Ltd, Tauranga. The *Quest* met all requirements for operation of the vibracorer including an 11 m reach hiab crane, and was equipped with its own GPS tracking system and echosounder. For providing positional stability, the vessel had an attached 10 m spud for use in shallower waters, and for deeper waters an anchor, which would not provide the same level of stability as the spud, as it would not prevent drifting of the barge.

### 4.4.2. Coring Procedure

#### 4.4.2.1. Timings

Of the five core sites, only sampling for CS5 required specific tidal timings. The exact coring location was slightly ambiguous, with the intent of the sampling to travel as far up through the Western Channel, and approaching the tidal flats, as the water depth allowed. Thus, the site was sampled first to coincide with high tide on the day.

The remaining sites were all relatively easily accessible and were simply sampled in the order that they were crossed travelling from CS5, through the Western Channel towards the port (i.e. CS4 – CS3 – CS2 – CS1).

At each location, the spud was deployed to provide positional stability so that the vessel would not sway with the strong ebb currents. However, site CS4 was in water depths greater than the spud could reach. Thus, anchoring had to be used instead at the site, which in turn required more time to establish the vessel position, and required a relatively quick deployment and retrieval of the vibracore unit to mitigate the effects of drift.

#### 4.4.2.2. Coring

The core sites were located utilising the vessel's GPS, with a chart and a secondary handheld GPS confirming each location. Core barrels were attached and secured at each location to the vibrating head. The vessel crane and winch system was used to lift the vibracorer off the vessel and deploy onto the channel bed (*Figure 4.3*). The vibracorer was operated for a maximum of 30 sec, or until there was evidence that core penetration had ceased (i.e. a slackening of a rope attached to vibrating head). The vibracorer was then lifted from the sea bed back onto the vessel. A scribe at the base of the tower would scratch the core as it descended past the base, marking the depth of penetration (*Figure 4.4*). A core catcher at the bottom of the core barrel prevented sediment escaping through the bottom of the core.


***Figure 4.03: Example of the vibracorer deployment. Features of the vibracorer are labelled (frame, head and core barrel). The vessel crane lifts the unit and deploys it off the vessel into the water.***

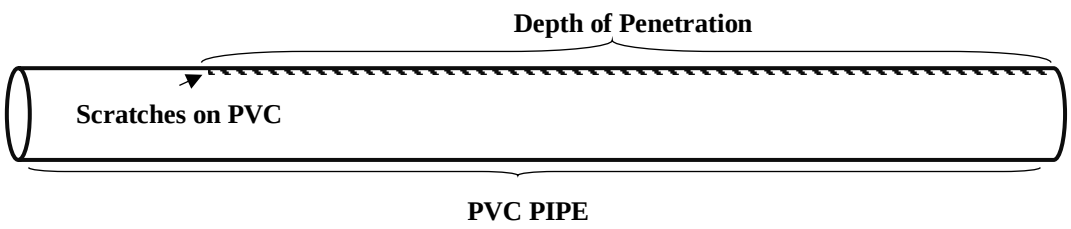


***Figure 4.4: An idealised example of a retrieved core indicating penetration depth***

### *4.4.3.* Post Coring

#### *4.4.3.1. Labelling*

Core penetration was recorded, with the penetration for the sites ranging from 230 cm to 320 cm. The retrieved cores were then cut into two or three sections, each 1-1.5 m long, plugged with foam and capped. The caps were sealed with three colours of tape (red, blue, white), which were also used as a labelling mechanism (*Figure 4.5*). Red tape marked the top of a core section and blue tape marked the bottom. Additionally, white tape on top of red or blue marked the very top of a core series (TOC) or bottom of a core series (BOC). Finally, black tape was used to mark the core site, with the number of bands marking the core location (e.g. CS1 had 1 band of black tape, CS4 had 4 bands of black tape).

(a)

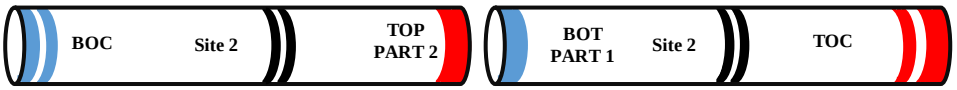


(b)

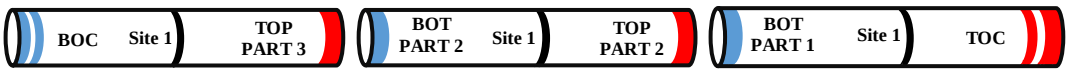


***Figure 4.5: Example of the labelling system utilised across both two and three piece core series.***

#### *4.4.3.2. Storage*

Sampled cores were laid horizontally at a secure location on the vessel while in the field, and similarly in the vehicle during transport from the field site to the University. Vertical alignment of cores was avoided to prevent compaction of the core contents. At the University, they were placed in refrigerated storage at 4°C for several days before splitting.

#### *4.4.3.3. Splitting*

Core barrels were split lengthwise using a dedicated saw table (*Figure 4.6*) that can control the depth of the saw cut into the core. The saw table cut the PVC on opposite sides of a core in two motions, as opposed to directly through the core which would cause disturbance of the sediment. A knife was then passed through the centre of the core to separate the core contents into two halves, and then the core could be opened. PVC residue from the core barrel was scattered throughout the exposed core, and so the exposed sections had the top 1-2 mm scraped off. All cores were photographed after cleaning, and subsequently logged and returned to storage.


***Figure 4.6: Saw table for splitting cores. Cores are laid flat in the central groove of the table, the PVC an the exposed side is split, the core is rotated 180° and once again the exposed PVC is split***

## 4.5. Analytical Methods

### *4.5.1.* Visual Logging

Stratigraphic logging was undertaken immediately following core splitting. The analysis involved describing all horizons identified within each core on the basis of:

(I) Colour: Using the Munsell colour chart

(II) Sediment texture: observable changes to the sorting, grading or shape

(III) Observed mineralogy: volcanic (primary/secondary), biogenic content

(IV) Shell composition: coarseness, abundance, and species compositions

### *4.5.2.* Laser Sizing

Subsamples for laser sizing were taken from each core at 5 cm intervals. The laser sizing provided grainsize variations that could be simplified into:

(I) Clay (Cl): < 3.9 um
(II) Silt (Si): 3.9 – 62.5 um
(III) Very Fine Sand (Vfs): 62.5 – 125 um
(IV) Fine Sand (Fs): 125 – 250 um
(V) Medium Sand (Ms): 0.25 – 0.5 mm
(VI) Coarse Sand (Cs): 0.5 – 1 mm
(VII) Very Coarse Sand (Vcs): 1 – 2mm

However two cores also featured sections with high levels of gravel sediment (g: >2 mm). These sections were sampled, stored in an oven for a week to dry the sediment, and the gravel sand and finer components were sieved and weighed.

### *4.5.3.* Stratigraphic Logs

Stratigraphic logs were created in Adobe Illustrator by combining the results of the visual logging and laser sizing. Horizons and facies were identified through a hierarchical process:

(I) A distinct visual change and laser sizing denotes a clear grainsize variation
(II) A distinct colour change though no apparent grainsize change
(III) Grainsize analysis shows slight change and visually appears homogenous
(IV) Shell composition changed gradually with depth

Essentially, Factors I and II constituted a separate facies. Instances of Factors III and IV were marked with dashed to lines to indicate a horizon change, as evolutionary changes occurring within a facies, which did not constitute a facies label on their own.

Although dateable material was present in the cores, there was no budget available to allow for dating..

## 4.6. Stratigraphic Analysis

### *4.6.1.* Core Site 1

At CS1 seven horizons, split into four facies (facies 1 = horizon 1, facies 2 = horizons 2, facies 3 = horizons 3-4, facies 4 = horizons 5-7) were identified down to a depth of 245 cm. *Figures 4.7* and *4.8*, and *Table 4.1* summarise the sedimentary analysis:

**Facies 1**: From 0 to 35 cm, a greyish orange, poorly sorted, gravel occurs. The gravel content is composed of two types of iron stained pumice (dark and lightly coloured). The pumice are rounded to sub-rounded, and reach up to a couple cm in size. A well-defined boundary with the horizon beneath is present. The modal grain size is gravel (33% by weight), with significant medium sand (25%) and coarse sand (24%) also present.

**Facies 2:** From 35 to 105 cm, a pale yellowish brown, well sorted, medium-coarse sand occurs. There is a well-defined boundary with the top horizon. A few scattered pebbles are found in the horizon, however, they occur along the core wall and so are speculated to have been dragged down from the top, as the core descended. Small, angular shell fragments can be found throughout the horizon and two whole shells were observed, with an *Austrovenus stutchburyi* (cockle) at 36.5 cm, and a *Paphies australis* (pipi) at 82 cm. The modal grain size is medium sand (44%) with coarse sand also comprising a significant composition (38%). Fine sand contributes a lower composition (9%) that decreases moving down through the horizon.

**Facies 3**: Composed of two horizons. Horizon 3 occurs from 105 to 135 cm, and Horizon 4 occurs from 135 to 150 cm.

> From 105 to 135 cm, a pale yellowish brown, well sorted, iron stained, medium-coarse sand occurs. While very similar to the horizon above, it differs through being a slightly darker hue, containing more, and larger shell fragments. However, no whole shell fragments are found in this horizon. Similar to above, medium sand is the modal grain size (48%), although the coarse composition has gone down slightly (33%). while the fine sand composition has increased concurrently (13%).

From 135 to 155 cm, facies 3 continues, with a dip observed in the medium sand composition (39%), while the coarse sand composition increasing concurrently (38%). Additionally the very coarse sediment composition has increased (9%) while the fine sand composition has dipped (10%) making the two very similar.

**Facies 4**: Is made up of three horizons. Horizon 5 is from 155 to 175 cm, Horizon 6 is from 175 to 205 cm, and Horizon 7 is from 205 to 240 cm.

From 155 to 175, a pale yellowish brown, well-sorted, coarse-medium sand occurs. This horizon indicates a marked increase in the shell composition and size, although there is still no whole shell pieces. However, the size of the shell fragments allows for their identification as cockles. Coarse sand is modal here (43%), with a significant medium sand contribution (38%), while very coarse sand (10%) and fine sand (7%) contribute similar amounts.

Moving down through the core, Horizon 5 shows a band of sediment where the shell composition is decreased, and the grain composition varies slightly with more fine sands present. Medium sand (44%) and coarse sand (37%) have effectively switched in abundance, and a similar trend is seen with the fine sand (11%) and very coarse sand (8%).

The bottom 35 cm of the core are effectively the same as Horizon 5. Again coarse sand is modal (43%), while medium sand is also significant (35%). The very coarse sand (13%) is also essentially double the fine sand (7%)

In addition, all the above horizons contain varying minor levels of very fine sand, silts and clays, with the silts experiencing a spike. The silt proportion varies from 0.73% to 2.9%. Horizon 1 includes the widest range of grain sizes, consistent with its' poor sorting.


***Figure 4.7: Image of two open cut core sections from CS1. Colour wheel present as a reference for cross-core comparison and measuring tape spread between the components as a reference for length***

***Table 4.1: Grainsize composition with horizon change through CS1***

| Horizons | Clay | Silt | Very Fine Sand | Fine Sand | Medium Sand | Coarse Sand | Very Coarse Sand | Gravel |
|---|---|---|---|---|---|---|---|---|
| **1 0-35 cm** | 0.351 | 2.942 | 0.870 | 5.873 | 25.200 | 24.382 | 7.459 | 32.92 |
| **2 35–100 cm** | 0 | 0.767 | 0.085 | 9.402 | 44.249 | 38.241 | 7.255 | 0 |
| **3 105–135 cm** | 0.037 | 1.553 | 0.091 | 13.254 | 48.487 | 32.530 | 4.048 | 0 |
| **4 140–155 cm** | 0.082 | 2.773 | 0.666 | 10.364 | 38.791 | 38.386 | 8.938 | 0 |
| **5 160–175 cm** | 0 | 1.139 | 0.239 | 6.974 | 38.407 | 42.789 | 10.452 | 0 |
| **6 180–205 cm** | 0 | 0.849 | 0.120 | 10.629 | 44.265 | 36.069 | 8.069 | 0 |
| **7 210–240 cm** | 0 | 0.731 | 0.223 | 6.599 | 35.262 | 42.706 | 13.478 | 0 |

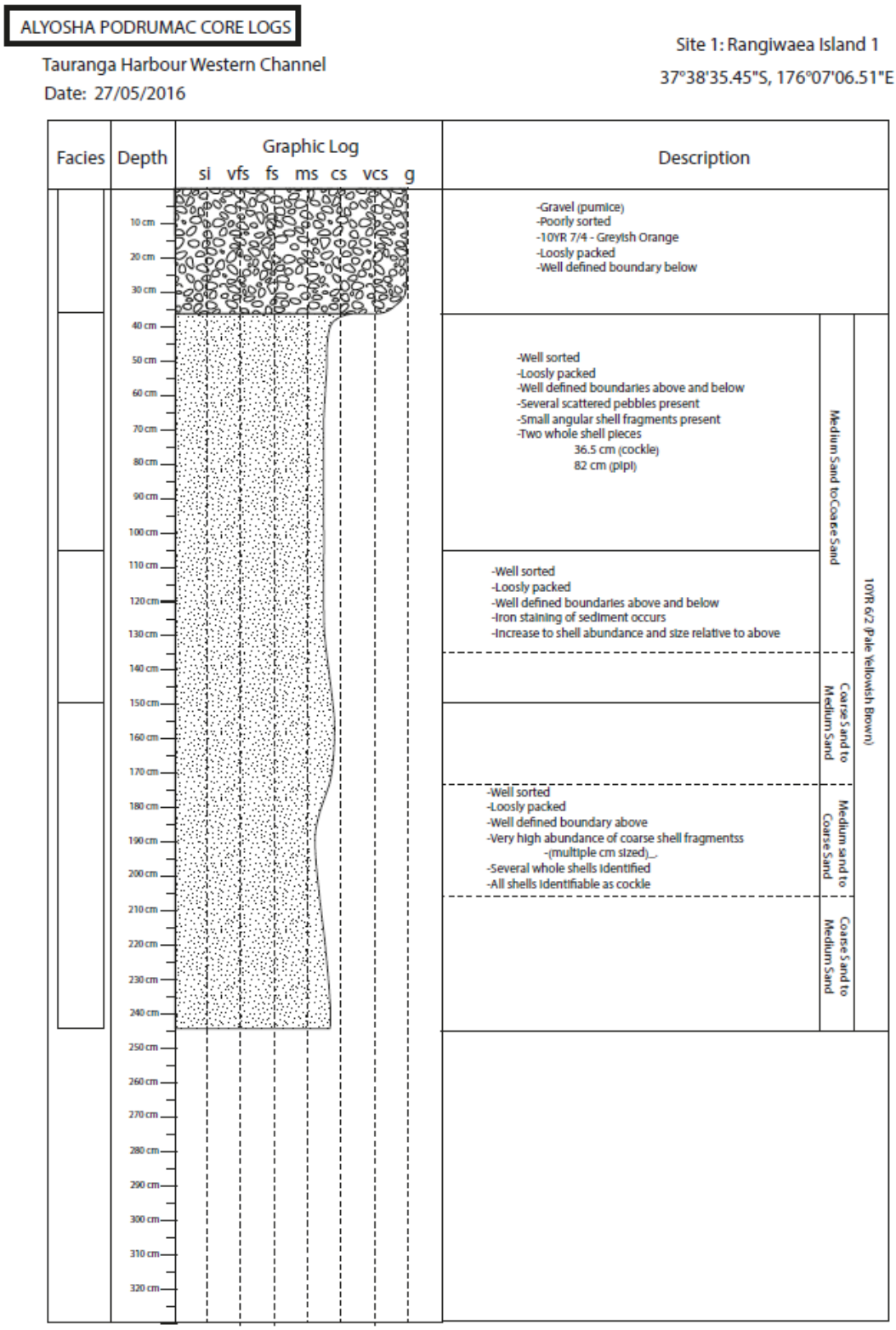


***Figure 4.8: Stratigraphic log for CS1***

### 4.6.2. CS2

CS2 was split into two components with the top 1/3 analysed independently of the bottom 2/3, due to some problems with core recovery. Additionally, the top 1/3 will just cover the visual aspect and interpretation of what is observed, while for the bottom, *Figures 4.9* and *4.10* and *Table 4.2* are complimentary to the analysis.

#### *4.6.2.1. Top Component*

The top component contains ~75 cm of sparsely filled core, with 30 cm of empty core present at the bottom, before the continuous fill of the bottom core component. Within this top component, there is an abundance of driftwood fragments and some gravels (pumice), along with sandy sediment. It is speculated that driftwood settled on the seafloor initially didn't allow the vibracorer to drill through the sea floor. Upon breaking through the driftwood, the topmost core contents settled loosely, and consequently moved with the water in the core.

#### *4.6.2.2. Bottom Component*

The bottom component is made up of 250 cm of continuous core and comprised of four horizons coinciding with four facies:

**Facies 1**: The top 30 cm of the core can be identified as a yellowish grey, poorly sorted gravel, with a discernible boundary with the horizon beneath. The gravel is identified as two types of iron stained pumice. All pumice clasts are rounded to sub-rounded, and up to 2 cm in size. The total gravel composition is ~30% (by weight). Subsequently, medium sand (27%) and coarse sand (25%) make up significant portions of the remaining sedimentary composition.

**Facies 2**: From 30 to 95 cm, a pale yellowish brown, well sorted, coarse-medium sand is identified. A distinct boundary occurs with the top horizon. Some pebbles (pumice) are still scattered through the horizon. However, the pebbles are believed to be derived from the top horizon, and dragged along the side of the core as it vibrated into the sediment. Shells become noticeable in the horizon in the form of small (mm sized), angular fragments. The coarse sand (41%) and medium sand (39%) compositions are nearly identical. The very coarse sand (11%) and fine sand

(10%) compositions are likewise nearly identical. At 55 cm, a slight increase in the shell composition (size and abundance) is noted.

**Facies 3**: From 95 to 150 cm, a dusky yellowish brown, well sorted, iron stained, medium-coarse sand is identified. The modal grain size here is medium sand (44%) and coarse sand is the second highest (36%). However, fine sand (15%) and very coarse sand (6%) are no longer similar. The top 30 cm features an initial decrease in shell abundance, followed by an increase in both size and abundance, through the bottom 25 cm. Species composition appears to be cockle.

**Facies 4**: The bottom metre of the core is identified as a dusky yellowish brown, well sorted, coarse-medium sand. The shell composition does not differ overtly from above, though the sediment composition shows a coarsening trend. Increases to coarse sand (43%) and very coarse sand (10%) occur, while decreases to medium sand (39%) and fine sand (7%) also occur.

Additionally, the levels of very fine sand, silt, and clay are greatly reduced, although a small spike in the silt component of the core occurs. The silt composition ranges from 0.50% to 2.0%. Horizon 1 includes the widest range of grain sizes, consistent with its' poor sorting.


***Figure 4.9: Image of three open cut core sections from CS2. Colour wheel present as a reference for cross-core comparison and measuring tape spread between the components as a reference for length***

***Table 4.2: Grainsize composition with horizon change through CS2***

| Horizons | Clay | Silt | Very Fine Sand | Fine Sand | Medium Sand | Coarse Sand | Very Coarse Sand | Gravel |
|---|---|---|---|---|---|---|---|---|
| **1 0 – 30 cm** | 0.046 | 2.020 | 0.235 | 8.157 | 27.518 | 25.174 | 6.849 | ~30 |
| **2 30 – 95 cm** | 0 | 0.926 | 0.136 | 9.767 | 38.410 | 40.718 | 11.105 | 0 |
| **3 95 – 150 cm** | 0 | 2.088 | 0.265 | 14.925 | 43.712 | 35.674 | 5.687 | 0 |
| **4 155 – 250 cm** | 0 | 0.500 | 0.105 | 7.338 | 38.871 | 43.048 | 10.139 | 0 |

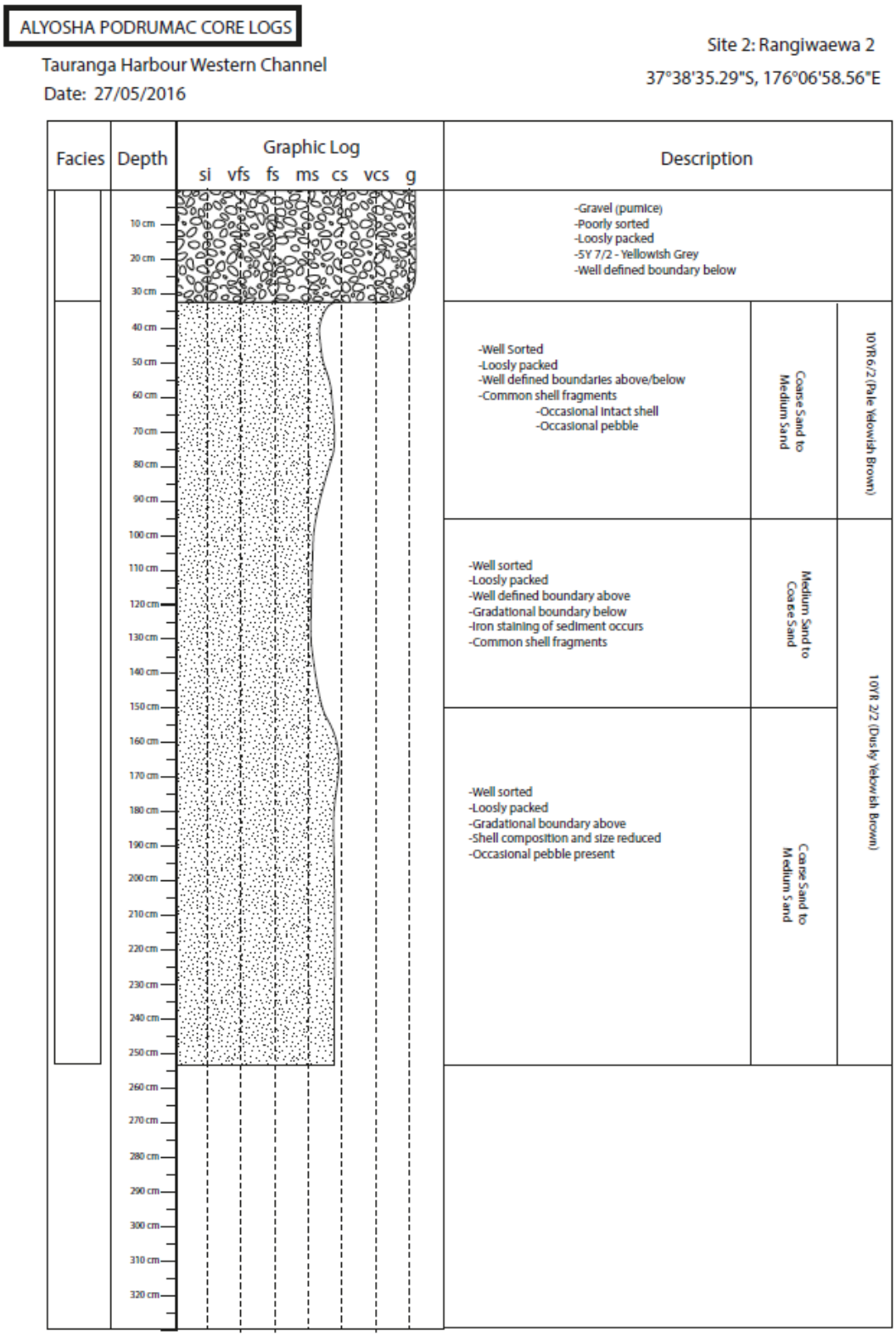


***Figure 4.10: Stratigraphic log for CS2***

### *4.6.3.* CS3

At CS3, nine horizons are split into two facies (facies 1 = horizon 1, facies 2 = horizons 2- 9), identified over a depth of 310 cm. *Figures 4.11* and 4*.12*, and *Table 4.3* are complimentary to the sedimentary interpretation:

**Facies 1**: The top 15 cm is greyish blue green, fine-medium sand. The layer has a very sharp and well defined boundary with the horizon beneath it. A high shell proportion is present that ranges in size from very small fragments to a whole cockle shell (3 X 2 cm). The modal grain size is medium sand (33%) with similar contributions of fine and coarse sands (both 24%).

**Facies 2:** Eight horizons are identifiable that occur as a gradational sequence:

From 20 to 90 cm, horizons 2 and 3 two horizons are identified as a light brownish grey, well sorted sand. A well-defined boundary occurs between horizons 1 and 2. A gradational trend in sediment texture occurs, with medium sand modal (33%) in Horizon 2 (20 to 30 cm) to fine sand modal (42%) in Horizon 3 (30 to 90 cm).

From 90 to 115 cm, a light olive grey, moderately sorted, silt to very fine sand with bimodality observed in silt (29%) and fine sand (28%). A large, whole cockle (3 cm X 3 cm), occurs within the horizon.

From 115 to 130 cm and 130 to 195 cm, two light olive grey, silt horizons are identified, distinguished by their variable silt composition (50% at Horizon 5 and 63% at Horizon 6). Several small shell fragments are scattered through Horizon 7.

The bottom 115 cm finds three horizons that display the same trends as horizons 2-4, but in reverse. The same colour (light brown grey) and shell compositions are observed (e.g.h7 = h4, h8 = h3, h9 = h2), as are highly similar sediment compositions.


***Figure 4.11: Image of three open cut core sections from CS3. Colour wheel present as a reference for cross-core comparison and measuring tape spread between the components as a reference for length***

***Table 4.3: Grainsize composition with horizon change through CS3***

| Horizons | Clay | Silt | Very Fine Sand | Fine Sand | Medium Sand | Coarse Sand | Very Coarse Sand | Gravel |
|---|---|---|---|---|---|---|---|---|
| **1 0–15 cm** | 0.752 | 6.003 | 6.852 | 23.339 | 33.483 | 24.226 | 5.345 | 0 |
| **2 20–30 cm** | 0.992 | 5.154 | 8.652 | 31.118 | 32.736 | 17.037 | 4.310 | 0 |
| **3 30–90 cm** | 3.134 | 13.999 | 18.727 | 41.500 | 21.019 | 1.573 | 0.047 | 0 |
| **4 90–115 cm** | 7.724 | 29.465 | 23.437 | 27.850 | 10.237 | 1.252 | 0.034 | 0 |
| **5 115–130 cm** | 12.366 | 50.188 | 24.377 | 11.724 | 1.337 | 0.008 | 0 | 0 |
| **6 130–195 cm** | 16.301 | 62.646 | 14.139 | 5.320 | 1.495 | 0.099 | 0 | 0 |
| **7 195–205 cm** | 9.926 | 32.993 | 15.105 | 27.316 | 14.496 | 0.164 | 0 | 0 |
| **8 205–280 cm** | 3.649 | 15.035 | 14.693 | 42.634 | 23.128 | 0.818 | 0.043 | 0 |
| **9 280–310 cm** | 0.729 | 4.591 | 12.716 | 49.511 | 29.289 | 3.147 | 0.019 | 0 |

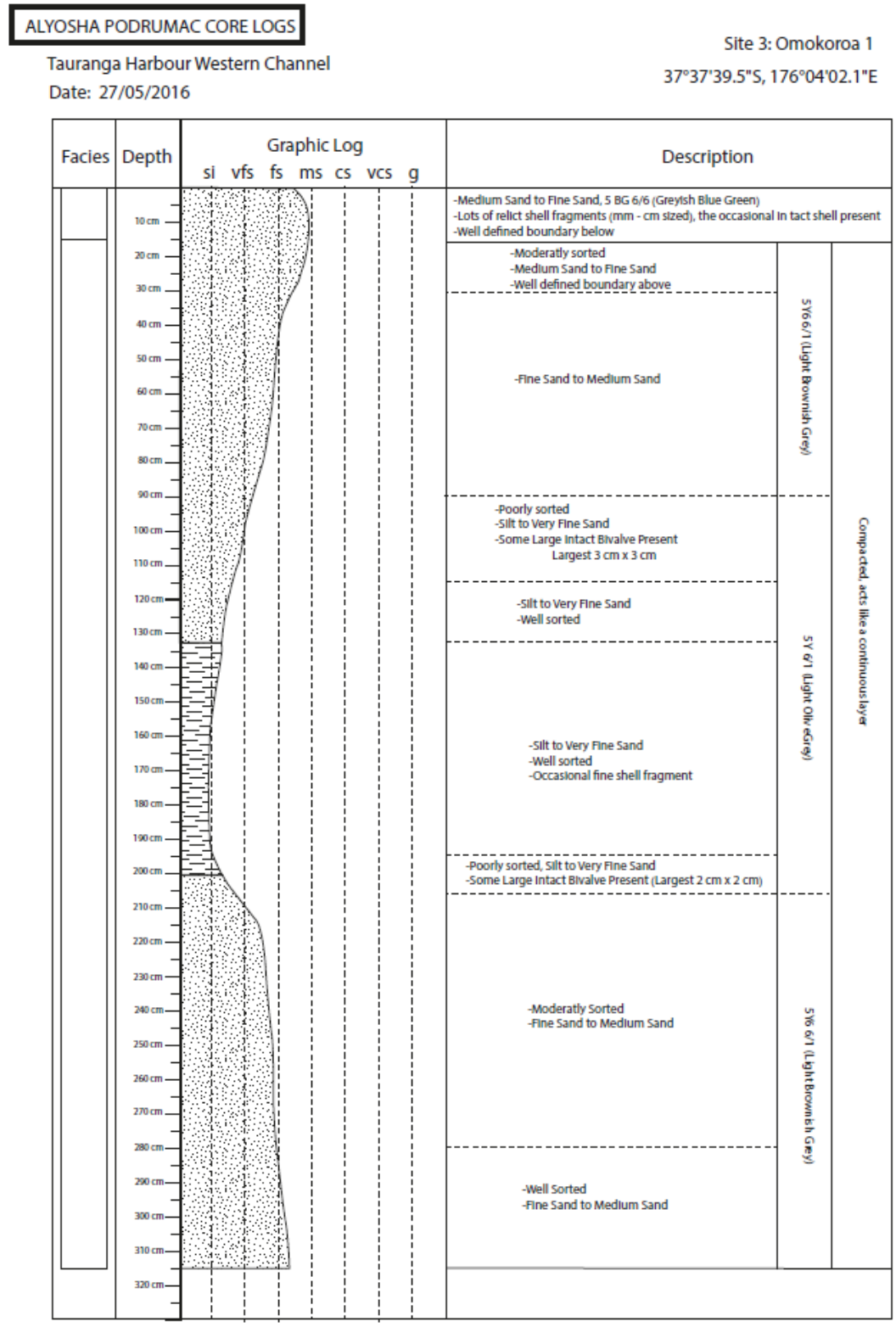


***Figure 4.12 Stratigraphic log for CS3***

### *4.6.4.* CS4

At CS4, four horizons are split into two facies (facies 1 = horizons 1-3, facies 2 = horizon 4), to a depth of 305 cm. No sharp boundaries are observed in the core. *Figures 4.13* and *4.14*, and *Table 4.4* are complimentary to the sedimentary analysis:

**Facies 1**: Three gradational horizons are identified from 0 to 25 cm, 25 to 165 cm, and 165 to 255 cm:

> The top 25 cm is pale yellowish green, well sorted medium sand. The modal grain size is medium sand (44%) with similar contributions of fine sand (20%) and coarse sand (25%). No shells are observed here, although occasional pebble fragments are observed scattered throughout.
>
> From 25 to 165 cm, the presence of very small, rare shell fragments can be identified, which increase in size an abundance with depth. Additionally, a decrease to coarse sands (11%) occurs with a concurrent increase to fine sands (35%) relative to horizon 1.
>
> From 165 to 255 cm, there are minimal changes to the grain size composition, although very coarse sands have increased (17%) while fine sands have decreased (29%). However, the colour changes slightly, now identifiable as Pale Green. Additionally, the shell abundance and size continues to increase, with a 10-15% shell proportion present.

**Facies 2**: The bottom 50 cm of the core is a greyish orange, medium sand. The horizon features a high proportion of shell, which fluctuates in bands from ~20% to >50%. The sand composition shows a very even spread with medium sand modal (37%), whilst fine sand (23%) and coarse sand (26%) are similar.

All horizons contain reduced very fine sands, silts and clays, with silts featuring a small spike, ranging in composition from 2.5% to 6.4%.


***Figure 4.13: Image of three open cut core sections from CS4. Colour wheel present as a reference for cross-core comparison and measuring tape spread between the components as a reference for length***

***Table 4.4: Grainsize composition with horizon change through CS4***

| Horizons | Clay | Silt | Very Fine Sand | Fine Sand | Medium Sand | Coarse Sand | Very Coarse Sand | Gravel |
|---|---|---|---|---|---|---|---|---|
| **1 0–25 cm** | 0.034 | 6.368 | 2.228 | 20.816 | 43.615 | 25.270 | 1.703 | 0 |
| **2 30–165 cm** | 0 | 3.348 | 1.590 | 35.879 | 48.502 | 10.357 | 0.323 | 0 |
| **4 165–255 cm** | 0.003 | 2.727 | 1.197 | 29.660 | 46.459 | 17.098 | 2.860 | 0 |
| **5 255–305 cm** | 0 | 2.554 | 1.383 | 22.333 | 36.909 | 25.739 | 11.082 | 0 |

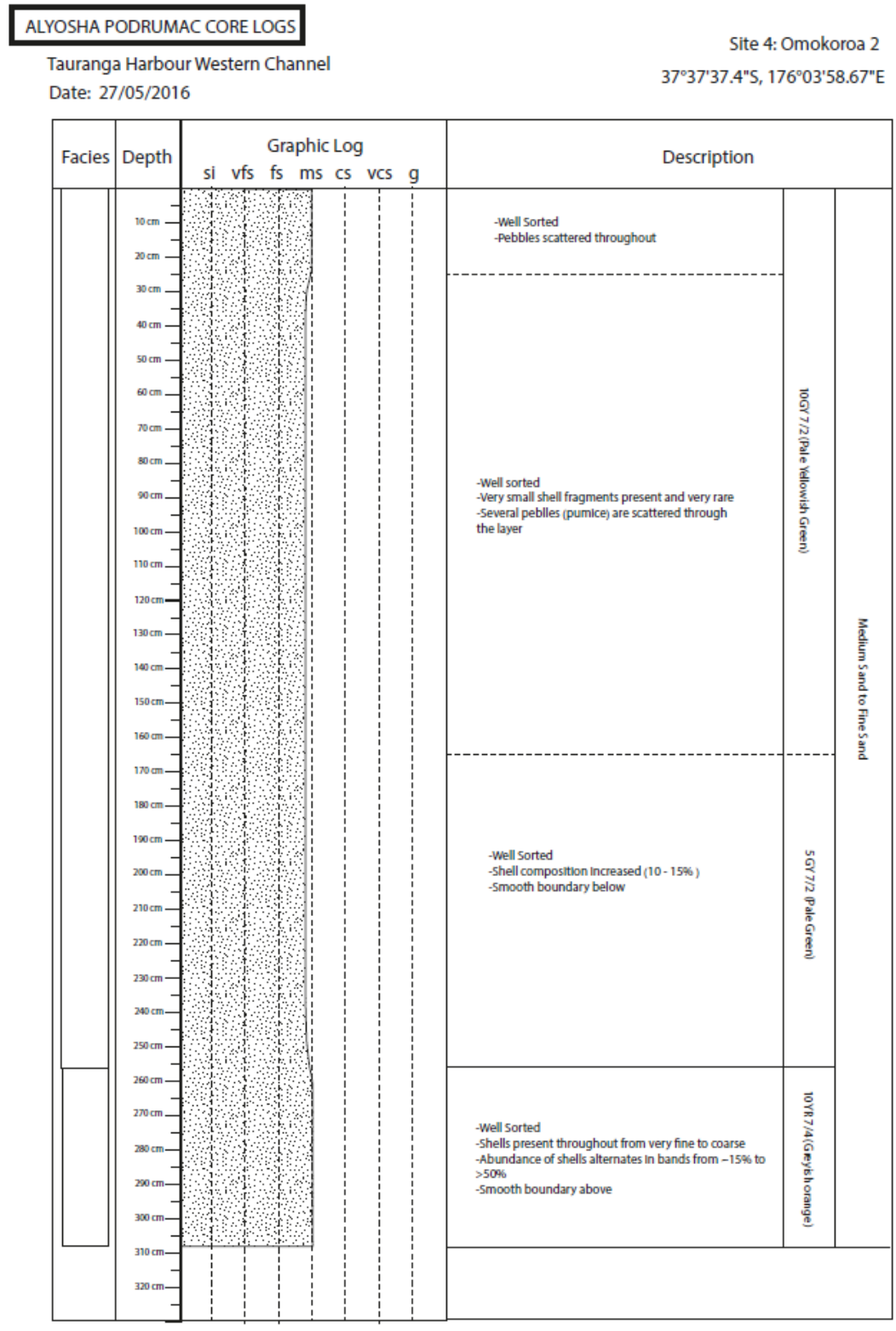


***Figure 4.14: Stratigraphic log for CS4***

### *4.6.5.* CS5

At CS5, four horizons are split into three facies (facies 1 = horizon 1, facies 2 = horizon 2, facies 3 = horizons 3 – 4), to a depth of 220 cm. *Figures 4.15* and *4.16*, and *Table 4.5* are complimentary to the sedimentary interpretation:

**Facies 1**: The top 35 cm is a moderate olive brown, well sorted, medium-fine sand. A clear colour boundary is observed with the layer beneath. Very fine shell fragments occur scattered throughout the horizon. The modal grain size is medium sand (46%) while fine sand (29%) and coarse sand (12%) also contribute significant amounts to the sedimentary composition.

**Facies 2**: From 35 to 130 cm, a pale yellowish brown, moderately sorted, medium sand occurs. Sharp boundaries occur at both the surrounding layers. The proportion of shell increases initially with depth, then reduces slightly over the bottom 30 cm. A whole cockle is present at 75 cm. Modal grain size is medium sand (42%), with lesser proportions of fine sand (31%) and coarse sand (15%).

**Facies 3**: Two gradation horizons occur from 130 to 165 cm:

> From 130 to 165 cm, a pale yellowish brown, moderately sorted medium sand occurs. A boundary can be noted with the layer above with a sudden decline in the shell composition. Additionally, several gastropods occur in the horizon, and a much reduced scatter of very fine shell fragments is present. The modal grain size is still medium sand (46%), with fine sand also high (33%), while coarse sand has reduced (6%).
>
> From 165 to 215 cm, a pale yellowish brown, moderately sorted medium sand occurs. The top half of the horizon is visually similar to horizon 3, though the bottom features a slight increase in the shell composition. The most evident difference in the horizons is the sedimentary composition, with medium sand still modal (43%), although fine sand decreases markedly (24%), while coarse sands increases (21%).

All horizons contain silt, much like the other cores. However, it is notable that the silt concentrations are much greater, now ranging from 7% – 12%.


***Figure 4.15: Image of two open cut core sections from CS5. Colour wheel present as a reference for cross-core comparison and measuring tape spread between the components as a reference for length***

***Table 4.5: Grainsize composition with horizon change through CS5***

| Horizons | Clay | Silt | Very Fine Sand | Fine Sand | Medium Sand | Coarse Sand | Very Coarse Sand | Gravel |
|---|---|---|---|---|---|---|---|---|
| **1 0 –35 cm** | 0.466 | 9.029 | 3.433 | 28.872 | 45.571 | 12.439 | 0.190 | 0 |
| **2 35 –130 cm** | 0.085 | 6.551 | 5.274 | 30.694 | 42.122 | 14.893 | 0.381 | 0 |
| **3 130 – 165 cm** | 0.707 | 11.673 | 1.790 | 33.028 | 46.434 | 6.367 | 0 | 0 |
| **4 165 – 220 cm** | 0.339 | 7.370 | 2.900 | 24.196 | 42.759 | 20.618 | 1.820 | 0 |

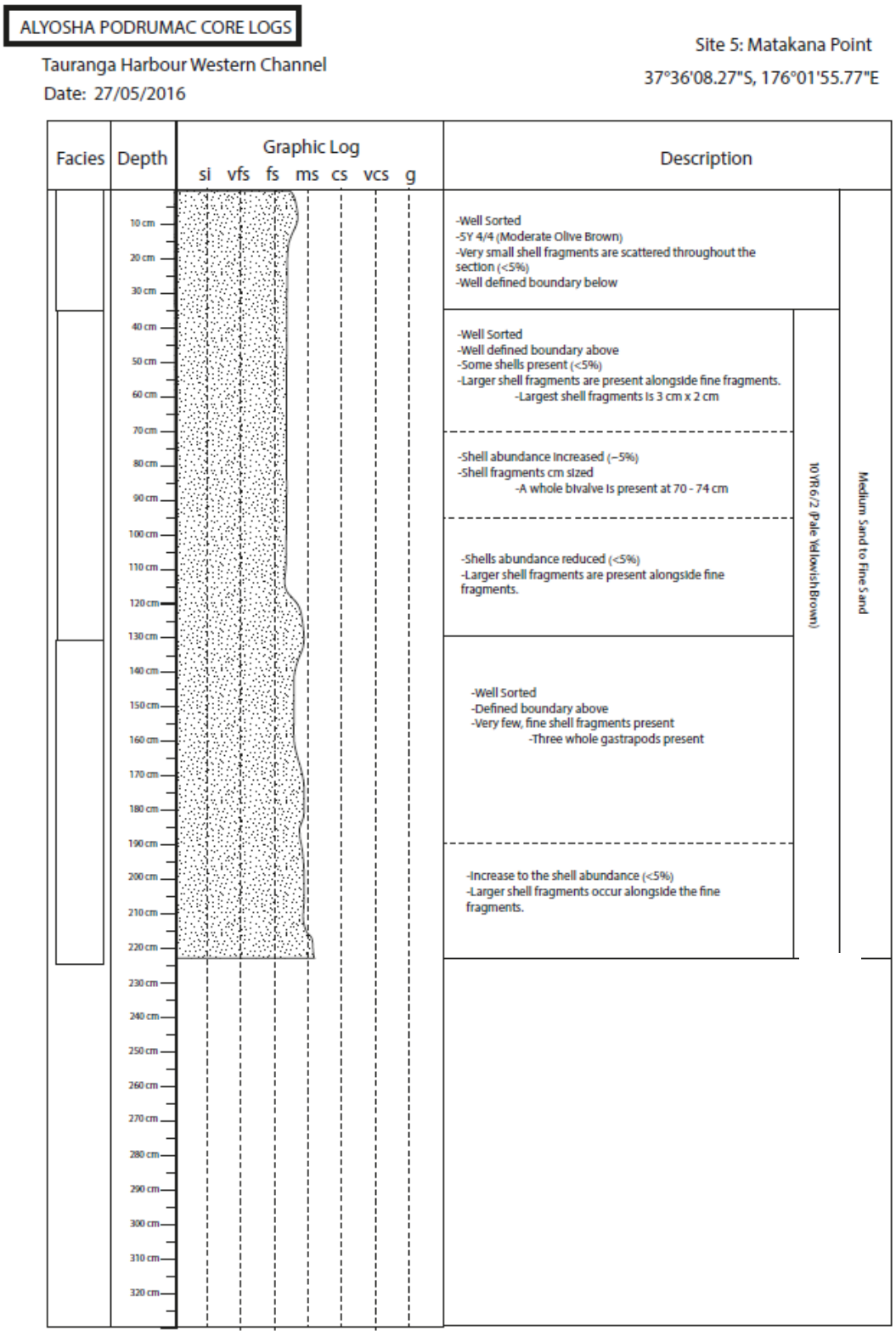


***Figure 4.16: Stratigraphic log for CS5***

## 4.7. Facies Interpretation

A facies analysis of each core group is presented, summarising the trends observed in the stratigraphic interpretation.

### *4.7.1.* CG1

At CG1, both CS1 and CS2 display the same sedimentary structure with depth. Essentially two depositional facies are identifiable. The top ~30 cm in the area is a pumice rich deposit, while beneath that is sandy-shelly sediment. Two types of pumice can be identified (dark and light material), which suggests a dual origin, and the rounding of clasts indicates secondary transport, post primary deposition (Carey et al., 2001). The sharp boundary between the top facies and the one beneath, indicates a change in the depositional environment. Additionally, beneath facies 2, another sharp boundary with a subsequent presence of iron stained deposits is identified, suggesting a significant age difference. Beneath ~150 cm, the two cores differ, with CS1 featuring more large and abundant shells, while CS2 remains similar to the overlying facies.

### *4.7.2.* CG2

Unlike CG1, the two cores of CG2 (CS3 and CS4) are highly variable. CS3 can be split into two environment facies. The top ~15 cm is a sandy, shell rich deposit. Beneath that is a very sharp boundary, separating the remainder of the core, which is composed of dark, compact and fine sediment. Changes to the dominant sediment grain size occur with depth through facies 2, which starts as a medium sand, transitions down to silt, and then to a fine sand at the bottom of the core. The changes observed are all very smooth, which indicates an undisturbed environmental evolution. Several shells can also be identified with depth, including two intact cockles.

CS4 can also be split into two facies, although the entire structure of the core is identifiable as medium sand. The first facies occurs to a depth of 255 cm, as a medium sand that has a gradually increasing shell composition. No shells are observed in the more recent sediment, whilst 10-15% shell is present at the bottom of the facies. The second facies can also be identified as a medium sand, although

a change in colour, and rapid increases to shell composition occur. At the bottom of the core, facies 2 consists of >50% shell.

The differences between the cores suggests that CS3 has been uplifted, and prior to the formation of the top facies has been eroded. The top facies itself, has been deposited rapidly and does not dictate a change in the environment. CS4 meanwhile, indicates a very high sedimentation rate that is likely fuelled by the erosion of CS3.

### *4.7.3.* CG3

At CG3 three facies are identified. The top 35 cm clearly a different colour to the rest of the core. The first facies change, between facies 1 and 2, shows a sharp change in colour and features an erosional boundary, suggesting a significant age difference. The core then shows sediment coarsening down to a depth of 130 cm, with the shell composition increasing with depth also. A second boundary can be observed at 130 cm, where the horizon from 130 cm to 190 cm, becomes finer, and features a change in shell composition, with several gastropod shells present alongside very fine bivalve fragments. The bottom component of the cores shows a coarsening of sediment again and an increase in the bivalve composition. Thus, an environmental change is predicted between facies 2 and 3.

### *4.7.4.* Silt Composition

Although the levels of silts and clays are generally low, they are higher than would be expected from the NIWA sediment modelling study that indicated that this silts are exported out of the harbour from the main channels (**Chapter 2**). The size distribution for facies 1 in CG1 is also inconsistent with the predictions of Kwoll and Winter (2011) based on the hydrodynamics.

## 4.8. Summary

- Vibracoring operates on the principles of thixotropy, by sending vibrations through a drill rod, reducing the shear resistance of sediment and penetrating through the ground under very limited pressure. It is a preferred method to traditional coring techniques for semi- to un-consolidated sedimentary

environments, in marine, coastal, estuarine, fluvial, and some terrestrial settings. Unlike traditional coring mechanisms, vibracoring causes minimal to no disturbance of grains as it penetrates the sediment.

- Five cores sites were sampled through the Western Channel and split into three groups. The three groups are distributed to gauge how sedimentation patterns vary along the upper Western Channel, with CG1 at the southeastern boundary of the field area, CG2 at roughly midway, and CG3 at the northwestern extent of the field area. Additionally, CG1 and CG2 are comprised of two core sites each to ascertain how sedimentation patterns vary locally at the two sites, and to assess if there is evidence for fault displacement.
- Sediment cores were described and a facies interpretation is presented:
    - CG1 identifies 5 facies. The top 3 facies of the two cores are similar, while the bottom facies of CS1 is seemingly older than the bottom facies of CS2. There is likely a large age difference between facies 2 and 3 in CG1 also.
    - CG2 is comprised of two very different cores. CS3 features two facies, a shelly sand at the top with a sharp erosional boundary, into a series of gradational horizons. CS4 also features two facies, both identifiable as medium sand from top to bottom, with a smooth boundary between the facies and an increasing shell abundance with depth. CG2 provides evidence for a fault with CS3 uplifted and CS4 downthrown.
    - CG3 identified 3 facies, with distinct boundaries between each facies. The grainsize varied minimally with depth, although shell composition differences are observable, as is a clear colour change between facies 1 and 2. A significant age difference is also suggested between facies 1 and 2.
- All sites also showed a reduced presence of silts, which is inconsistent with NIWA sediment modelling, and the top facies of CG1 is inconsistent predictions based on hydrodynamic

# CHAPTER 5
# DISCUSSION

## 5.1 Introduction

This chapter creates a conceptual model for the evolution of the upper Western Channel based on the results of **Chapter 3: Seismic Survey Interpretation** and **Chapter 4: Sediment Coring Interpretation**, and compares the findings with existing literature. The interpretation is split into **5.2. Evolution of Upper Western Channel Sedimentary Deposits** – where sedimentation patterns along the Western Channel are discussed in relation to the development of the channel over time, **5.3. Structural Interpretation** – where the faulting identified through the field area is discussed, and **5.4. Summary** – where the key points of the chapter are summarised.

## 5.2 Evolution of Upper Western Channel Sedimentary Deposits

The sedimentary evolution is split into three components; (1) a discussion of Holocene fluvial sedimentation patterns, (2) a discussion of Holocene tsunami deposits, and (3) a brief discussion on the pre-Holocene deposits identified. *Table 5.1* shows how the facies identified in the sedimentary cores (**Chapter 4**) relate to the three categories.

***Table 5.1: Correlation of Core Site and Core Group facies, to one of three categories; Fluvial Holocene Deposits, Tsunami Holocene Deposits, or Pre-Holocene Deposits***

| Core Group | Core Site | Fluvial Holocene | Tsunami Holocene | Pre-Holocene |
|---|---|---|---|---|
| **CG1** | CS1 | Facies 2 | Facies 1 | Facies 3,5 |
| | CS2 | Facies 2 | Facies 1 | Facies 3-4 |
| **CG2** | CS3 | N/A | Facies 1 | Facies 2 |
| | CS4 | Facies 1-2 | N/A | N/A |
| **CG3** | CS5 | Facies 1 | N/A | Facies 2-3 |

### 5.2.1 Fluvial Deposits

Holocene estuarine deposits are identified as facies 1 in CS4 and CG3, and facies 2 in CG1 (*Table 5.1*). These deposits are composed of predominantly sand, with very minor silt compositions (**see Chapter 4: Sediment Coring Interpretation**). The relative sand compositions vary along the channel, which provides an indication of the hydrodynamic influence on sedimentation patterns. Locally, the sediment composition and texture also varies with depth beneath the seabed, allowing a reconstruction on the hydrodynamic changes over time for each site. Thirdly, combining the knowledge of the hydrodynamics and sedimentary sequences, with a review of harbour sedimentary sources, the relative contributions of the local sources can be inferred. Finally, the rates of sedimentation can be calculated for the core sites, and compared with other locations through the harbour. Thus, relative rates of infilling can be estimated for the Western Channel, on the basis of channel dynamics.

#### *5.2.1.1 Sedimentary Change through the Harbour*

A comparison of the sedimentary texture along the Western Channel, from the tidal flats (CG5) towards the central harbour (CG1), shows a trend of coarsening sediment from medium-fine sand to medium-coarse sand. Additionally, the silt proportion shows a similar but opposite trend, with the highest proportions near the tidal flats close to Matakana Point (~9%), and the lowest towards the Centre Bank end of the channel (<3%).

These patterns are consistent with patterns in other estuaries around New Zealand (Heap and Nichol, 1997; Abrahim et al., 2008; Kennedy et al., 2008), and can be considered a consequence of stronger tidal currents occurring closer to the tidal inlet, and weaker currents closest to the central tidal flats. Stronger currents exhibit more potential to transport finer grades of sediment (through suspension) out towards the open coast, while also having potential to mobilise increasingly coarser sediment through saltation. As a result, a sequence from finer to coarser sand deposits are typically observed along major tidal channels heading seaward through estuaries.

However, the distribution of sandwaves discussed in **Chapter 3**, modifies this pattern. The sediment within the sandwaves tends to be coarser than the adjacent

regions without sandwaves. The sandwaves also occur in patches. Hence, although there is a general trend of coarsening towards the harbour entrance, in areas of enhanced flow and possibly increased sediment input, there are localised deviations from this trend.

#### *5.2.1.2 Sediment Change with Depth*

At CG1, there are minimal changes within the Holocene sediments with increasing depth, although there is a slight trend of increasing shell abundance and size. This is interpreted as a consequence of increasing estuary infilling, with the initial (young) estuary having a larger tidal prism and therefore stronger currents, resulting in greater transport of shelly deposits.

At CS4, two Holocene facies are identified with a gradational boundary observed between the two. The facies change is attributed to a hydrodynamic change at the site during the Holocene. The area around the Omokoroa Peninsula, before the formation of the Matakana Barrier Island, drained out to the ocean through a tidal inlet around present day Hunters Creek (Shepherd et al, 1997; Christophers, 2015). With the closure of the inlet soon after the establishment of modern sea levels around 5.2 ka (*Figure 5.1a/b*), the drainage of the area surrounding Omokoroa shifted, possibly to the modern tidal inlet in the east. The change in facies observed in CS4 between facies 1 and 2 are inferred to be a result of this shift. Essentially, the older facies is a much more shell rich deposit, consistent with facies that form near tidal inlets and under strong currents (Healy, 1985), and reflecting the higher densities of shellfish within sediments close to the tidal inlet (Cole et al, 2000). Subsequently, the adjustment of the tidal discharge to a more distal inlet meant reduced currents through the area, and resulted in the observed phenomenon of a rapidly reducing shell proportion.

At CG3, much like CG1, minimal change with depth below the seabed is observed through the Holocene facies. However, the key factor to consider here is a low sedimentation rate. Evidence within the core shows an anoxic environment upon retrieval (*Figure 5.2*). The anoxic environment indicates a low energy and/or high productivity (Demaison and Moore, 1980), both of which are consistent with a rapidly shallowing channel at the location.

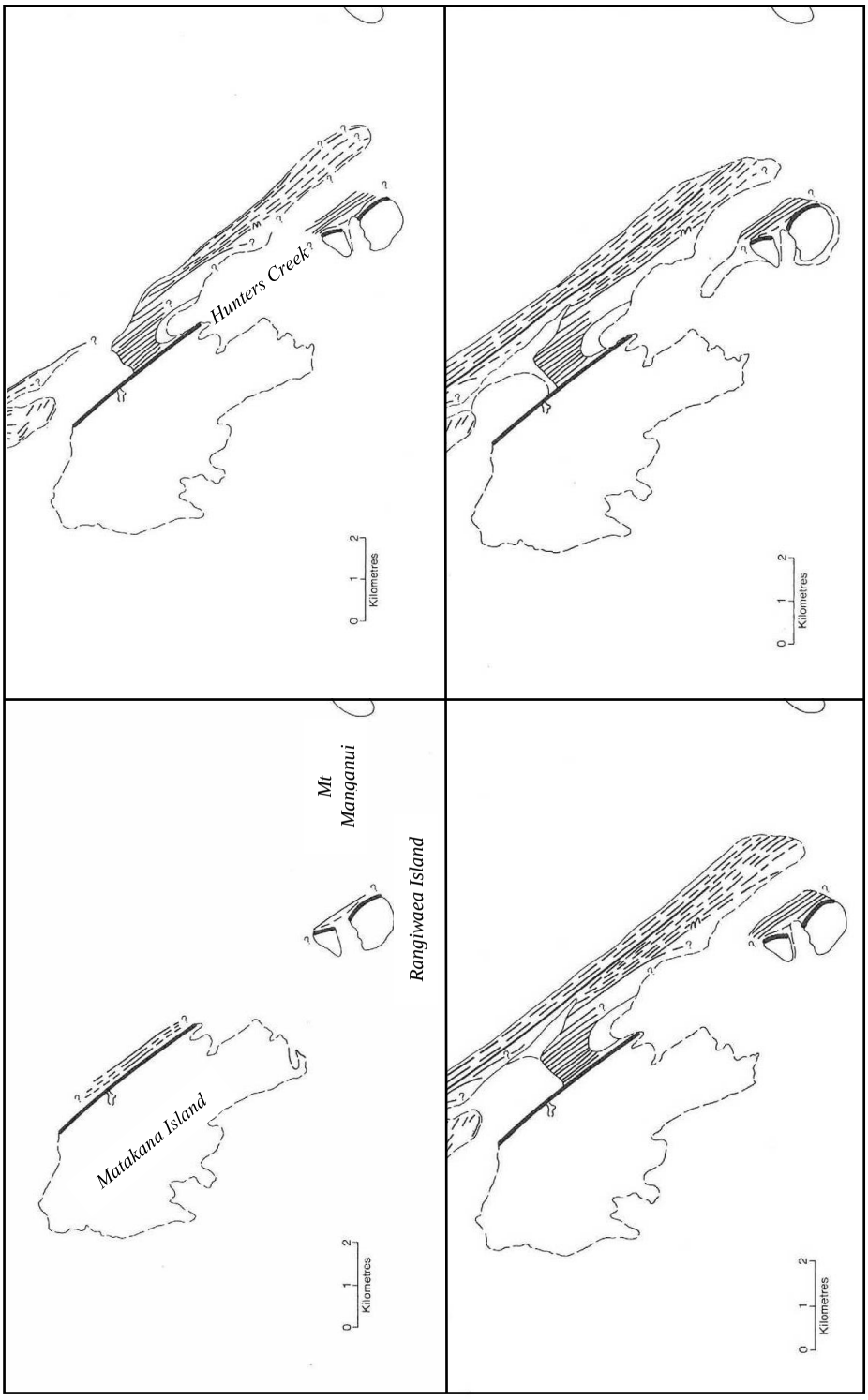


***Figure 5.1: Evolution of the Matakana Barrier Island. (a)6,000 Cal BP, (b)4,000 Cal BP, (c)1,750 Cal BP, and (D) 600 Cal BP. From Shepherd et al (1997)***

***Figure 5.2: Anoxic units seen in CS5 in the upper 20 cm. These units rapidly oxidised once the core was opened.***

#### *5.2.1.3 Sedimentary Sources*

Potential sediment sources that have been identified for the Tauranga Harbour include local erosion (MacGibbon, 2011; Christophers, 2015), terrestrial inputs (THSS, 2009), and storm and tsunami overwash of Matakana Island (Shepherd, 1997).

At each location where sandwaves are evident (**Chapter 3)**, a local erosional source of sedimentation can also be identified in the form of eroding coastal cliffs. This suggests that sedimentation within the harbour is driven primarily through locally sourced erosion. This hypothesis is supported by a comparison of the sediment core stratigraphies. CS4 has the most evident source of a locally sourced sediment, derived from erosion of the uplifted surface at CS3. Comparing CS4 to the other core sites through harbour, CS4 also has the most distinctly thick Holocene deposit (>250 cm), significantly more than observed at any other core site.

Meanwhile, the THSS (2009) showed that the terrestrial input of sediment from the catchments discharging into Tauranga Harbour are mostly silts. It is still possible for even a minimal sand sediment yield from catchments to fuel rapid accretion under the correct conditions (Kuehl et al., 2016). However, the upper Western Channel is located some distance from the fluvial catchments on the mainland, and there are no significant fluvial discharges from Matakana Island. Shepherd et al (1997) have identified that erosion of Matakana Island during storm events can also provide a flux of sediment into the harbour. However, this appears to have primarily occurred during the early development of the Holocene deposits of Matakana Island, and does not appear to have occurred over at least the last 3000 years.

Hence, it is concluded that there is sufficient evidence (with particular reference to CG2 and sandwave occurrence), to suggest that sedimentation within the harbour is driven primarily through locally sourced erosion, while the other sources have reduced impacts.

#### *5.2.1.4 Rates of Sedimentation*

Due to budget limitations, dating of material within the cores did not occur. Instead ages were inferred mostly from the presence of erosional boundaries between facies and the degree of weathering indicated by colour. Consequently, the rate of sedimentation was calculated based on the *inferred* Holocene sediment thickness, and the time since the establishment of modern sea level for New Zealand, taken as 7,200 cal ky BP (de Lange et al., 2015).

At CG1, the Holocene sediment is ~65 cm thick, beneath a surficial tsunami deposit correlated to 1400 – 1500 AD (*discussed below in **5.3***). This gives a sedimentation rate of 0.0977 mm/yr (7,200 BP – 500±50 BP). At CG2, only one of the two cores (CS4) has a clearly defined Holocene facies. However, the entire recovered core (305 cm) is believed to be Holocene. Thus, accurately stating the Holocene sediment is even more problematic, given that the total depth of Holocene sediment remains unknown. Consequently, the sedimentation rate is stated as a minimum of 0.436 mm/yr (7,200 BP), with the rate likely to be greater if the Holocene sediment is thicker than the core sampled. CG3 contains the thinnest Holocene facies, with 35 cm. Thus, the sedimentation at the site can be calculated as 0.0482 mm/yr (7,200 BP).

The highest rate of sedimentation (CS4) occurred at a location experiencing large sandwaves in the Western Channel (SS3). A similar area of sandwaves was observed at SS1, and so a similar rate of sedimentation is predicted for that location. Meanwhile, the seismic profiles at CG1 did not display any sandwaves, and so the rate determined there is presumed to be representative of the flat (no sandwave) surfaces through much of the central Western Channel, from Rangiwaea Island to the Omokoroa Peninsula. No coring was undertaken of sandwave structures observed at SS2 and SS4. Given that sandwaves observed at these locations were significantly smaller in height and wavelength than those at SS1 and SS3, the sedimentation rate is assumed to lie between those calculated at CG1 and CG2,

although likely closer to the CG1 rate than the latter. Finally, CG3, which correlated to SS5 is found to have the lowest rate of Holocene sedimentation within the Upper Western Channel, despite the sandwaves present.

Thus, the controls on sedimentation rates through the Western Channel can be linked to two factors: sediment supply and current strength. Effectively, where currents can sufficiently mobilise more sediment, greater rates of sedimentation are observed (e.g. CG1 vs CG3). Additionally, where there is a more readily available source of sediment, greater sedimentation rates will be experienced (e.g. CS4 vs CG1). In the instances identified through the Western Channel, the sedimentation process is likely driven by local erosion (e.g. CS4 sediment is sourced from erosion at CS3).

Comparing the sedimentation rates to other locations through the harbour, the two central Western Channel sites are accreting at rates greater than has been observed elsewhere in the harbour. This is consistent with literature, due to highly mobile sediment present in the channels (Bokuniewicz et al., 1977). The upper channel site is meanwhile accreting at a rate similar to the tidal flats of eastern Omokoroa Peninsula (Christophers, 2015). The similar sedimentation rate is further evidence of a local erosional source of sediment for CG3 (from Matakana and Flax Points), with sedimentation at eastern Omokoroa maintained by erosion of the Omokoroa Peninsula.

#### *5.2.1.5 Tsunami Deposits*

Two facies identified appear to be anomalous compared to their present day environments. These are the pumice rich deposit found atop the two cores of CG1, and the sandy shelly deposit atop CS3 (*Table 5.1*). These two deposits can be classed as "event deposits" – an episodic deposit of short duration of unusual or high energy processes relative to everyday normal conditions or "background deposits" (Bourgeois, 2009). Event deposits can occur due to a range of factors, including storm events and tsunamis. In the instance of the deposits at CG1 and CS3, they are considered as probable tsunami deposits.

Characteristics of tsunami deposits are discussed in a range of research papers including Atwater, (1987), de Lange et al. (1991), Carey et al. (2001), Goff et al.

(2001), Tuttle et al. (2004), Dawson and Stewart, (2007), de Lange and Moon (2007), Morton et al. (2007), Bourgeois (2009), Goff et al. (2012) and Goto et al. (2012), with following criteria observed in the deposits of CG1 and CS3:

(I) Lower contact is often unconformable or erosional

(II) Deposits can range in clast size from mud to boulders, though will commonly be in the form of an anomalous unit (e.g. a sand in a peat formation)

(III) Deposits can be either:

a. A single homogenous, structureless layer indicative of rapid deposition, as occurs when the flow decelerates between the uprush and backwash

OR

b. Display normal grading, due to transport in suspension with coarser fragments near the bottom

(IV) Shell rich layers, commonly of larger or intact shells as opposed to shell hash, and often found transported farther than other tsunami deposits

(V) Pumice layers, often found transported farther than other tsunami deposits due to low density. May display grading with larger clasts featuring lower density

(VI) Deposits can be up to 1 m thick, though most commonly are 25 cm and less

**CG1**

The gravel rich deposit of CG1 agrees with factors (I), (II), (IIIa), (V), and (VI). The sharp contact is indicative of erosion associated with tsunami events before the depositional phase. The depositional phase has shown a clearly different sedimentary composition with the presence of pumice fragments, and the thickness of the deposit fits within the range of tsunami deposits identified.

Considering the pumice origin, two types of pumice are identified, a dark and a lightly coloured pumice. All pumice fragments are rounded to sub-rounded, a feature consistent with secondary transport as aggradation occurs through grain to grain interactions (Carey et al., 2001). The dark pumice is identified as the Loisels pumice, which has an origin from a submarine volcanic eruption (Mt Healy), and

is traced along much of the northeast coastline of New Zealand (de Lange and Moon, 2007) , and given an inferred age of 610±20 $C^{14}$ BP (Lowe et al., 2000). The other light pumice is believed to be a distal airfall deposit from the TVZ that has been deposited through the BOP. Notable deposits include the Taupo Tephra (1815-1725 cal BP), and the Kaharoa Tephra (600 cal BP) (Shepherd et al., 1997).

Along the truncated Purukau shoreline, both the Loisels pumice, and Kaharoa Tephra can be identified. Considering the evolution of eastern Matakana Island (***Figure 2.3, Chapter 2***), there is significant evidence to suggest that a tsunami event, which occurred pre-formation of the eastern Matakana Island, caused erosion of the Purukau Shoreline and created the deposit identified in CG1. Considering the paleo tsunami records, several tsunami events are known to have occurred in the recent history of New Zealand that may have resulted in the tsunami deposit (Goff, 2002). I believe that the deposits are consequence of a local tsunami event that occurred between AD 1400 and AD 1500.

**CS3**

The second identified tsunami deposit is the sandy, shelly layer atop CS3, that matches with the criteria of (I), (II), (IIIa), (IV), and (VI). Again, sharp contact with the facies below marks erosion, while the sedimentary composition is very different to below. The layer this time is a massive deposit, consistent with very rapid deposition, and the shell composition and thickness are also consistent with distal tsunami deposits. Furthermore, considering the perceived uplift and subsequent erosion that has occurred at the site, prior to the deposition of the top facies, it is unlikely to have formed through ordinary fluvial deposition. The deposit is similar to a nearby shelly/sandy deposit identified on the Omokoroa Peninsula, and correlated to a tsunami event, dated at 1652±20 cal y BP (Christophers, 2015).

However, the deposits in the Western Channel are significantly thicker and coarser than the unit at Omokoroa and contain Loisels Pumice, which is not present at Omokoroa, but is associated with the tsunami deposit on Matakana Island at the Purakau Shoreline. The lack of a similar deposit in CS4 is attributed to the high sediment mobility at the site, indicating that any tsunami deposit there was likely to have been reworked.

### 5.2.2 Pre Holocene

Aside from CS4, all cores are partially composed of pre-Holocene material. However, the interpretation of the deposit ages is entirely speculative, based on degree of weathering and comparisons with literature. The evidence of deposits predicted to be pre-Holocene is presented below. The evidence each core group is analysed independently of the others.

#### *5.2.2.1 Diagenesis*

A prime indicator of pre-Holocene material is evidence of diagenetic trends. Upon deposition and burial, fluids will alter the sedimentary composition of deposits through chemical weathering. Shells will commonly experience a change to their mineralogy, where a dissolution of calcite occurs with an efflux of dissolved calcium carbonate. Where shell fossils are preserved, other minerals (usually silicates) will influx to replace the calcium carbonate that has leached out (Maliva and Siever, 1988; Nelson and Smith, 1996; van der Zee et al., 2003). In environments such as the Tauranga Harbour, which are comprised of volcanogenic sediments, manganese is concentrated in these sediments and will commonly replace the calcium carbonate composition of shells (Lynn and Bonatti, 1965; Homoky et al., 2011).

#### *5.2.2.2 CG1*

At CG1, beneath the Holocene sediment, both cores (CS1 and CS2) show signs of an iron stained sandy shelly deposit. The iron staining provides evidence of post depositional alteration, and thus provide a basis for the deposits being pre Holocene.

Comparing the deposits with other locations around the harbour, recent capital dredging of the main shipping channels for the Port of Tauranga excavated a cemented yellowish orange coarse sand with manganese cockle shell casts from Stella Passage (Moon, pers comm.). This deposit was predicted to be Pleistocene estuarine deposits before dredging commenced. Additionally, at the Omokoroa Peninsula, a sandy deposit with minor silt and small shell fragments has been identified beneath a 20 ka dated peat. As such, there appears sufficient evidence to suggest these deposits as Pleistocene.

#### *5.2.2.3 CG2*

At CS3, the site has evidently experienced uplift and subsequent erosion. The silty composition indicates formation at a period when sea level was much lower than present, while the compaction indicates that the sediment has been buried. However, there is also a presence of large cockles that have not experienced diagenesis. Thus, without dating it is difficult to ascertain the age of the deposit. A similar Pleistocene deposit has been identified at the Omokoroa Peninsula, underlying a peat deposit dated at 7,676±50 BP (Christophers, 2015). The lack of diagenesis can be considered a consequence of the thick shells of cockles, which are more resistant to weathering, in combination with minimal groundwater movement to drive the diagenetic processes. Alternatively, similar silty deposits have been identified at other New Zealand estuarine sites, as early Holocene deposits that formed when sea levels were much lower (Abrahim et al., 2008; Kennedy et al., 2008). However, given the deposits identified at Omokoroa and the evidence of extensive erosion experienced, I believe the deposit is more likely from the Pleistocene.

#### *5.2.2.4 CG3*

At CG3, there is again a lack of diagenetic evidence. However, a sharp boundary between facies 1 and 2, and the anoxic conditions of facies 1, reinforces the greatly reduced Holocene sedimentation rates calculated for the site. Thus, facies 2 is believed to be Pleistocene, with the sharp boundary indicating an erosional period in the early Holocene.

## 5.3 Structural Interpretation

The Tauranga region is known to be tectonically active. Through paleotsunami records, a number of tsunamis have been recognised as affecting the BOP coastline. Some of these are believed to have been generated by local earthquakes, which implies local faulting. Furthermore, evidence of subsidence of areas within the Tauranga Harbour has been previously suggested based on submergence of archaeological sites (Shoefield, 1968; Shepherd et al., 1997). More recently an area of doming around Omokoroa has also been suggested (Christophers, 2015).

Considering the evidence from Chapters 3 and 4 for faulting through the Western Channel, three faults have been identified. FS1 and FS3 were only evident in the

seismic profiles: with FS1 suggesting a fault propagated fold (though there may be a fracture >1.5 m below the seabed); while FS3 did not mark a direct fault trace, although it did suggest one nearby. FS2, meanwhile, had what appeared to be a fault rupturing the surface. Further evidence of a fault was provided by the coring, where the uplifted side was composed of finer, darker, and presumably older sediment, and indicated an erosional environment. The downthrown side was composed entirely of Holocene sands.

The review of literature found that the orientation of rivers and peninsulas along the western margin is linked to deep seated faults believed to be orientated to the north-northeast (Briggs, 1996). Additionally, there are also a series of hotsprings that can be found across the Tauranga Region. These hotsprings are also thought to be partly fault controlled (Briggs, 1996), which suggests leakage of crustal elements through the fault traces. Stewart (2016) sampled radium concentration throughout Tauranga Harbour with the hope of identifying enriched concentrations along fault traces, where the element would leak to the surface (radium is orders of magnitude more enriched in the crust than normally found within seawater) (*Figure 5.3*).

Based on the geomorphology and radium concentrations, the locations of the faults can be split into two groups. The first group consists of FS1 to the southeast, where subsidence is believed to be occurring. Meanwhile, the second group is composed of FS2 and FS3 around Omokoroa, where doming is believed to be occurring.

### 5.3.1 Doming Evidence

Considering the positioning the fault traces, a radium hotspot is found directly above the FS2. Extrapolating the trace northeast and southwest sees the hotspot link up with another hotspot directly to the southeast. Additionally, the trace also links up with Plummers Point and the sandbank between Motuhoa Island and the Omokoroa Peninsula, with the sandbank forming on the uplifted side, and a channel on the downthrown side. This evidence suggests the existence of a fault parallel to, and to the east of the fault identified at the Omokoroa Peninsula by Christophers (2015). Similarly, to the west of the Omokoroa Peninsula, where seismic profiles suggested a fault presence without identifying a fault trace itself, two radium hotspots link up to form another parallel fault orientated to the northeast, also linking up with the Waipapa River.

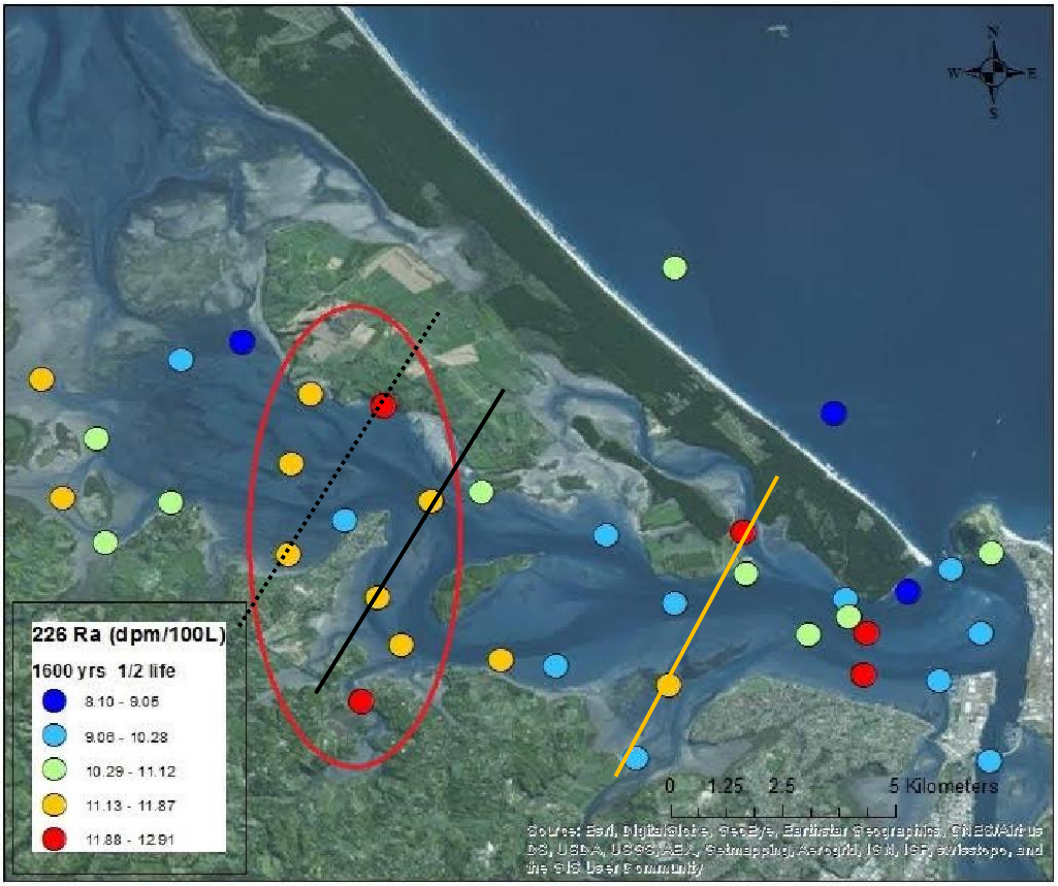


***Figure 5.3: Radium concentration through the harbour overlain on a map from Google Earth. Radium concentrations are provided from (Stewart, 2016). The solid black line marks the projected orientation of FS2 where the fault trace is known from the Seismic, and the dashed line marks the fault trace of FS3, where seismic did not directly mark the location of a fault trace and is so more speculative. Additionally, a solid yellow line marks evidence of a fault to the east of FS1, with no Radium hotspots identified at the location of FS1 itself.***

Christophers (2015) had suggested a doming of the Omokoroa Peninsula, on the basis of the fault cutting through the peninsula, and the closure of the tidal inlet to the northeast on Matakana Island. FS2 and FS3 provide evidence that may support this hypothesis. If doming was occurring, the central fault forms as stress builds up in the sedimentary structure and causes a fracture. As the doming proceeds, built up stress can then cause fractures that occur parallel to the original (Fossen, 2016) (*Figure 5.4*). Doming of the area also coincides with the evolution of Matakana Island (*Figure 5.2*) identified by Shepherd et al (1997), which shows the presence of a core of Pleistocene sediment flanked by two tidal inlets.

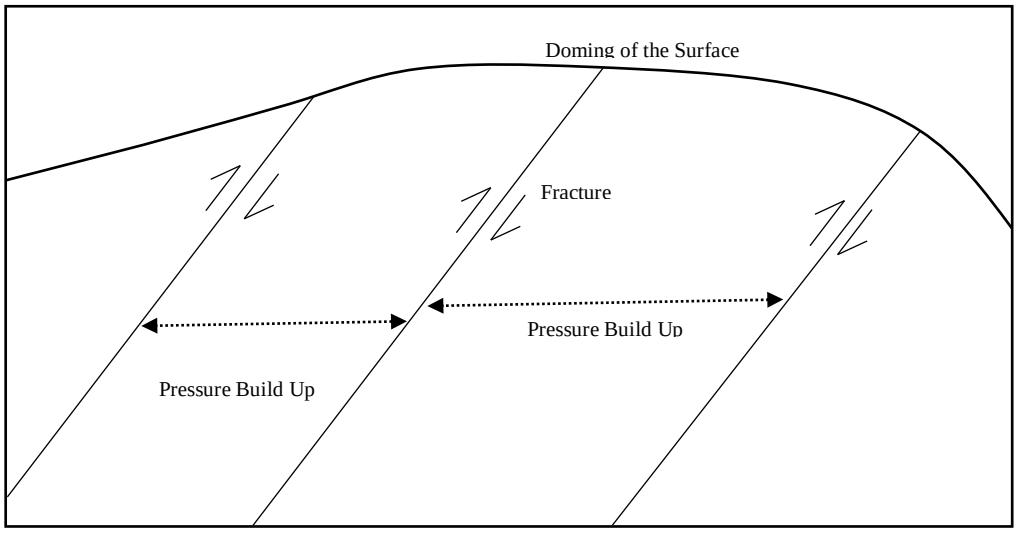


***Figure 5.4: Parallel fracturing forming as stress builds up in the subsurface due to doming.***

### 5.3.2 Subsidence Evidence

The fault evidence at FS1 does not link up as well with the radium concentrations as FS2 and FS3, with instead reduced levels noted at this site. As FS1 did not feature a fault break the surface, and instead a fold propagated fault was identified, the lower radium concentration observed can thus be considered a consequence of this. Because no direct path of leaking to the surface is present, the radium must instead pass through sedimentary sequences and is so reduced. However, to the east of the fault site, a northeast orientation shows two radium hotspots linking up with the Wairoa River. Suggesting parallel fracturing as occurs around Omokoroa, there may be evidence of faulting occurring around Rangiwaea Island also, associated with local subsidence.

## 5.4 Summary

- A longitudinal distribution of coarsening sand is observed in the sedimentary texture along the upper Western Channel, moving out from the tidal flats towards the tidal inlet. The pattern can experience local variations however, with current amplification or proximity to a sedimentary source affected the sediment texture.
- CG1 and CG3 both experience minimal sedimentary changes with depth below the seabed. CG2 meanwhile shows a shell rich facies, which grades

into a shell poor facies, associated with a change in drainage patterns due to the closure of the Hunters Creek Inlet to the immediate northeast.

- Evidence suggests local erosion as the primary source of sediment to the harbour, with particular reference to sandwave occurrence and CS4. Other sources (e.g. terrestrial and storm overwash) are considered to play a lesser role in sediment supply.
- Sedimentation rates are controlled by two key factors: current strength, with greater sedimentation rates occurring where stronger currents occur due to more mobile sediment; and proximity to a sediment source, with the greatest sedimentation rate occurring immediately adjacent a local erosional source.
- Two tsunami deposits are identified by matching a range of criteria established for tsunami deposits. The deposits are identified south of Rangiwaea Island, and east of the Omokoroa Peninsula, and correlated to tsunami events of AD 1400 – 1500, and 1652 ± 20 cal ky BP respectively.
- Pre-Holocene deposits are identified on the basis of diagenetic trends, and correlation to other pre-Holocene deposits identified through the harbour.
- A doming of the Omokoroa region a suggested on active faulting evident in the region, with a series of parallel fault traces identified. This is further backed the closure of a tidal inlet to the northeast indicating greater sedimentation. Additionally, a fault trace in the southeast backs earlier suggestions of subsidence occurring in the region.

# CHAPTER 6
# CONCLUSION

## 6.1 Summary of Research Findings

This chapter summarises the research findings for this research project, with particular reference to the research aim and objectives set out in Chapter 1. Additionally, recommendations for future work are presented based on the findings of this project.

The aim of this research was to investigate the Holocene evolution of the Upper Western Channel within Tauranga Harbour by characterising the stratigraphy and structural features of the sedimentary deposits underlying the channel. The specific objectives of the project were:

*(I) Mapping of the Upper Western Channel utilizing seismic reflection to identify: (a) patterns of sedimentation (facies) and (b) areas of active faulting;*

A seismic reflection survey mapped the Upper Western Channel, from Rangiwaea Island to Matakana Point. Seismic surveys within Tauranga Harbour had previously been focused nearer the tidal inlet, including the Lower Western Channel and part of the Upper Western Channel through to Rangiwaea Island. From the seismic profile data:

(a) Sandwaves were used to identify locations of active mobile sediment. The locations of sandwaves were found to correlate to areas where significant changes to the local hydrodynamics occur, and where a local erosional source of sediment could be identified. Sediment transport within the sandwaves is controlled by the dominant residual currents at each location; and

(b) Three fault sites were identified along the Channel: FS1 occurs south of Rangiwaea Island and consisted of a monoclinical fold. FS2 occurs east of the Omokoroa Peninsula, where a reverse fault is observed breaking the surface, with the eastern side uplifted and the western downthrown. FS3 occurs west of the Omokoroa Peninsula. No fault trace could be

identified within the seismic profile. However the existence of a fault was inferred from, sharply slanted subsurface units, truncated by an erosional surface.

*(II) Sediment coring of the Western Channel to observe how local sedimentary structure varies through the harbour and with depth, and identify the presence of faults;*

Vibracore samples were obtained at five locations through the Upper Western Channel, consisting of three groups of cores:

(a) CG1 is composed of two cores (CS1 & CS2) that have a similar stratigraphic sequence. The top three facies spanning ~150 cm differ very little from one another. However, the bottom metre of the cores have different sedimentary compositions, with CS1 having experienced erosion.

(b) CG2 is composed of two cores (CS3 & CS4) with highly variable sedimentary compositions. CS3 has a thin shell sandy facies at the surface, before a sharp erosional boundary transitions to a series of silty-sand deposits. CS4 meanwhile is made of two gradational medium sand facies that show an increasing shell composition with depth. CG2 correlates to FS2 and reinforces the fault location, with CS3 occurring on the uplifted surface and CS4 on the downthrown.

(c) CG3 is composed of one core, which can be split into three facies separated by sharp boundaries. The grainsize composition varies little, but the colour and shell proportions change significantly between facies.

*(III) To identify patterns of sedimentation: (a) along the Upper Western Channel; (b) locally with depth; (c) the sources of sediment; and (d) approximate rates of sedimentation;*

Patterns of sedimentation were identified through an amalgamation of sedimentation data from the seismic survey and sediment coring chapter, and compared with existing literature:

(a) From the tidal flats, along the Upper Western Channel towards the harbour entrance, a coarsening trend of sediment texture is observed.

Local variations can occur with current amplification or proximity to a sedimentary source.

(b) CS4 is the only core composed of two Holocene deposits. An increasing shell composition with depth, from no shells at the surface to >50% at 300 cm, associated with a change in drainage patterns due to the closure of a mid-Holocene inlet.

(c) Fluvial sedimentation is driven by locally sourced erosion. Both the seismic and coring interpretation identified thicker Holocene deposits near active erosional sources. Additionally, two tsunami facies have been identified in surface deposits in CG1 and CS3, and correlate to a regional tsunami event around AD 1400-1500.

(d) Rates of sedimentation for each core group are calculated as: CG1 0.0977 mm/yr (7,200 BP – 500±50 BP), CG2 0.436 mm/yr (7,200 cal ky BP) and CG3 0.0482 mm/yr (7,200 BP). The CG1 rate is believed representative of the areas without sandwaves identified through the Upper Western Channel. The CG2 rate is the greatest identified and coincide with SS3. The sedimentation rate here is believed to also be representative of SS1, where a similar sandwave structure was observed. CG3 had the lowest calculated rate of sedimentation at 0.0482 mm/yr (7,200 BP), consistent with reduced currents approaching the tidal flats, and similar to the sedimentation rates reported for intertidal flats around eastern Omokoroa Peninsula.

*(IV) To interpret the structural integrity of the Western Channel.*

Two faults (FS2 and FS3) were identified from seismic profiles, one either side of the Omokoroa Peninsula that are consistent with groundwater radium concentrations and headland orientation. An earlier theorised doming of the Omokoroa matches with the evidence of faulting identified in this study. FS1 in the southeast meanwhile, is associated with local subsidence.

## 6.2 Future Work

Due to budgetary constraints, no dating of dateable material was conducted. Consequently, the ages of deposits are largely speculative, despite backing by

literature. Thus, dating of the deposits, in particular facies 3 in CG1, the large shells in CS3, and facies 2 in CG3 should be undertaken. These would confirm the Holocene deposits as identified in this thesis, and allow for more accurate calculation on the rates of sedimentation.

Future sedimentary analysis is then recommended for Hunters Creek, to observe the geomorphological evolution the location. This would allow for the confirmation of the interpretation provided for CS4, and the shifting drainage pattern of the Omokoroa region from Hunters Creek to the modern Tauranga Inlet, around 5.2 ka.

# REFERENCES


Abrahim, G. M., Nichol, S. L., Parker, R. J., & Gregory, M. R. (2008). Facies depositional setting, mineral maturity and sequence stratigraphy of a Holocene drowned valley, Tamaki Estuary, New Zealand. *Estuarine, Coastal and Shelf Science, 79*(1), 133-142.

Allen, J. (1980). Sand waves: a model of origin and internal structure. *Sedimentary Geology, 26*(4), 281-328.

Atwater, B. F. (1987). Evidence for great Holocene earthquakes along the outer coast of Washington State. *Science, 236*(4804), 942-944.

Barnes, H. A. (1997). Thixotropy—a review. *Journal of Non-Newtonian fluid mechanics, 70*(1), 1-33.

Barnett, A. (1985). Overview and Hydrodynamics, Tauranga Harbour Study, Parts I & III. *Tauranga, New Zealand: Bay of Plenty Harbour Board, 74p*

Barrow, J. C. (1994). The resonant sonic drilling method: an innovative technology for environmental restoration programs. *Groundwater Monitoring & Remediation, 14*(2), 153-160.

Bell, R., Goff, J., Downes, G., Berryman, K., Walters, R., Chague-Goff, C., Barnes, P., & Wright, I. (2004). *Tsunami hazard for the Bay of Plenty and eastern Coromandel Peninsula*. Bay of Plenty Regional Council: NIWA, GeoEnvironmental Ltd, GNS

Bokuniewicz, H., Gordon, R., & Kastens, K. (1977). From and migration of sand waves in a large estuary, Long Island Sound. *Marine Geology, 24*(3), 185-199.

Bourgeois, J. (2009). Geologic effects and records of tsunamis. *The sea, 15*, 53-91.

Brannigan, A. M. (2009). *Change in geomorphology, hydrodynamics and surficial sediment of the Tauranga Entrance tidal delta system.* University of Waikato.

Briggs, R., Houghton, B., McWilliams, M., & Wilson, C. (2005). 40Ar/39Ar ages of silicic volcanic rocks in the Tauranga-Kaimai area, New Zealand: Dating the transition between volcanism in the Coromandel Arc and the Taupo Volcanic Zone. *New Zealand Journal of Geology and Geophysics, 48*(3), 459-469.

Briggs, R. M. (1996). *Geology of the Tauranga Area: Sheet U14 1: 50 000*: Department of Earth Sciences, University of Waikato.

Carey, S., Morelli, D., Sigurdsson, H., & Bronto, S. (2001). Tsunami deposits from major explosive eruptions: an example from the 1883 eruption of Krakatau. *Geology, 29*(4), 347-350.

Chappell, P. R. (2013). *The Climate and Weather of Bay of Plenty. 3rd edition*. NIWA

Christophers, A. J. (2015). *Paleogeomorphic reconstruction of the Omokoroa Domain, Bay of Plenty, New Zealand*. University of Waikato.

Clement, A. J., Sloss, C. R., & Fuller, I. C. (2010). Late quaternary geomorphology of the Manawatu coastal plain, North Island, New Zealand. *Quaternary International, 221*(1), 36-45.

Cole, R., Hull, P., & Healy, T. R. (2000). Assemblage structure, spatial patterns, recruitment, and post-settlement mortality of subtidal bivalve molluscs in a large harbour in north-eastern New Zealand. *New Zealand Journal of Marine and Freshwater Research, 34*(2), 317-329.

Danišík, M., Shane, P., Schmitt, A. K., Hogg, A., Santos, G. M., Storm, S., Evans, N.J., Fifield, L.K., & Lindsay, J. M. (2012). Re-anchoring the late Pleistocene tephrochronology of New Zealand based on concordant radiocarbon ages and combined 238 U/230 Th disequilibrium and (U–Th)/He zircon ages. *Earth and Planetary Science Letters, 349*, 240-250.

Davies-Colley, R., & Healy, T. (1978). Sediment and hydrodynamics of the Tauranga Entrance to Tauranga Harbour. *New Zealand Journal of Marine and Freshwater Research, 12*(3), 225-236.

Davis, R. A., & Healy, T. R. (1993). Holocene coastal depositional sequences on a tectonically active setting: southeastern Tauranga Harbour, New Zealand. *Sedimentary Geology, 84*(1), 57-69.

Dawson, A. G., & Stewart, I. (2007). Tsunami deposits in the geological record. *Sedimentary Geology, 200*(3), 166-183.

Day, J. (1981). Summaries of current knowledge of 43 estuaries in southern Africa. *Estuarine ecology with particular reference to southern Africa*, 251-329.

de Lange, W., & Gibb, J. (2000). Seasonal, interannual, and decadal variability of storm surges at Tauranga, New Zealand. *New Zealand Journal of Marine and Freshwater Research, 34*(3), 419-434.

de Lange, W., & Moon, V. (2007). Tsunami washover deposits, Tawharanui, New Zealand. *Sedimentary Geology, 200*(3), 232-247.

de Lange, W., Moon, V., & Johnstone, R. (2015. *Evolution of the Tauranga Harbour Entrance: Influences of tsunami, geology and dredging*. Paper

presented at the Australasian Coasts & Ports Conference 2015, Auckland, New Zealand

de Lange, W. P., Moon, V. G., & Healy, T. R. (1991). Problems with predicting the transport of pumiceous sediments in the coastal environment *Coastal Sediments* (pp. 990-996): ASCE.

Demaison, G., & Moore, G. T. (1980). Anoxic environments and oil source bed genesis. *Organic Geochemistry, 2*(1), 9-31.

Elliot, A., Parshotam, A., & Wadhwa, S. (2009). *Tauranga Harbour Sediment Study: Catchment Model Results*. Bay of Plenty Regional Council: NIWA.

Erslev, E. A. (1991). Trishear fault-propagation folding. *Geology, 19*(6), 617-620.

Fiechter, J., Steffen, K. L., Mooers, C. N., & Haus, B. K. (2006). Hydrodynamics and sediment transport in a southeast Florida tidal inlet. *Estuarine, coastal and shelf science, 70*(1), 297-306.

Fossen, H. (2016). *Structural geology*: Cambridge University Press.

Friedrichs, C. (2011). 3.06-Tidal Flat Morphodynamics: A Synthesis. *Treatise on Estuarine and Coastal Science, edited by E. Wolanski and D. McLusky*, 137-170.

Garae, C. (2015). *Estimating patterns and rates of coastal cliff retreat around Tauranga Harbour*. University of Waikato

Goff, J. (2002). *Preliminary study of tsunami record on Coromandel East Coast*. Environment Waikato, Environment Bay of Plenty: GeoEnvironmental Ltd

Goff, J., Chagué-Goff, C., & Nichol, S. (2001). Palaeotsunami deposits: a New Zealand perspective. *Sedimentary Geology, 143*(1), 1-6.

Goff, J., Chagué-Goff, C., Nichol, S., Jaffe, B., & Dominey-Howes, D. (2012). Progress in palaeotsunami research. *Sedimentary Geology, 243*, 70-88.

Goto, K., Chagué-Goff, C., Goff, J., & Jaffe, B. (2012). The future of tsunami research following the 2011 Tohoku-oki event. *Sedimentary Geology, 282*, 1-13.

Green, M. O. (2009). *Tauranga Harbour Sediment Study: Implementation and Calibration of the USC-3 Model*. Bay of Plenty Regional Council: NIWA.

Green, M. O. (2009). *Tauranga Harbour Sediment Study: Predictions of Harbour Sedimentation Under Future Scenarios*. Bay of Plenty Regional Council: NIWA.

Gumenskii, B. M., & Komarov, N. S. (1961). Soil drilling by vibrations. *New York Consultants Bureau (translated from Russian)*, 80pp.

Hancock, N., Hume, T. M., & Swales, A. (2009). *Tauranga Harbour Sediment Study: Harbour Bed Sediments*. Bay of Plenty Regional Council: NIWA.

Hay, D. N., de Lange, W., & Healy, T. (1991). Storm and oceanographic databases for the Western Bay of Plenty *Coastal Engineering: Climate for Change; Proceedings of 10th Australasian Conference on Coastal and Ocean Engineering, 1991* (p. 139): Water Quality Centre, DSIR Marine and Freshwater.

Healy, T. (1985). Field collection programme and morphological study, Tauranga Harbour study, Parts II and V. *Tauranga, New Zealand: Bay of Plenty Harbour Board, 25p*

Healy, T., & Kirk, R. (1982). Coasts *Landforms of New Zealand* (pp. 80-104): Longman Paul Auckland, New Zealand.

Heap, A., & Nichol, S. (1997). The influence of limited accommodation space on the stratigraphy of an incised-valley succession: Weiti River estuary, New Zealand. *Marine Geology, 144*(1), 229-252.

Heath, R. (1979). Significance of storm surges on the New Zealand coast. *New Zealand Journal of Geology and Geophysics, 22*(2), 259-266.

Herbst, P. H., Schuler, A. A., & Lawrie, A. (2002). *Erosion Protection Works: Guidelines for Tauranga Harbour*. Environment Bay of Plenty

Homoky, W., Hembury, D., Hepburn, L., Mills, R., Statham, P., Fones, G., & Palmer, M. (2011). Iron and manganese diagenesis in deep sea volcanogenic sediments and the origins of pore water colloids. *Geochimica et Cosmochimica Acta, 75*(17), 5032-5048.

Hughes, M. W., Quigley, M. C., van Ballegooy, S., Deam, B. L., Bradley, B. A., & Hart, D. E. (2015). The sinking city: Earthquakes increase flood hazard in Christchurch, New Zealand. *GSA Today, 25*(3)

Hull, A. G. (1986). Pre-AD 1931 tectonic subsidence of Ahuriri Lagoon, Napier, Hawke's Bay, New Zealand. *New Zealand journal of geology and geophysics, 29*(1), 75-82.

Hume, T. M., Green, M. O., & Elliot, S. (2009). *Tauranga Harbour Sediment Study: Assessment of Predictions for Management*. Bay of Plenty Regional Council: NIWA.

Hume, T. M., & Herdendorf, C. E. (1988). A geomorphic classification of estuaries and its application to coastal resource management—a New Zealand example. *Ocean and Shoreline Management, 11*(3), 249-274.

Hume, T. M., & Herdendorf, C. E. (1992). Factors controlling tidal inlet characteristics on low drift coasts. *Journal of Coastal Research*, 355-375.

Hume, T. M., & Herdendorf, C. E. (1993). On the use of empirical stability relationships for characterising estuaries. *Journal of Coastal Research*, 413-422.

Hume, T. M., Snelder, T., Weatherhead, M., & Liefting, R. (2007). A controlling factor approach to estuary classification. *Ocean & Coastal Management, 50*(11), 905-929.

Hunt, S., Bryan, K. R., & Mullarney, J. C. (2015). The influence of wind and waves on the existence of stable intertidal morphology in meso-tidal estuaries. *Geomorphology, 228*, 158-174.

Jorat, M., Moon, V., Hepp, D., Kreiter, S., de Lange, W., Feldmann, S., & Morz, T. (2016). Subseafloor Investigation of Sediments at Southern Tauranga Harbour, New Zealand, before Capital Dredging. *Journal of Coastal Research, Under Review*

Kennedy, D. M., Paulik, R., & Millar, M. (2008). Infill of a structurally controlled estuary: An example from southern Whanganui Inlet, New Zealand. *New Zealand Geographer, 64*(1), 20-33.

Krüger, J., & Healy, T. R. (2006). Mapping the morphology of a dredged ebb tidal delta, Tauranga Harbour, New Zealand. *Journal of coastal research*, 720-727.

Kuehl, S. A., Alexander, C. R., Blair, N. E., Harris, C. K., Marsaglia, K. M., Ogston, A. S., Orpin, A.R., Roering, J.J., Bever, A.J., Bilderback, E. L., & Carter, L. (2016). A source-to-sink perspective of the Waipaoa River margin. *Earth-Science Reviews, 153*, 301-334.

Kwoll, E., & Winter, C. (2011). Determination of the initial grain size distribution in a tidal inlet by means of numerical modelling. *Journal of Coastal Research* (64), 1081.

Le Hir, P., Roberts, W., Cazaillet, O., Christie, M., Bassoullet, P., & Bacher, C. (2000). Characterization of intertidal flat hydrodynamics. *Continental shelf research, 20*(12), 1433-1459.

LINZ. (2016). Chart NZ 5411 Tauranga Harbour, Katikati Entrance to Mount Maunganui. https://data.linz.govt.nz/layer/1402-chart-nz-5411-tauranga-harbour-katikati-entrance-to-mount-maunganui/

Liu, J. T., & Aubrey, D. G. (1993). Tidal residual currents and sediment transport through multiple tidal inlets. *Formation and evolution of multiple tidal inlets*, 113-157.

Lowe, D. J. (2011). Tephrochronology and its application: a review. *Quaternary Geochronology, 6*(2), 107-153.

Lowe, D. J., Newnham, R. M., McFadgen, B. G., & Higham, T. F. (2000). Tephras and New Zealand archaeology. *Journal of Archaeological Science, 27*(10), 859-870.

Ludwick, J. C. (1975). Variations in the boundary-drag coefficient in the tidal entrance to Chesapeake Bay, Virginia. *Marine Geology, 19*(1), 19-28.

Lynn, D., & Bonatti, E. (1965). Mobility of manganese in diagenesis of deep-sea sediments. *Marine Geology, 3*(6), 457-474.

MacGibbon, R., Hamill, K., Muirhead, S., Tozer, C., & McConchie, J. (2011). *Tauranga Harbour Sediment Management Review*. Bay of Plenty Regional Council: OPUS

Maliva, R. G., & Siever, R. (1988). Mechanism and controls of silicification of fossils in limestones. *The Journal of Geology*, 387-398.

McCave, I. (1971). Sand waves in the North Sea off the coast of Holland. *Marine geology, 10*(3), 199-225.

Moon, V., de Lange, W., Garae, C., Mörz, T., Jorat, M., & Kreiter, S. (2015). Monitoring the landslide at Bramley Drive, Tauranga, NZ.

Morton, R. A., Gelfenbaum, G., & Jaffe, B. E. (2007). Physical criteria for distinguishing sandy tsunami and storm deposits using modern examples. *Sedimentary Geology, 200*(3), 184-207.

Nelson, C. S., & Smith, A. M. (1996). Stable oxygen and carbon isotope compositional fields for skeletal and diagenetic components in New Zealand Cenozoic nontropical carbonate sediments and limestones: a synthesis and review. *New Zealand Journal of Geology and Geophysics, 39*(1), 93-107.

NIWA. (2013). *Estuary Types.* Retrieved from https://www.niwa.co.nz/coasts-and-oceans/nz-coast/learn-about-coastal-environments/estuary-types

Oliver, R. C. (1997). A geotechnical characterisation of volcanic soils in relation to coastal landsliding on the Maungatapu Peninsula, Tauranga, New Zealand.

Parker, B. B. (1991). TIDAL INTERACTIONS (REVIEW). *Tidal hydrodynamics*, 237.

Parshotam, A., Hume, T. M., Elliot, S., Green, M. O., & Wadhwa, S. (2008). *Tauranga Harbour Sediment Study: Specification of Scenarios*. Bay of Plenty Regional Council: NIWA.

Parshotam, A., Wadhwa, S., & Mullan, B. (2009). *Tauranga Harbour Sediment Study: Sediment Load Model Implementation and Validation*. Bay of Plenty Regional Council: NIWA.

Penrose, J., Siwabessy, P., Gavrilov, A., Parnum, I., Hamilton, L., Bickers, A., Brooke, B., Ryan, D., & Kennedy, P. (2005). Acoustic techniques for seabed classification. *Cooperative Research Centre for Coastal Zone Estuary and Waterway Management, Technical Report, 32*

Pluet, J., & Pirazzoli, P. (1991). *World atlas of Holocene sea-level changes*: Elsevier.

Quaternary Resources PTY Limited (2016). *Vibracore Operations Manual: Model QR 300*

Pritchard, D. W. (1967). What is an estuary: physical viewpoint. *Estuaries, 83*, 3-5.

Pritchard, M., & Gorman, R. (2009). *Tauranga Harbour Sediment Study: Hydrodynamics and Sediment Transport Modelling*. Bay of Plenty Regional Council: NIWA.

Santos, I. R., Bryan, K. R., Pilditch, C. A., & Tait, D. R. (2014). Influence of porewater exchange on nutrient dynamics in two New Zealand estuarine intertidal flats. *Marine Chemistry, 167*, 57-70.

Schock, S. G., LeBlanc, L. R., & Mayer, L. A. (1989). Chirp subbottom profiler for quantitative sediment analysis. *Geophysics, 54*(4), 445-450.

Schofield, J. (1968). Dating of recent low sea level and Maori rock carvings Ongari Point.

Shepherd, M., McFadgen, B., Betts, H., & Sutton, D. G. (1997). *Formation, landforms and palaeoenvironment of Matakana Island and implications for archaeology*: Department of Conservation.

Soulsby, R. (1997). *Dynamics of marine sands: a manual for practical applications*: Thomas Telford.

Stewart, B. (2016). *Untitled Research*. University of Waikato. In Press.

Suppe, J. (1985). *Principles of structural geology*: Prentice Hall.

Surman, M., Clarke, R., & Carter, M. (1999). *Tauranga Harbour Sediment Source Survey*. Bay of Plenty Regional Council:

Tay, H., Bryan, K., de Lange, W., & Pilditch, C. (2013). The hydrodynamics of the southern basin of Tauranga Harbour. *New Zealand Journal of Marine and Freshwater Research, 47*(2), 249-274.

Terwindt, J. H. (1971). Sand waves in the Southern Bight of the North Sea. *Marine Geology, 10*(1), 51-67.

Terwindt, J. H., & Brouwer, M. J. (1986). The behaviour of intertidal sandwaves during neap-spring tide cycles and the relevance for palaeoflow reconstructions. *Sedimentology, 33*(1), 1-31.

Tuttle, M. P., Ruffman, A., Anderson, T., & Jeter, H. (2004). Distinguishing tsunami from storm deposits in eastern North America: the 1929 Grand Banks tsunami versus the 1991 Halloween storm. *Seismological Research Letters, 75*(1), 117-131.

Van de Kreeke, J., & Hibma, A. (2005). Observations on silt and sand transport in the throat section of the Frisian Inlet. *Coastal engineering, 52*(2), 159-175.

van der Zee, C., Van Raaphorst, W., Helder, W., & de Heij, H. (2003). Manganese diagenesis in temporal and permanent depositional areas of the North Sea. *Continental shelf research, 23*(6), 625-646.

Whitbread-Edwards, A. (1994). *The volcanic geology of the western Tauranga Basin*. University of Waikato, Unpublished.

Wilson, C., Rhoades, D., Lanphere, M., Calvert, A., Houghton, B., Weaver, S., & Cole, J. (2007). A multiple-approach radiometric age estimate for the Rotoiti and Earthquake Flat eruptions, New Zealand, with implications for the MIS 4/3 boundary. *Quaternary Science Reviews, 26*(13), 1861-1870.